

DIRAC NEUTRALINOS AND ELECTROWEAK SCALAR BOSONS OF $N=1/N=2$ HYBRID SUPERSYMMETRY AT COLLIDERS

S. Y. Choi,¹ D. Choudhury,² A. Freitas,³ J. Kalinowski,⁴ J. M. Kim,⁵ and P. M. Zerwas⁶

¹*Department of Physics and RIPC, Chonbuk National University, Jeonju 561-756, Korea*

²*Department of Physics and Astrophysics, University of Delhi, Delhi 110007, India*

³*Department of Physics & Astronomy, University of Pittsburgh, 3941 O'Hara St, PA 15260, USA*

⁴*Faculty of Physics, University of Warsaw, 00681 Warsaw, Poland, and
Theory Division, CERN, CH-1211 Geneva 23, Switzerland*

⁵*Physikalisches Institut and Bethe Center for Theoretical Physics,
Universität Bonn, Nussallee 12, D-53115 Bonn, Germany*

⁶*Institut für Theoretische Teilchenphysik und Kosmologie,
RWTH Aachen University, D-52074 Aachen, Germany, and
Deutsches Elektronen-Synchrotron DESY, D-22603 Hamburg, Germany*

(Dated: November 21, 2018)

In the $N=1$ supersymmetric extension of the Standard Model, neutralinos associated in supermultiplets with the neutral electroweak gauge and Higgs bosons are, as well as gluinos, Majorana fermions. They can be paired with the Majorana fermions of novel gaugino/scalar supermultiplets, as suggested by extended $N=2$ supersymmetry, to Dirac particles. Matter fields are not extended beyond the standard $N=1$ supermultiplets in $N=1/N=2$ hybrid supersymmetry to preserve the chiral character of the theory. Complementing earlier analyses in the color sector, central elements of such an electroweak scenario are analyzed in the present study. The decay properties of the Dirac fermions $\tilde{\chi}_D$ and of the scalar bosons σ are worked out, and the single and pair production-channels of the new particles are described for proton collisions at the LHC, and electron/positron and $\gamma\gamma$ collisions at linear colliders. Special attention is paid to modifications of the Higgs sector, identified with an $N=2$ hypermultiplet, by the mixing with the novel electroweak scalar sector.

1. INTRODUCTION

Neutral electroweak gauge bosons are described by self-conjugate fields with two degrees of freedom before symmetry breaking. In $N=1$ supersymmetry [1–3] the gaugino partners \tilde{G} of the gauge bosons G_μ in the supermultiplets $\hat{G} = \{G_\mu, \tilde{G}\}$ are correspondingly self-conjugate Majorana fields with two independent components for the two helicities. They mix with neutral higgsinos to form the neutralino fields $\tilde{\chi}^0$. However, in $N=2$ extended supersymmetric scenarios, *cf.* Ref. [4–11], gauginos \tilde{G}' with scalar partners σ are introduced in novel $N=1$ chiral supermultiplets $\hat{\Sigma} = \{\tilde{G}', \sigma\}$, which together with the original $N=1$ gauge supermultiplets constitute the $N=2$ gauge hypermultiplets $\mathcal{G} = \{\hat{G}, \hat{\Sigma}\}$. For suitable mass matrices, the new gauginos can be combined with the original ones to form Dirac fields $\tilde{G}_D = \tilde{G} \oplus \tilde{G}'$. Including the higgsinos, the neutralino fields can thus be identified with Dirac fields $\tilde{\chi}_D^0$.

The transition from Majorana to Dirac fields renders the theory [partially] R -symmetric [12]. R -symmetry, a continuous extension of the R -parity concept, is associated with global transformations of the fermionic coordinates,

$\theta \rightarrow e^{i\alpha}\theta$ and $\bar{\theta} \rightarrow e^{-i\alpha}\bar{\theta}$. All Standard Model (SM) fields carry vanishing R -charge. Assigning the R -charge $+1$ to θ , the gauge superfields and the matter chiral superfields carry R -charges 0 and $+1$, respectively. As a result, the kinetic part of the action is R -symmetric. In gauge superfields the R -charges of the gaugino components \tilde{G} are $+1$, and equally for the scalar components of the matter lepton and quark superfields. Higgs superfields are assigned R -charges 0 , giving rise to $\{0, -1\}$ for the R -charges of the Higgs fields themselves and the higgsino fields. Thus the tri-linear Yukawa terms in the superpotential carry R -charge $+2$ and the corresponding action is R -invariant, unlike the μ -term for which the associated action, with $R = -2$, is not R -invariant. Soft Majorana mass terms of gauginos and the tri-linear scalar coupling terms, which break supersymmetry, carry $R = +2$ so that the corresponding Lagrangians are not R -invariant. However, assigning $R = 0$ to the chiral superfields $\hat{\Sigma}$, the new gaugino \hat{G}' fields carry R -charge -1 . Thus, Dirac mass terms, combining the old and the new gaugino fields, are R -invariant.

The conservation of R -charges, initially motivated by the transition from Majorana to Dirac gauginos, has important physical implications. The theory naturally suppresses the baryon and lepton number violating operators and the μ term in the superpotential. Since it also forbids soft SUSY breaking gaugino Majorana masses in the Lagrangian and Higgs couplings to sfermion pairs, SUSY flavor-changing and CP-violating contributions, for instance, are reduced significantly, widening the potential parameter space for supersymmetric theories [13]. The more restrictive Dirac gaugino masses, on the other hand, are allowed. Moreover, since the scalar components σ of the chiral superfields $\hat{\Sigma}$ have R -charge 0 , they can couple to SM particles so that σ particles can be produced singly in standard particle collisions. In addition, they can decay to pairs of SM particles [and, similarly, to pairs of supersymmetric particles].

The $N=1$ chiral supermultiplets within the $N=2$ gauge hypermultiplets contain scalar sigma fields σ in the adjoint representations of the gauge groups $SU(1)_C$, $SU(2)_I$ and $U(1)_Y$. In the electroweak $SU(2)_I$ and $U(1)_Y$ sectors the scalar fields can acquire non-zero vacuum expectation values and they can mix with the original Higgs fields. As a result, the properties of the Higgs particles are modified in this scenario.

In $N=2$ supersymmetric theories the standard $N=1$ L/R matter supermultiplets are complemented with new L/R matter multiplets [14]. To keep the theory chiral, in agreement with experimental observations, the masses of the new multiplets must be chosen very large so that $N=2$ supersymmetry is effectively reduced to $N=1$ supersymmetry in this sector. Exceptions are the two Higgs doublets which can be associated with the two supermultiplets within a Higgs hypermultiplet. Since the gauge and Higgs sectors are framed in the $N=2$ formalism, but the matter sector in $N=1$ is not, the theory is conventionally termed $N=1/N=2$ hybrid theory.

The transition from the Majorana-type Minimal Supersymmetric Standard Model (MSSM) to a Dirac theory by expanding the gauge sector can be formulated in a smooth way by suitable transitions of the parameters in the $\{\tilde{G}, \tilde{G}'\}$ mass matrix. We start with an infinitely large \tilde{G}' Majorana mass at the beginning of the path, which is congruent with the original MSSM. Lowering the Majorana masses to zero and generating non-diagonal entries in the mass matrix at the end of the path, the two Majorana fields can be combined to a Dirac field if the two mass eigenvalues have equal moduli but opposite signs. In this way, the characteristics of the Majorana theory can systematically be tagged in the evolution to the Dirac theory, and implications of the Dirac theory can be connected with experimental analyses.

The Dirac theory, including the scalar sigma fields, has been analyzed in two earlier studies [7, 8] primarily in the colored sector, and experimental consequences have been discussed for the proton collider LHC. Basic elements of the electroweak sector, including the interaction of the Higgs field with the novel scalar fields, have been presented in Ref. [15], and implications for the relic density in the Universe have been discussed for such a Dirac theory [see also [16–18]]. In the present study we will focus on collider signatures of the electroweak chargino/neutralino and the novel sigma sectors at LHC and e^+e^- colliders. In addition, modifications of the properties of the Higgs particles by interactions with the novel scalars will be discussed. While the theoretical basis of the $N=1/N=2$ hybrid theory is summarized in the next section, phenomenological consequences are worked out for the chargino/neutralino and scalar/Higgs sectors thereafter.

superfields	SU(3) _C , SU(2) _I , U(1) _Y	Spin 1	Spin 1/2	Spin 0
\hat{G}_C / color	8, 1, 0	g^a	\tilde{g}^a	
\hat{G}_I / isospin	1, 3, 0	W^i	\tilde{W}^i	
\hat{G}_Y / hypercharge	1, 1, 0	B	\tilde{B}	
$\hat{\Sigma}_C$ / color	8, 1, 0		\tilde{g}'^a	σ_C^a
$\hat{\Sigma}_I$ / isospin	1, 3, 0		\tilde{W}'^i	σ_I^i
$\hat{\Sigma}_Y$ / hypercharge	1, 1, 0		\tilde{B}'	σ_Y^0

Table I: The $N=2$ gauge hypermultiplets for the color $SU(3)_C$, isospin $SU(2)_I$ and hypercharge $U(1)_Y$ groups. The superscripts $a = 1-8$ and $i = 1-3$ denote the $SU(3)_C$ color and $SU(2)_I$ isospin indices, respectively.

2. THEORETICAL BASIS: $N=1/N=2$ HYBRID THEORY

2.1. Hyper/Superfields and Interactions

The $N=1/N=2$ hybrid model, which can be evolved from the MSSM continuously to a Dirac gaugino theory, includes a large spectrum of fields. The $N=2$ gauge hypermultiplets $\mathcal{G} = \{\hat{G}, \hat{\Sigma}\}$ can be decomposed into the usual $N=1$ vector supermultiplets of gauge and gaugino fields $\hat{G} = \{G_\mu, \tilde{G}\}$, complemented by chiral supermultiplets of novel gaugino and scalar fields $\hat{\Sigma} = \{\tilde{G}', \sigma\}$. The new gauge/gaugino/scalar fields, together with the MSSM fields, are shown explicitly for the color $SU(3)_C$ and the electroweak isospin $SU(2)_I$ and hypercharge $U(1)_Y$ gauge groups in Tab. I.

In parallel to the gauge fields, the neutral gaugino fields \tilde{G} are self-conjugate Majorana fields with two helicity components, analogously the novel gaugino fields \tilde{G}' . [The notation $G_\mu, \tilde{G}, \tilde{G}', \sigma$ is used generically for gauge, gaugino and σ fields; when specific gauge groups are referred to, the notation follows Table I.] To match the two gaugino degrees of freedom in the new chiral supermultiplet, the components of the scalar fields σ are complex. Suitable mass matrices provided, the two gaugino Majorana fields \tilde{G} and \tilde{G}' can be combined to a Dirac field \tilde{G}_D .

In a similar way, the two Higgs-doublet superfields \hat{H}_d and \hat{H}_u^\dagger of the MSSM can be united to an $N=2$ hyperfield $\mathcal{H} = \{\hat{H}_d, \hat{H}_u^\dagger\}$ [19, 20]. It may be noted that, after diagonalizing the off-diagonal 2×2 mass matrix, the two neutral higgsinos can be interpreted as a Dirac field.

In contrast, the observed chiral character of the Standard Model precludes the extension of the usual (s)lepton and (s)quark supermultiplets \hat{Q} to hypermultiplets of L/R symmetric particles and mirror-particles. Moreover, including such a large number of new matter fields would make the entire theory asymptotically non-free. Equivalent to introducing very heavy masses, the mirror fields can just be eliminated from the system of matter fields *ad hoc*. This supposition generates the $N=1/N=2$ hybrid character of the theory.

Corresponding to the complex spectrum of fields, the sum of a set of actions with different bases and characteristics describes the $N=1/N=2$ hybrid theory. The $N=2$ action of the gauge hypermultiplet $\mathcal{G} = \{\hat{G}, \hat{\Sigma}\}$ consists of the usual $N=1$ action of the gauge supermultiplet \hat{G} plus the action of the chiral supermultiplet $\hat{\Sigma}$ which couples the new gaugino and scalar fields to the gauge superfield:

$$\mathcal{A}_G = \sum \frac{1}{16g^2k} \int d^4x d^2\theta \operatorname{tr} \hat{G}^\alpha \hat{G}_\alpha, \quad (2.1)$$

$$\mathcal{A}_\Sigma = \sum \int d^4x d^2\theta d^2\bar{\theta} \hat{\Sigma}^\dagger \exp[\hat{G}] \hat{\Sigma}, \quad (2.2)$$

with the sums running over the gauge groups $SU(3)_C$, $SU(2)_I$ and $U(1)_Y$. g are the gauge couplings (denoted by

g_s, g and g' for color, isospin and hypercharge) and k are the corresponding quadratic Casimir invariants $C_2(G)$. $\hat{G}_\alpha = 2g\hat{G}_\alpha T^a$ are the gauge superfield-strengths, T^a the generators in the adjoint representation; the traces run over the gauge-algebra indices. To this class of actions belongs also the standard (s)lepton/(s)quark gauge action

$$\mathcal{A}_Q = \sum \int d^4x d^2\theta d^2\bar{\theta} \hat{Q}^\dagger \exp[\hat{G}] \hat{Q}, \quad (2.3)$$

summed over the standard matter chiral superfields, denoted generically as \hat{Q} .

These actions are complemented by gauge-invariant $N=1$ supersymmetric Majorana mass terms M for the new gauge superfields and Dirac mass terms M^D coupling the original and new gauge superfields:

$$\mathcal{A}_M = \int d^4x d^2\theta M \text{tr} \hat{\Sigma} \hat{\Sigma}, \quad (2.4)$$

$$\mathcal{A}_D = \int d^4x d^2\theta M^D \theta^\alpha \text{tr} \hat{G}_\alpha \hat{\Sigma}. \quad (2.5)$$

\mathcal{A}_M , which is bi-linear in the Σ fields, is part of the superpotential of the theory and contributes to the masses of the chiral supermultiplets. The Dirac mass term can be generated, *e.g.*, by the interaction $\sqrt{2}\hat{X}^\alpha \hat{G}_\alpha \hat{\Sigma}/M_X$ when a hidden-sector $U(1)'$ spurion superfield acquires a D -component vacuum expectation value $\hat{X}^\alpha = \theta^\alpha D_X$, giving rise to the Dirac mass $M^D = D_X/M_X$ [21].

According to the general rules, this set of actions generates D -terms bi-linear in the usual slepton and squark fields and linear in the new scalar sigma field with a coefficient given by the Dirac mass M^D . When the auxiliary fields D are eliminated through their equations of motion, the sigma fields get coupled to bi-linears of the slepton and squark fields with strength M^D .

The Higgs sector is rendered more complicated by the interactions with the non-colored scalar sigma fields. The Higgs supermultiplets \hat{H}_d and \hat{H}_u^\dagger are coupled to the $SU(2)_I \times U(1)_Y$ supergauge fields in the usual way,

$$\mathcal{A}_H = \sum_{i=u,d} \int d^4x d^2\theta d^2\bar{\theta} \hat{H}_i^\dagger \exp[\hat{G}_I + \hat{G}_Y] \hat{H}_i. \quad (2.6)$$

The part of the superpotential which includes Higgs fields, consists of the standard $N=1$ bi-linear μ -term,

$$\mathcal{A}_\mu = \int d^4x d^2\theta \mu \hat{H}_u \cdot \hat{H}_d, \quad (2.7)$$

and the tri-linear Higgs Yukawa terms involving the matter fields, which can be adopted from the $N=1$ theory:

$$\mathcal{A}'_Q = \int d^4x d^2\theta \sum g_Q \hat{q}^c \hat{Q} \cdot \hat{H}_q, \quad (2.8)$$

the dots denoting the asymmetric contraction of the $SU(2)_I$ doublet components. New tri-linear interactions are predicted in $N=2$ supersymmetry [5] which couple the two supercomponents of the Higgs hypermultiplet with the new chiral superfields in the superpotential:

$$\mathcal{A}'_H = \int d^4x d^2\theta \frac{1}{\sqrt{2}} \hat{H}_u \cdot (\lambda_I \hat{\Sigma}_I + \lambda_Y \hat{\Sigma}_Y) \hat{H}_d. \quad (2.9)$$

In $N=2$ supersymmetry the couplings λ_I, λ_Y are identified with the $SU(2)_I$ and $U(1)_Y$ gauge couplings,

$$\lambda_I = g/\sqrt{2} \quad \text{and} \quad \lambda_Y = -g'/\sqrt{2}. \quad (2.10)$$

In our phenomenological analyses we will treat them generally as independent couplings.

It may be noticed that the Majorana action \mathcal{A}_M , the μ -term \mathcal{A}_μ and the tri-linear Higgs-sigma term \mathcal{A}'_H are manifestly not R -invariant.

Finally, the bi-linear and tri-linear soft supersymmetry breaking terms must be added to the gauge, Higgs and matter Lagrangians:

$$\begin{aligned}
\mathcal{L}_{\text{gauge,soft}} &= -\frac{1}{2}M_{\tilde{B}} \tilde{B} \tilde{B} - \frac{1}{2}M_{\tilde{W}} \left(\tilde{W}^+ \tilde{W}^- + \tilde{W}^- \tilde{W}^+ + \tilde{W}^0 \tilde{W}^0 \right) - \frac{1}{2}M_{\tilde{g}} \tilde{g}^a \tilde{g}^a + \text{h.c.} \\
&\quad -\frac{1}{2}M'_{\tilde{B}} \tilde{B}' \tilde{B}' - \frac{1}{2}M'_{\tilde{W}} \left(\tilde{W}'^+ \tilde{W}'^- + \tilde{W}'^- \tilde{W}'^+ + \tilde{W}'^0 \tilde{W}'^0 \right) - \frac{1}{2}M'_{\tilde{g}} \tilde{g}'^a \tilde{g}'^a + \text{h.c.} \\
&\quad -m_Y^2 |\sigma_Y^0|^2 - \frac{1}{2} (m_Y'^2 (\sigma_Y^0)^2 + \text{h.c.}) - m_I^2 |\sigma_I^j|^2 - \frac{1}{2} (m_I'^2 (\sigma_I^j)^2 + \text{h.c.}) \\
&\quad -m_C^2 |\sigma_C^a|^2 - \frac{1}{2} (m_C'^2 (\sigma_C^a)^2 + \text{h.c.}) , \tag{2.11}
\end{aligned}$$

$$\begin{aligned}
\mathcal{L}_{\text{Higgs,soft}} &= -m_{H_u}^2 \left(|H_u^+|^2 + |H_u^0|^2 \right) - m_{H_d}^2 \left(|H_d^-|^2 + |H_d^0|^2 \right) \\
&\quad - [B_\mu (H_u^+ H_d^- - H_u^0 H_d^0) + \text{h.c.}] \\
&\quad - [A_Y \lambda_Y \sigma_Y^0 (H_u^+ H_d^- - H_u^0 H_d^0) + A_I \lambda_I \sigma_I^i (H_u \cdot \tau^i H_d) + \text{h.c.}] , \tag{2.12}
\end{aligned}$$

with i and a being the $SU(2)_I$ and $SU(3)_C$ indices, τ^i the Pauli matrices, and moreover,

$$\begin{aligned}
\mathcal{L}_{\text{matter,soft}} &= - \left(m_Q^2 \right)_{ij} \left(\tilde{u}_{iL}^* \tilde{u}_{jL} + \tilde{d}_{iL}^* \tilde{d}_{jL} \right) - \left(m_u^2 \right)_{ij} \tilde{u}_{iR}^* \tilde{u}_{jR} - \left(m_d^2 \right)_{ij} \tilde{d}_{iR}^* \tilde{d}_{jR} \\
&\quad - \left(m_L^2 \right)_{ij} \left(\tilde{\nu}_{iL}^* \tilde{\nu}_{jL} + \tilde{e}_{iL}^* \tilde{e}_{jL} \right) - \left(m_e^2 \right)_{ij} \tilde{e}_{iR}^* \tilde{e}_{jR} \\
&\quad - (A_u f_u)_{ij} \tilde{u}_{iR}^* (\tilde{d}_{jL} H_u^+ - \tilde{u}_{jL} H_u^0) - (A_d f_d)_{ij} \tilde{d}_{iR}^* (\tilde{u}_{jL} H_d^- - \tilde{d}_{jL} H_d^0) + \text{h.c.} \\
&\quad - (A_e f_e)_{ij} \tilde{e}_{iR}^* (\tilde{\nu}_{jL} H_d^- - \tilde{e}_{jL} H_d^0) + \text{h.c.} , \tag{2.13}
\end{aligned}$$

with i, j now denoting the matter generations. Here, the convention is adopted to use subscripts C, I, Y for parameters corresponding to color, isospin and hypercharge gauge groups, respectively. Capitalized mass parameters M are the Majorana gaugino masses [M^D for Dirac], while lower-case m denotes soft scalar masses. The Majorana mass terms, $M'_{\tilde{B}}$, $M'_{\tilde{W}}$ and $M'_{\tilde{g}}$, for the new gauge adjoint fermions are soft $N=1$ SUSY breaking parameters and add to the Majorana mass parameters, M_Y, M_I and M_C , introduced in Eq. (2.4) as part of the $N=1$ supersymmetric superpotential.

From this set of actions and Lagrangians, and after eliminating the auxiliary D^a fields through their equations of motion, the masses and mixings of the Higgs and gauge-adjoint scalar particles and their interactions can be read off, and correspondingly those of their superpartners as will be detailed below. The final form of the Lagrangians are collected in the following list which, in general, includes only interactions of the new fields:¹

(i) $SU(3)_C \times SU(2)_I \times U(1)_Y$ gauge boson/sigma sector:

The gauge interactions of the adjoint sigma fields are determined from the scalar kinetic term $(D_\mu \sigma)^\dagger (D^\mu \sigma)$ with the covariant derivative $D_\mu = \partial_\mu + ig_s T^a g_\mu^a + ig T^i W_\mu^i$. In addition to their kinetic terms, the term generates the Lagrangian for the derivative three-point and seagull four-point interaction terms:

$$\mathcal{L}_{\sigma_C, \text{gauge}} = -g_s f^{abc} g_\mu^a (\sigma_C^{b*} \overleftrightarrow{\partial}^\mu \sigma_C^c) + g_s^2 f^{ace} f^{bde} g_\mu^a g^{\mu b} \sigma_C^{*c} \sigma_C^d , \tag{2.14}$$

$$\mathcal{L}_{\sigma_I, \text{gauge}} = -g \epsilon_{ijk} W_\mu^i (\sigma_I^{j*} \overleftrightarrow{\partial}^\mu \sigma_I^k) + g^2 \epsilon_{ikm} \epsilon_{jlm} W_\mu^i W^{\mu j} \sigma_I^{*k} \sigma_I^l , \tag{2.15}$$

where f^{abc} and ϵ_{ijk} are the $SU(3)_C$ and $SU(2)_I$ structure constants, respectively, and $A \overleftrightarrow{\partial}^\mu B \equiv A \partial^\mu B - (\partial^\mu A) B$.

¹ Many of the mass parameters and couplings defining the $N=1/N=2$ hybrid model can be complex in general. Nevertheless, for the sake of simplicity all the parameters are assumed to be real throughout this paper.

(ii) $SU(3)_C$ sfermion/gaugino/sigma sector:

The interaction Lagrangian of the sigma field σ_C with the squarks is given by

$$\mathcal{L}_{\sigma_C(\sigma_C)\tilde{q}\tilde{q}} = -\sqrt{2}g_s M_C^D (\sigma_C^a + \sigma_C^{a*}) \left(\tilde{q}_L^* \frac{\lambda^a}{2} \tilde{q}_L - \tilde{q}_R^* \frac{\lambda^a}{2} \tilde{q}_R \right) + i g_s^2 f^{abc} \sigma_C^{a*} \sigma_C^b \tilde{q}^\dagger \frac{\lambda^c}{2} \tilde{q}, \quad (2.16)$$

where λ^a ($a = 1-8$) are the Gell-Mann matrices. Therefore, the L - and R -chiral squarks contribute with opposite signs as demanded by the general form of the super-QCD D -terms. On the other hand, the interactions of the two gluino fields, \tilde{g} and \tilde{g}' , with the $SU(3)_C$ sigma field σ_C and with the squark and quark fields are described by the Lagrangians:

$$\mathcal{L}_{\tilde{g}\tilde{g}'\sigma_C} = -\sqrt{2}i g_s f^{abc} \overline{\tilde{g}_L^a} \tilde{g}_R^b \sigma_C^c + \text{h.c.}, \quad (2.17)$$

$$\mathcal{L}_{\tilde{g}\tilde{q}\tilde{q}} = -\sqrt{2}g_s \left(\overline{\tilde{q}_L} \frac{\lambda^a}{2} \tilde{g}_R^a \tilde{q}_L - \overline{\tilde{q}_R} \frac{\lambda^a}{2} \tilde{g}_L^a \tilde{q}_R \right) + \text{h.c.}, \quad (2.18)$$

Only the standard gluino couples to squark fields since, as required by $N=2$ supersymmetry, the new gluino \tilde{g}' couples only to mirror matter fields, which in the hybrid model are assumed to be absent.

(iii) $SU(2)_I \times U(1)_Y$ sfermion/gaugino/sigma sector:

In the weak basis, the R -chiral sfermions \tilde{f}_R are $SU(2)_I$ singlets so that only the L -chiral sfermions \tilde{f}_L interact with the $SU(2)_I$ sigma field σ_I through the interaction Lagrangians:

$$\mathcal{L}_{\sigma_I(\sigma_I)\tilde{f}\tilde{f}} = -\sqrt{2}g M_I^D (\sigma_I^i + \sigma_I^{i*}) \tilde{f}_L^\dagger \frac{\tau^i}{2} \tilde{f}_L + i g^2 \epsilon_{ijk} \sigma_I^{j*} \sigma_I^k \tilde{f}_L^\dagger \frac{\tau^i}{2} \tilde{f}_L, \quad (2.19)$$

where \tilde{f}_L is any matter $SU(2)_I$ -doublet field. On the other hand, the Lagrangians governing the interactions of the winos, \tilde{W} and \tilde{W}' , with the $SU(2)_I$ sigma field σ_I and the (s)fermion fields are given by

$$\mathcal{L}_{\sigma_I\tilde{W}\tilde{W}'} = -\sqrt{2}i g \epsilon^{ijk} \overline{\tilde{W}_L^i} \tilde{W}_R^j \sigma_I^k + \text{h.c.}, \quad (2.20)$$

$$\mathcal{L}_{\tilde{W}\tilde{f}\tilde{f}} = -\sqrt{2}g \overline{\tilde{f}_L} \frac{\tau^i}{2} \tilde{W}_R^i \tilde{f}_L + \text{h.c.}. \quad (2.21)$$

Only the L -chiral sfermions \tilde{f}_L couple to the standard wino \tilde{W} .

The $U(1)_Y$ sigma field σ_Y is essentially a SM singlet state with no tree-level gauge interaction to any of the gauge bosons, gauginos and higgsinos. The singlet scalar field couples only to the Higgs bosons and the (s)fermion fields, with the latter being given by the Lagrangian:

$$\mathcal{L}_{\sigma_Y\tilde{f}\tilde{f}} = -\sqrt{2}g' M_Y^D (\sigma_Y^0 + \sigma_Y^{0*}) (Y_{f_L} |\tilde{f}_L|^2 - Y_{f_R} |\tilde{f}_R|^2), \quad (2.22)$$

and the standard bino \tilde{B} (but not the new bino \tilde{B}') couples to the (s)fermion fields through the interaction Lagrangian:

$$\mathcal{L}_{\tilde{B}\tilde{f}\tilde{f}} = -\sqrt{2}g' (Y_{f_L} \overline{\tilde{f}_L} \tilde{B}_R \tilde{f}_L - Y_{f_R} \overline{\tilde{f}_R} \tilde{B}_L \tilde{f}_R) + \text{h.c.}, \quad (2.23)$$

where Y_{f_L} and Y_{f_R} are the hypercharges of the L -chiral and R -chiral fermions, f_L and f_R , respectively.

(iv) $SU(2)_I \times U(1)_Y$ higgsino/sigma sector:

The superpotential (2.9) coupling the new $SU(2)_I \times U(1)_Y$ chiral superfields with the Higgs hypermultiplets leads to Yukawa-type interactions of the electroweak sigma fields with the higgsino fields. In the weak basis, the interactions are described by the Lagrangian

$$\begin{aligned} \mathcal{L}_{\sigma\tilde{H}\tilde{H}} = & -\lambda_Y \sigma_Y^0 (\overline{\tilde{H}_{uR}^-} \tilde{H}_{dL}^- - \overline{\tilde{H}_{uR}^0} \tilde{H}_{dL}^0) + \lambda_I \sigma_I^0 (\overline{\tilde{H}_{uR}^-} \tilde{H}_{dL}^- + \overline{\tilde{H}_{uR}^0} \tilde{H}_{dL}^0) + \text{h.c.} \\ & -\sqrt{2}\lambda_I (\sigma_1^- \overline{\tilde{H}_{uR}^-} \tilde{H}_{dL}^0 - \sigma_2^+ \overline{\tilde{H}_{uR}^0} \tilde{H}_{dL}^-) + \text{h.c.}, \end{aligned} \quad (2.24)$$

where we have introduced two charged scalars and one neutral scalar defined as

$$\sigma_1^- = \frac{1}{\sqrt{2}} (\sigma_I^1 + i\sigma_I^2), \quad \sigma_2^+ = \frac{1}{\sqrt{2}} (\sigma_I^1 - i\sigma_I^2), \quad \sigma_I^0 = \sigma_I^3, \quad (2.25)$$

with each of σ_I^i being complex.

Combining the above Lagrangian (2.24) with the Lagrangian (2.20) for the interactions of the sigma fields with gauginos will enable us to derive the vertices for the interactions of the sigma fields with charginos and neutralinos in the mass eigenstate basis.

(v) $SU(2)_I \times U(1)_Y$ Higgs/sigma sector :

The potential for the neutral and charged electroweak Higgs and scalar fields receives contributions from three different sources: the gauge kinetic terms, the superpotential, and the soft-breaking terms. Complementing the neutral field interactions noted in Ref. [15] by the charged fields, the potential $V_{\sigma H}$ for the charged and neutral electroweak Higgs and adjoint scalars can be written as a sum over four characteristic contributions:

$$V_{\sigma H|1} = m_{H_u}^2 (|H_u^+|^2 + |H_u^0|^2) + m_{H_d}^2 (|H_d^0|^2 + |H_d^-|^2) + [B_\mu (H_u^+ H_d^- - H_u^0 H_d^0) + \text{h.c.}], \quad (2.26)$$

$$\begin{aligned} V_{\sigma H|2} = & \frac{1}{2} [\sqrt{2} M_Y^D (\sigma_Y^0 + \sigma_Y^{0*}) + \frac{1}{2} g' (|H_u^+|^2 - |H_d^-|^2 + |H_u^0|^2 - |H_d^0|^2)]^2 \\ & + \frac{1}{2} |2M_I^D (\sigma_1^+ + \sigma_2^+) + \sqrt{2} g (\sigma_1^+ \sigma_I^0 - \sigma_2^+ \sigma_I^{0*}) + g (H_u^+ H_u^{0*} + H_d^0 H_d^+)|^2 \\ & + \frac{1}{2} [\sqrt{2} M_I^D (\sigma_I^0 + \sigma_I^{0*}) + g (|\sigma_2^+|^2 - |\sigma_1^-|^2) + \frac{1}{2} g (|H_u^+|^2 - |H_d^-|^2 - |H_u^0|^2 + |H_d^0|^2)]^2, \end{aligned} \quad (2.27)$$

$$\begin{aligned} V_{\sigma H|3} = & |(\mu + \lambda_Y \sigma_Y^0 - \lambda_I \sigma_I^0) H_d^- + \sqrt{2} \lambda_I \sigma_1^- H_d^0|^2 + |(\mu + \lambda_Y \sigma_Y^0 - \lambda_I \sigma_I^0) H_u^+ - \sqrt{2} \lambda_I \sigma_2^+ H_u^0|^2 \\ & + |(\mu + \lambda_Y \sigma_Y^0 + \lambda_I \sigma_I^0) H_d^0 + \sqrt{2} \lambda_I \sigma_2^+ H_d^-|^2 + |(\mu + \lambda_Y \sigma_Y^0 + \lambda_I \sigma_I^0) H_u^0 - \sqrt{2} \lambda_I \sigma_1^- H_u^+|^2 \\ & + |M_Y \sigma_Y^0 + \lambda_Y (H_u^+ H_d^- - H_u^0 H_d^0)|^2 + |M_I \sigma_I^0 - \lambda_I (H_u^+ H_d^- + H_u^0 H_d^0)|^2 \\ & + |M_I \sigma_1^- - \sqrt{2} \lambda_I H_u^0 H_d^-|^2 + |M_I \sigma_2^+ + \sqrt{2} \lambda_I H_u^+ H_d^0|^2, \end{aligned} \quad (2.28)$$

$$\begin{aligned} V_{\sigma H|4} = & m_Y^2 |\sigma_Y^0|^2 + m_I^2 (|\sigma_I^0|^2 + |\sigma_1^-|^2 + |\sigma_2^+|^2) + \frac{1}{2} (m_Y^2 (\sigma_Y^0)^2 + \text{h.c.}) + \frac{1}{2} [m_I^2 ((\sigma_I^0)^2 + 2\sigma_2^+ \sigma_1^-) + \text{h.c.}] \\ & + A_Y \lambda_Y \sigma_Y^0 (H_u^+ H_d^- - H_u^0 H_d^0) - A_I \lambda_I \sigma_I^0 (H_u^+ H_d^- + H_u^0 H_d^0) + \text{h.c.} \\ & + \sqrt{2} A_I \lambda_I (\sigma_1^- H_u^+ H_d^0 - \sigma_2^+ H_d^- H_u^0) + \text{h.c.} \end{aligned} \quad (2.29)$$

After shifting the neutral fields by their vacuum expectation values, the physical scalar masses and the tri- and quadri-linear interaction vertices can be read off.

2.2. Masses, Mixings and Dirac Fields

Introducing the vacuum expectation values of the scalar/Higgs fields in the Lagrangians of the previous subsection, their values are determined by the absence of terms linear in the fields, while from the terms bi-linear in the fields the mass matrices for the scalars/Higgs, the charginos and neutralinos can be read off. The vacuum expectation values (*vevs*) of the neutral Higgs and the neutral sigma fields² are defined as

$$\langle H_{u/d}^0 \rangle = \frac{1}{\sqrt{2}} v_{u/d}, \quad (2.30)$$

$$\langle \sigma_{Y/I}^0 \rangle = \frac{1}{\sqrt{2}} v_{Y/I}. \quad (2.31)$$

² Throughout the paper, we restrict ourselves to the case of a CP preserving and neutral vacuum with real vacuum expectation values.

As usual, the $vevs$ of the Higgs sector can be rewritten as

$$v = \sqrt{v_u^2 + v_d^2} \quad \text{and} \quad \tan \beta = \frac{v_u}{v_d}. \quad (2.32)$$

The masses of the electroweak vector bosons W, Z are generated by the interactions of the fields with the ground states of the neutral Higgs H_u^0, H_d^0 and the neutral scalar iso-triplet field σ_I^0 (while the hyper-singlet field σ_Y^0 does not couple)

$$m_Z^2 = \frac{1}{4}(g'^2 + g^2)v^2, \quad m_W^2 = \frac{1}{4}g^2v^2 + g^2v_I^2. \quad (2.33)$$

The iso-triplet vev shifts the tree-level ρ -parameter away from unity by the amount

$$\Delta\rho = \rho - 1 = 4v_I^2/v^2. \quad (2.34)$$

Allowing a maximum value $\Delta\rho \leq 10^{-3}$ for the shift [22], it turns out that the vacuum expectation value of the iso-triplet field must be very small, $v_I \leq 3$ GeV, *cf.* [15]. We will assume that the soft supersymmetry breaking scalar σ_I mass parameter m_I of order TeV drives v_I to the small value. As a result, the Higgs vev is close to the standard value $v = 246$ GeV, and $\tan \beta$ may be identified approximately with the corresponding MSSM parameter. And while almost any value for v_Y is phenomenologically quite consistent, a large m_Y would drive v_Y to small values.

1. Charginos

Defining the current bases, $\{\tilde{W}'_R^+, \tilde{W}_R^+, \tilde{H}_{uR}^+\}$ and $\{\tilde{W}'_L^-, \tilde{W}_L^-, \tilde{H}_{dL}^-\}$ for the two charged winos and the charged higgsino, the chargino mass matrix can be written as

$$\mathcal{M}_C = \begin{pmatrix} M'_2 & M_2^D - gv_I & -\lambda_I v_u \\ M_2^D + gv_I & M_2 & \frac{1}{\sqrt{2}}gv_d \\ \lambda_I v_d & \frac{1}{\sqrt{2}}gv_u & \mu_c \end{pmatrix}, \quad (2.35)$$

where

$$M_2 = M_{\tilde{W}}, \quad M'_2 = M'_{\tilde{W}} + M_I, \quad M_2^D = M_I^D \quad \text{and} \quad \mu_c = \mu + (\lambda_Y v_Y - \lambda_I v_I)/\sqrt{2}. \quad (2.36)$$

Three charginos, *i. e.* one degree of freedom more than in MSSM and related iso-singlet extensions like NMSSM or USSM, are predicted in the general $N=1/N=2$ hybrid model, labeled $\tilde{\chi}_1^\pm, \tilde{\chi}_2^\pm, \tilde{\chi}_3^\pm$ (ultimately for ascending mass values). The MSSM case is reached in the limit $M'_2 \rightarrow -\infty$ which corresponds to infinitely heavy \tilde{W}' . By raising the magnitude of the \tilde{W}' gaugino mass parameter M'_2 from $-\infty$ to 0 and lowering at the same time M_2 to 0 the Dirac limit is obtained. Though the 3×3 mass matrix can be diagonalized analytically for arbitrary parameters, we study instead the evolution of the eigenvalues analytically in the limit of small couplings, and numerically by varying $-\infty \leq M'_2 \leq 0$ from the MSSM to the Dirac limit.

For small gaugino/higgsino mixings in the area where the supersymmetry mass parameters M'_2, M_2, M_I^D, μ [and the size of their mutual differences] are much larger than the electroweak parameter v , the eigenvalues and mixing parameters can be calculated easily. This approximation leaves us with one higgsino mass eigenvalue

$$\overline{m}_3^\pm = \mu_c, \quad (2.37)$$

and a 2×2 gaugino mass submatrix with two eigenvalues

$$\overline{m}_{1,2}^\pm = \frac{1}{2}|\gamma_2 \mp \delta_2| \quad \text{where} \quad \gamma_2 = \sqrt{(M'_2 + M_2)^2 + 4g^2v_I^2} \quad \text{and} \quad \delta_2 = \sqrt{(M'_2 - M_2)^2 + 4(M_I^D)^2}, \quad (2.38)$$

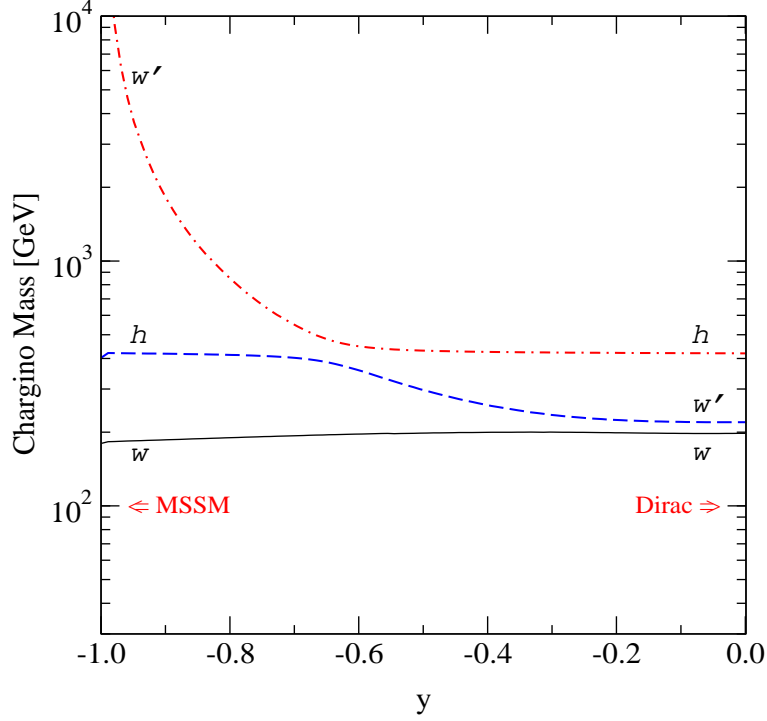


Figure 1: Evolution of the chargino masses as a function of the control parameter y from the MSSM doublet ($y = -1$) to the Dirac ($y = 0$) triplet along the path \mathcal{P}_C in Eq. (2.42) for $m = 200$ GeV, $\tan\beta = 5$, $v_I = v_Y = 3$ GeV and the $N=2$ values for the couplings $\lambda_{Y,I}$ in Eq. (2.10).

and the two mixing angles for the positive and negative states

$$\cos\theta_{\pm} \equiv c_{\pm} = \frac{1}{\sqrt{2}} \sqrt{1 - (M_2^{\prime 2} - M_2^2 \mp 4gv_I M_2^D)/\gamma_2 \delta_2}, \quad (2.39)$$

$$\sin\theta_{\pm} \equiv s_{\pm} = \frac{1}{\sqrt{2}} \sqrt{1 + (M_2^{\prime 2} - M_2^2 \mp 4gv_I M_2^D)/\gamma_2 \delta_2}, \quad (2.40)$$

With $M_2' = -\infty$ in the MSSM limit we get $c_{\pm} = 0$ and $s_{\pm} = 1$, while $c_+ = s_- = 1$ and $c_- = s_+ = 0$ in the Dirac limit with $M_2' = M_2 = 0$ and $M_2^D, v_I > 0$.

Switching on the weak couplings among the gaugino and higgsino sectors, the chargino mass eigenvalues and the mixing parameters derived from

$$\mathcal{M}_C^{\text{diag}} = U_+^T \mathcal{M}_C U_-, \quad (2.41)$$

can be calculated analytically in simple form.³ The results are presented in Appendix C.

In analogy to the color sector in Ref. [7] we study the evolution of the eigenvalues in Fig. 1 numerically by varying the mass parameters along the path

$$\begin{aligned} \mathcal{P}_C : \quad M_2' &= my/(1+y), \\ M_2 &= -my, \\ M_2^D &= m, \\ \mu &= 2m, \end{aligned} \quad (2.42)$$

³ In Appendix A we provide an analytic prescription for the singular value decomposition of a general 2×2 matrix and in Appendix B the small-mixing approximation.

for a fixed value of $m = 200$ GeV with the control parameter $-1 \leq y \leq 0$ running from the MSSM [$y = -1$] to the Dirac limit [$y = 0$]. This set corresponds to mass parameters giving rise to $m_{\tilde{\chi}_1^\pm} \approx m$ (fixed), $m_{\tilde{\chi}_2^\pm} \approx m[y + 1/(1 + y)]$, moving from ∞ to m , and $m_{\tilde{\chi}_3^\pm} \approx \mu$ (fixed) in the decoupled wino and higgsino sectors and for very small v_I . The other parameters in the chargino mass matrix (2.35) are chosen as $\tan \beta = 5$, $v_I = v_Y = 3$ GeV and the $N=2$ values for the couplings $\lambda_{Y,I}$ are adopted.

For the parameters chosen, the descending order of the physical masses in the figure reflects, in obvious notation, the pattern $w' \gg h > w$ in the MSSM limit. At some medium y , the states w' and h cross over to $h > w'$, keeping the ordering $h > w' > w$ until the Dirac limit is reached. The physical masses in the cross-over zone of the states w' and h cannot be described by the standard analytical expansion applied above. They must either be obtained numerically or by analytical expansions tailored specifically for cross-over phenomena, see Ref. [23].

2. Neutralinos

Six neutral electroweak Majorana fields are incorporated in the $N=1/N=2$ hybrid model. The mass matrix can be extracted from the bi-linear terms of the gaugino, gaugino' and higgsino fields in the Lagrangian of the preceding subsection, written in the current basis $\{\tilde{B}', \tilde{B}, \tilde{W}'^0, \tilde{W}^0, \tilde{H}_u^0, \tilde{H}_d^0\}$ as

$$\mathcal{M}_N = \begin{pmatrix} M'_1 & M_1^D & 0 & 0 & -\frac{1}{\sqrt{2}}\lambda_Y v_d & -\frac{1}{\sqrt{2}}\lambda_Y v_u \\ M_1^D & M_1 & 0 & 0 & \frac{1}{2}g'v_u & -\frac{1}{2}g'v_d \\ 0 & 0 & M'_2 & M_2^D & -\frac{1}{\sqrt{2}}\lambda_I v_d & -\frac{1}{\sqrt{2}}\lambda_I v_u \\ 0 & 0 & M_2^D & M_2 & -\frac{1}{2}g v_u & \frac{1}{2}g v_d \\ -\frac{1}{\sqrt{2}}\lambda_Y v_d & \frac{1}{2}g'v_u & -\frac{1}{\sqrt{2}}\lambda_I v_d & -\frac{1}{2}g v_u & 0 & -\mu_n \\ -\frac{1}{\sqrt{2}}\lambda_Y v_u & -\frac{1}{2}g'v_d & -\frac{1}{\sqrt{2}}\lambda_I v_u & \frac{1}{2}g v_d & -\mu_n & 0 \end{pmatrix}, \quad (2.43)$$

where

$$M_1 = M_{\tilde{B}}, \quad M'_1 = M'_{\tilde{B}} + M_Y, \quad M_1^D = M_Y^D, \quad \mu_n = \mu + (\lambda_Y v_Y + \lambda_I v_I)/\sqrt{2}. \quad (2.44)$$

and M_2, M'_2 are defined in Eq. (2.36). This 6×6 mass matrix is diagonalized by the unitary transformation

$$\mathcal{M}_N^{\text{diag}} = U_N^T \mathcal{M}_N U_N. \quad (2.45)$$

Six neutralinos, *i.e.* two degrees of freedom more than in MSSM, are predicted in the general $N=1/N=2$ hybrid model, labeled $\tilde{\chi}_{1\dots 6}^0$ (ordered according to ascending mass values). They evolve from the MSSM by raising the magnitude of the gaugino mass parameters $M'_{1,2}$ from $-\infty$ to finally 0 in the Dirac limit.

In general, the diagonalization of the 6×6 neutralino mass matrix cannot be carried out in analytic form. However, as before, in the limit in which the supersymmetry masses are much larger than the electroweak scale, approximate solutions can be found analytically. First switching off the electroweak mixings among the bino, wino and higgsino sectors leaves us with two bino mass eigenvalues, two wino mass eigenvalues and two higgsino mass eigenvalues:

$$\overline{m}_{1,2}^0 = \frac{1}{2} ||M_1 + M'_1| \mp \delta_1|, \quad (2.46)$$

$$\overline{m}_{3,4}^0 = \frac{1}{2} ||M_2 + M'_2| \mp \delta_2|, \quad (2.47)$$

$$\overline{m}_{5,6}^0 = \mu, \quad (2.48)$$

with $\delta_{1,2} = \sqrt{(M'_{1,2} - M_{1,2})^2 + 4(M_{1,2}^D)^2}$, and the block-diagonal mixing matrix

$$\overline{U}_N = \text{diag}(\overline{U}_1, \overline{U}_2, \overline{U}_h) \quad \text{with} \quad \overline{U}_{1,2} = \begin{pmatrix} c_{1,2} & -is_{1,2} \\ s_{1,2} & ic_{1,2} \end{pmatrix} \quad \text{and} \quad \overline{U}_h = \begin{pmatrix} i/\sqrt{2} & -1/\sqrt{2} \\ i/\sqrt{2} & 1/\sqrt{2} \end{pmatrix}, \quad (2.49)$$

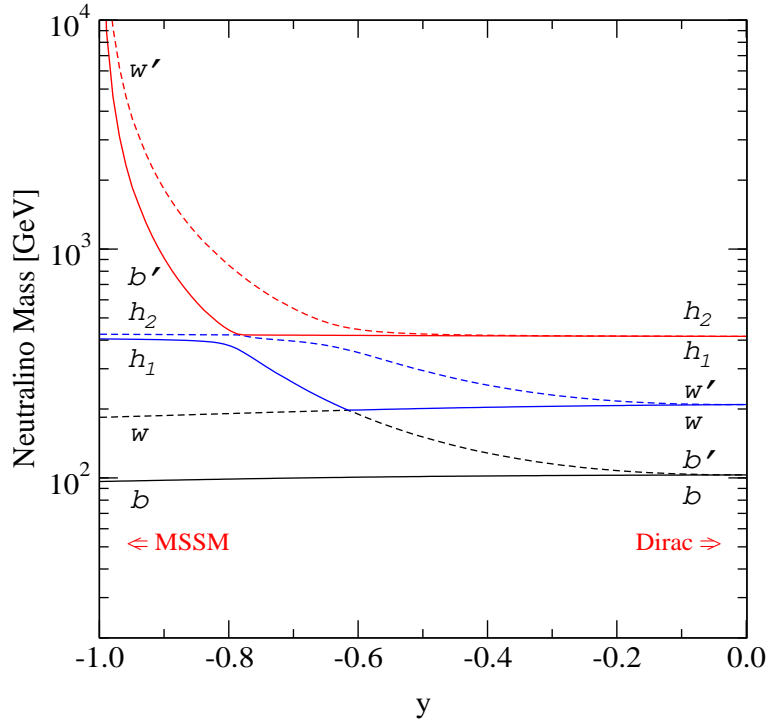


Figure 2: Evolution of the neutralino masses as a function of the control parameter y from the MSSM ($y = -1$) quartet to the Majorana sextet, merging to the Dirac triplet in the ($y = 0$) limit, for the same path (2.42) as in the chargino sector with bino/wino relations chosen as $M_1^{(D)}/M_2^{(D)} = 1/2$.

with the mixing angles $c_{1,2}/s_{1,2} = \sqrt{[1 \pm (M'_{1,2} - M_{1,2})/\delta_{1,2}]/2}$.

Switching on the weak couplings among the bino, wino gaugino sectors and the higgsino sector, the mass eigenvalues and mixing parameters are calculated using the block-diagonalization method described in Appendix B. The results of this procedure are relegated to Appendix C.

The numerical evolution of the neutralinos in the hybrid model is displayed in Fig. 2 as a function of the control parameter y for the same path and parameter set as in the chargino sector, Eq.(2.42), and supplemented by the bino/wino mass relations $M_1^{(D)} \approx M_2^{(D)}/2$, and setting $\tan\beta = 5$ and $v_I = v_Y = 3$ GeV.

The evolution of the neutralino masses follows the same pattern as the charginos, though being more complex due to the increased number of states. Starting from the mass pattern $w' > b' \gg h_1 \sim h_2 > w > b$ of the neutral states in the MSSM limit for the parameters chosen above, the first cross-over is observed for $b' \leftrightarrow h_1$, followed by $w' \leftrightarrow h_2$ and $b' \leftrightarrow w$ at roughly the same position. The mass system moves to the final pattern $h_1 = h_2 > w' = w > b' = b$ in the Dirac limit.

The transition from the Majorana to the Dirac theory in the limits M'_2, M_2 and $M'_1, M_1 \rightarrow 0$ can easily be studied by analyzing the mass matrix \mathcal{M}_N for vanishing gaugino/higgsino mixing. The eigenvalues of the matrix come in pairs of opposite signs: $\pm m_j$ for $j = 1, 2, 3$. The Majorana fields in each pair, denoted by $\tilde{\chi}_\pm$ according to the sign of the eigenvalue, can be combined to one Dirac field,

$$\tilde{\chi}_D = (\tilde{\chi}_+ + i\tilde{\chi}_-)/\sqrt{2}, \quad (2.50)$$

the superposition giving rise to vanishing contractions $\langle \tilde{\chi}_D \tilde{\chi}_D \rangle = 0$, as required for Dirac fields.

The \pm pairing of the eigenstates is not restricted to the hybrid neutralino mass matrix with vanishing gaugino/higgsino mixing but it is also realized if the gaugino/higgsino mixing is switched on and the couplings $\lambda_{Y,I}$ are

given by the $N=2$ relations, $\lambda_Y = -g'/\sqrt{2}$ and $\lambda_I = g/\sqrt{2}$ [15]. The key is the vanishing of the coefficients of odd powers of the eigenvalues in the characteristic eigenvalue equation:

$$\det(\mathcal{M}_N - m) = r_0 + r_2 m^2 + r_4 m^4 + r_6 m^6 = 0, \quad (2.51)$$

with the coefficients given by

$$\begin{aligned} r_6 &= 1, \\ r_4 &= -\frac{1}{2}\text{tr}(\mathcal{M}_N^2) = -[(M_Y^D)^2 + (M_I^D)^2 + \mu_n^2 + m_Z^2], \\ r_2 &= \frac{1}{8}[\text{tr}(\mathcal{M}_N^2)]^2 - \frac{1}{4}\text{tr}(\mathcal{M}_N^4) \\ &= (M_Y^D M_I^D)^2 + [(M_Y^D)^2 + (M_I^D)^2]\mu_n^2 + 2m_Z^2[(M_Y^D)^2 c_W^2 + 2(M_I^D)^2 s_W^2] - 2m_Z^2(M_Y^D s_W^2 + M_I^D c_W^2)\mu_n c_{2\beta} + m_Z^4, \\ r_0 &= -\frac{1}{48}[\text{tr}(\mathcal{M}_N^2)]^3 + \frac{1}{12}[\text{tr}(\mathcal{M}_N^3)]^2 + \frac{1}{8}\text{tr}(\mathcal{M}_N^4)\text{tr}(\mathcal{M}_N^2) - \frac{1}{6}\text{tr}(\mathcal{M}_N^6) \\ &= -(M_Y^D M_I^D \mu_n)^2 + 2m_Z^2 M_Y^D M_I^D \mu_n (M_Y^D c_W^2 + M_I^D s_W^2) c_{2\beta} - m_Z^4 (M_Y^D c_W^2 + M_I^D s_W^2)^2. \end{aligned} \quad (2.52)$$

The odd coefficients r_{2j+1} are linear in traces of odd powers of \mathcal{M}_N which vanish. While this is obvious for $\text{tr}(\mathcal{M}_N)$ in the Dirac limit $M_{1,2}, M'_{1,2} \rightarrow 0$, it can easily be proven also for odd powers of the mass matrix if the submatrix that mixes the mass submatrix of the gauginos with the mass submatrix of the higgsinos is orthogonal. This is satisfied in Eq. (2.43), a sufficient [but not necessary] condition for orthogonality being the $N=2$ symmetry of the basic Lagrangian.

If the lightest neutralino is the lightest supersymmetric particle (LSP) and stable, its Dirac or Majorana nature has important consequences for cold dark matter phenomenology. This is most clearly seen by inspecting, for example, the neutralino annihilation cross section into an electron-positron pair in the MSSM and Dirac limits. Assuming for simplicity a pure bino-type MSSM neutralino state $\tilde{\chi}_1^0 = \tilde{B}^0$, we obtain

$$\begin{aligned} \frac{d\sigma}{d\cos\theta}[\tilde{\chi}_1^0 \tilde{\chi}_1^0 \rightarrow e^- e^+] &= \frac{\pi^2 \alpha}{16 c_W^2 s} \beta^3 \left[\frac{\eta_{1L}^2 + (\eta_{1L}^2 - 4\eta_{1L} + 2 - \beta^2) \cos^2 \theta + \beta^2 \cos^4 \theta}{(\eta_{1L}^2 - \beta^2 \cos^2 \theta)^2} \right. \\ &\quad \left. + 16 \frac{\eta_{1R}^2 + (\eta_{1R}^2 - 4\eta_{1R} + 2 - \beta^2) \cos^2 \theta + \beta^2 \cos^4 \theta}{(\eta_{1R}^2 - \beta^2 \cos^2 \theta)^2} \right], \end{aligned} \quad (2.53)$$

due to the t - and u -channel L - and R -chiral selectron exchange where $c_W = \cos\theta_W$, θ is the c.m. scattering angle, $\beta = (1 - 4m_{\tilde{\chi}_1^0}^2/s)^{1/2}$ and $\eta_{1L,R} = 1 + 2(m_{eL,R}^2 - m_{\tilde{\chi}_1^0}^2)/s$. On the other hand, in the Dirac theory with the pure bino-type Dirac neutralino state $\tilde{\chi}_{D1}^0 = \tilde{B}_L^0 + \tilde{B}_R^0$ we obtain for the annihilation cross section

$$\frac{d\sigma}{d\cos\theta}[\tilde{\chi}_{D1}^0 \tilde{\chi}_{D1}^{0c} \rightarrow e^- e^+] = \frac{\pi \alpha^2}{32 c_W^2 s} \beta \left[\frac{(1 - \beta \cos\theta)^2}{(\eta_{1L} - \beta \cos\theta)^2} + 16 \frac{(1 + \beta \cos\theta)^2}{(\eta_{1R} + \beta \cos\theta)^2} \right]. \quad (2.54)$$

In other words, in the limit of $\beta \rightarrow 0$, the annihilation cross section (2.53) in the MSSM shows a P -wave suppression behavior $\sim \beta^3$, while in the Dirac case, the cross section (2.54) shows only a S -wave suppression behavior $\sim \beta$. As a result, the P -wave suppression of the MSSM LSP annihilation cross sections requires a significant fine-tuning of the spectra to be consistent with the WMAP observations [24]. In contrast, the annihilation of Dirac gauginos into a fermion and anti-fermion pair has a non-vanishing S -wave contribution even in the limit of vanishing fermion masses. Thus, the annihilation to fermions does not require the chirality flip in the final state, giving rise to enhanced decay branching fractions to leptons. This opens the parameter space that fits the WMAP measurements [15, 17]. Moreover, in contrast to the Majorana case, Dirac gauginos with non-vanishing higgsino fraction can lead to spin-independent scattering cross sections off nuclei via the Z -boson exchange [18], thus significantly altering the prospects for dark matter detection experiments.

3. Scalar/Higgs Particles

The scalar/Higgs sector involves various components in the basic Lagrangian: terms derived from the $N=2$ Higgs-Higgs-scalar interactions, the superpotential, the D -terms and the soft breaking terms. Expanding the scalar/Higgs potential about the vacuum expectation values of the neutral fields, $v_{u/d}, v_{Y/I}$, linear and bi-linear terms of the physical fields associated with the masses are generated, while tri- and quadri-linear terms describe the self-interactions of the physical scalar/Higgs fields.

To stabilize the system, the coefficients of the linear terms must vanish; this condition connects the vacuum expectation values with the basic parameters of the Lagrangian:

$$\begin{aligned}
v_Y &= \frac{v^2}{4\tilde{m}_Y^2\tilde{m}_I^2 - \lambda_Y^2\lambda_I^2v^4} \left\{ 2\tilde{m}_I^2 \left[g'M_Y^D c_{2\beta} - \sqrt{2}\lambda_Y\mu + (M_Y + A_Y)\lambda_Y s_{2\beta}/\sqrt{2} \right] \right. \\
&\quad \left. + \lambda_Y\lambda_I v^2 \left[gM_I^D c_{2\beta} + \sqrt{2}\lambda_I\mu - (M_I + A_I)\lambda_I s_{2\beta}/\sqrt{2} \right] \right\} \\
&\sim \frac{v^2}{2\tilde{m}_Y^2} \left[g'M_Y^D c_{2\beta} - \sqrt{2}\lambda_Y\mu + (M_Y + A_Y)\lambda_Y s_{2\beta}/\sqrt{2} \right] \quad \text{for } \tilde{m}_{Y,I} \gg \lambda_{Y,I}v, \tag{2.55}
\end{aligned}$$

$$\begin{aligned}
v_I &= \frac{v^2}{4\tilde{m}_Y^2\tilde{m}_I^2 - \lambda_Y^2\lambda_I^2v^4} \left\{ 2\tilde{m}_Y^2 \left[-gM_I^D c_{2\beta} - \sqrt{2}\lambda_I\mu + (M_I + A_I)\lambda_I s_{2\beta}/\sqrt{2} \right] \right. \\
&\quad \left. - \lambda_Y\lambda_I v^2 \left[g'M_Y^D c_{2\beta} - \sqrt{2}\lambda_Y\mu + (M_Y + A_Y)\lambda_Y s_{2\beta}/\sqrt{2} \right] \right\} \\
&\sim -\frac{v^2}{2\tilde{m}_I^2} \left[gM_I^D c_{2\beta} + \sqrt{2}\lambda_I\mu - (M_I + A_I)\lambda_I s_{2\beta}/\sqrt{2} \right] \quad \text{for } \tilde{m}_{Y,I} \gg \lambda_{Y,I}v, \tag{2.56}
\end{aligned}$$

with the abbreviations $c_{2\beta} = \cos 2\beta$ and $s_{2\beta} = \sin 2\beta$, and

$$\tilde{m}_Y^2 = m_Y^2 + m_Y'^2 + M_Y^2 + 4(M_Y^D)^2 + \frac{1}{2}\lambda_Y^2v^2, \tag{2.57}$$

$$\tilde{m}_I^2 = m_I^2 + m_I'^2 + M_I^2 + 4(M_I^D)^2 + \frac{1}{2}\lambda_I^2v^2. \tag{2.58}$$

The Higgs *vevs* $v_{u,d}$ are determined by

$$\begin{aligned}
0 &= (m_{H_u}^2 + \mu^2)v_u - B_\mu v_d + \frac{1}{8}(g'^2 + g^2)(v_u^2 - v_d^2)v_u + \frac{1}{2}(\lambda_Y^2 + \lambda_I^2)v_u v_d^2 \\
&\quad + (\sqrt{2}\lambda_Y\mu + g'M_Y^D)v_Y v_u + (\sqrt{2}\lambda_I\mu - gM_I^D)v_I v_u \\
&\quad - \frac{1}{\sqrt{2}}(M_Y + A_Y)\lambda_Y v_Y v_d - \frac{1}{\sqrt{2}}(M_I + A_I)\lambda_I v_I v_d + \frac{1}{2}(\lambda_Y v_Y + \lambda_I v_I)^2 v_u, \tag{2.59}
\end{aligned}$$

$$\begin{aligned}
0 &= (m_{H_d}^2 + \mu^2)v_d - B_\mu v_u - \frac{1}{8}(g'^2 + g^2)(v_u^2 - v_d^2)v_d + \frac{1}{2}(\lambda_Y^2 + \lambda_I^2)v_d^2 v_u \\
&\quad + (\sqrt{2}\lambda_Y\mu - g'M_Y^D)v_Y v_d + (\sqrt{2}\lambda_I\mu + gM_I^D)v_I v_d \\
&\quad - \frac{1}{\sqrt{2}}(M_Y + A_Y)\lambda_Y v_Y v_u - \frac{1}{\sqrt{2}}(M_I + A_I)\lambda_I v_I v_u + \frac{1}{2}(\lambda_Y v_Y + \lambda_I v_I)^2 v_d, \tag{2.60}
\end{aligned}$$

after inserting the *vevs* $v_{Y,I}$ from Eq. (2.56). The values of $v_{u,d}$ and v_I can be determined phenomenologically in terms of the observables $\tan \beta$ and m_W^2, m_Z^2 , *vide* Eqs. (2.32) and (2.33).

The terms in the Lagrangian which are bi-linear in the fields build up the scalar/Higgs mass matrices. Decomposing the neutral fields into ground-state values, real and imaginary parts,

$$H_u^0 = \frac{1}{\sqrt{2}} [s_\beta(v+h) + c_\beta H + i(c_\beta A - s_\beta a)], \quad H_u^+ = c_\beta H^+ - s_\beta a^+, \tag{2.61}$$

$$H_d^0 = \frac{1}{\sqrt{2}} [c_\beta(v+h) - s_\beta H + i(s_\beta A + c_\beta a)], \quad H_d^- = s_\beta H^- + c_\beta a^-, \tag{2.62}$$

with the abbreviations $c_\beta = \cos \beta$ and $s_\beta = \sin \beta$, and

$$\sigma_Y^0 = \frac{1}{\sqrt{2}}(v_Y + s_Y + ia_Y), \quad (2.63)$$

$$\sigma_I^3 = \frac{1}{\sqrt{2}}(v_I + s_I + ia_I), \quad \sigma_I^1 = \frac{1}{\sqrt{2}}(\sigma_2^+ + \sigma_1^-), \quad \sigma_I^2 = \frac{i}{\sqrt{2}}(\sigma_2^+ - \sigma_1^-), \quad (2.64)$$

it can be ascertained that the matrix of the imaginary fields involves a massless Goldstone field a , and likewise the charged fields involve $a_G^\pm = [va^\pm + \sqrt{2}v_I(\sigma_1^\pm + \sigma_2^\pm)]/\sqrt{v^2 + 4v_I^2}$. These are absorbed to provide masses to the neutral and charged gauge bosons. The neutral fields h, H, s_Y, s_I are parity-even scalars while A, a_Y, a_I are parity-odd pseudoscalars; the charged fields H^\pm mix with the associated charged scalar fields $s_{1,2}^\pm$, defined later in Eq. (2.80). These elements build up the neutral pseudoscalar 3×3 mass matrix, the neutral scalar 4×4 mass matrix and the charged scalar 3×3 mass matrix:

(i) neutral pseudoscalars:

In the $\{A, a_Y, a_I\}$ basis, the 3×3 real and symmetric pseudoscalar mass matrix squared is given by

$$\mathcal{M}_P^2 = \begin{pmatrix} M_A^2 & -\frac{1}{\sqrt{2}}(M_Y - A_Y)\lambda_Y v & -\frac{1}{\sqrt{2}}(M_I - A_I)\lambda_I v \\ -\frac{1}{\sqrt{2}}(M_Y - A_Y)\lambda_Y v & \tilde{m}_Y'^2 & \frac{1}{2}\lambda_Y \lambda_I v^2 \\ -\frac{1}{\sqrt{2}}(M_I - A_I)\lambda_I v & \frac{1}{2}\lambda_Y \lambda_I v^2 & \tilde{m}_I'^2 \end{pmatrix}, \quad (2.65)$$

where

$$M_A^2 = 2 \left[B_\mu + \lambda_Y v_Y (M_Y + A_Y)/\sqrt{2} + \lambda_I v_I (M_I + A_I)/\sqrt{2} \right] / s_{2\beta}, \quad (2.66)$$

$$\tilde{m}_Y'^2 = m_Y^2 - m_Y'^2 + M_Y^2 + \frac{1}{2}\lambda_Y^2 v^2, \quad (2.67)$$

$$\tilde{m}_I'^2 = m_I^2 - m_I'^2 + M_I^2 + \frac{1}{2}\lambda_I^2 v^2. \quad (2.68)$$

This matrix can easily be diagonalized in approximate form in the limit of the genuine supersymmetry parameters, $m_{Y,I}$ being much larger than the electroweak scale v , *i.e.* $v/m_{Y,I} \ll 1$. This leaves us with three approximately unmixed states with their masses

$$\overline{M}_{A_1}^2 = M_A^2, \quad \overline{M}_{A_2}^2 = \tilde{m}_Y'^2, \quad \overline{M}_{A_3}^2 = \tilde{m}_I'^2. \quad (2.69)$$

The expressions for the mass eigenvalues and mixing elements, when the weak coupling among the $\{A, a_Y, a_I\}$ states is retained, are given in Appendix C.

(ii) neutral scalars:

In the $\{h, H, s_Y, s_I\}$ basis, the real and symmetric 4×4 scalar mass matrix squared \mathcal{M}_S^2 is given by

$$\mathcal{M}_S^2 = \begin{pmatrix} m_Z^2 + \delta_H c_{2\beta} & \delta_H c_{2\beta} & -\frac{v_Y}{v}(2\tilde{m}_Y'^2 - \lambda_Y^2 v^2) & -\frac{v_I}{v}(2\tilde{m}_I'^2 - \lambda_I^2 v^2) \\ \delta_H c_{2\beta} & M_A^2 - \delta_H s_{2\beta} & \Delta_Y & \Delta_I \\ -\frac{v_Y}{v}(2\tilde{m}_Y'^2 - \lambda_Y^2 v^2) & \Delta_Y & \tilde{m}_Y'^2 & \frac{1}{2}\lambda_Y \lambda_I v^2 \\ -\frac{v_I}{v}(2\tilde{m}_I'^2 - \lambda_I^2 v^2) & \Delta_I & \frac{1}{2}\lambda_Y \lambda_I v^2 & \tilde{m}_I'^2 \end{pmatrix}, \quad (2.70)$$

where

$$\delta_H = [(\lambda_Y^2 + \lambda_I^2)v^2 - 2m_Z^2] s_{2\beta}/2, \quad (2.71)$$

$$\Delta_Y = g' M_Y^D v s_{2\beta} - \frac{1}{\sqrt{2}}\lambda_Y (M_Y + A_Y)v c_{2\beta}, \quad (2.72)$$

$$\Delta_I = -g M_I^D v s_{2\beta} - \frac{1}{\sqrt{2}}\lambda_I (M_I + A_I)v c_{2\beta}. \quad (2.73)$$

Note that δ_H vanishes in the $N=2$ SUSY limit. Thus, in this limit, the eigenvalues of the Higgs submatrix $\{h, H\}$ are just m_Z^2 and M_A^2 [20], with no dependence on $\tan \beta$, a feature markedly different from the MSSM. This submatrix

receives several radiative corrections, the most important one accruing from stop/top loops, due to their large Yukawa couplings. As a result, the Higgs submatrix is modified to

$$\begin{pmatrix} m_Z^2 + \delta_H s_{2\beta} & \delta_H c_{2\beta} \\ \delta_H c_{2\beta} & M_A^2 - \delta_H s_{2\beta} \end{pmatrix} \rightarrow \begin{pmatrix} m_Z^2 + \delta_H s_{2\beta} + \epsilon_H & \delta_H c_{2\beta} + \epsilon_H/t_\beta \\ \delta_H c_{2\beta} + \epsilon_H/t_\beta^2 & M_A^2 - \delta_H s_{2\beta} + \epsilon_H/t_\beta \end{pmatrix}, \quad (2.74)$$

where

$$\epsilon_H \simeq \frac{3G_F m_t^4}{\sqrt{2}\pi^2} \ln \frac{m_{\tilde{t}_1} m_{\tilde{t}_2}}{m_t^2}. \quad (2.75)$$

The transition from the current basis to the diagonal 2×2 Higgs matrix with eigenvalues

$$\overline{M}_{S_1}^2 \approx m_Z^2 + \delta_H s_{2\beta} + \epsilon_H - \frac{(\delta_H c_{2\beta} + \epsilon_H/t_\beta)^2}{M_A^2 - m_Z^2}, \quad (2.76)$$

$$\overline{M}_{S_2}^2 \approx M_A^2 - \delta_H s_{2\beta} + \epsilon_H/t_\beta^2 + \frac{(\delta_H c_{2\beta} + \epsilon_H/t_\beta)^2}{M_A^2 - m_Z^2}, \quad (2.77)$$

is carried out by an orthogonal transformation with the mixing element given by

$$\tan \theta_h = \frac{m_Z^2 + \delta_H s_{2\beta} + \epsilon_H - \overline{M}_{S_1}^2}{|\delta_H c_{2\beta} + \epsilon_H/t_\beta|}, \quad (2.78)$$

with $0 \leq \theta_h \leq \pi/2$.

In the limit of $m_{Y,I}$ being much larger than the electroweak scale v , the $\{s_Y, s_I\}$ submatrix leads to the two approximate mass eigenvalues

$$\overline{M}_{S_3}^2 = \tilde{m}_Y^2, \quad \overline{M}_{S_4}^2 = \tilde{m}_I^2. \quad (2.79)$$

The $\{h, H\}$ and $\{s_Y, s_I\}$ systems are weakly coupled at the order $v/M_A, v/m_{Y,I}$, and the block diagonalization allows to derive the results given in Appendix C.

(iii) charged scalars:

After the charged Goldstone bosons a_G^\pm are absorbed into the charged gauge bosons, there remain three physical charged scalar states $\{H^\pm, s_1^\pm, s_2^\pm\}$ with the second and third states defined by

$$s_1^\pm = (\sigma_1^\pm - \sigma_2^\pm)/\sqrt{2} \quad \text{and} \quad s_2^\pm = \frac{v(\sigma_1^\pm + \sigma_2^\pm)/\sqrt{2} - 2v_I a^\pm}{\sqrt{v^2 + 4v_I^2}}. \quad (2.80)$$

The real symmetric 3×3 charged scalar mass matrix squared $\mathcal{M}_{H^\pm}^2$ is then given in the $\{H^\pm, s_1^\pm, s_2^\pm\}$ basis by

$$\mathcal{M}_{H^\pm}^2 = \begin{pmatrix} \tilde{M}_{H^\pm}^2 & \Delta_\pm & -\sqrt{\rho} \Delta_I \\ \Delta_\pm & \tilde{m}_I'^2 + g^2 v_I^2 & \frac{1}{2}\sqrt{\rho} (\lambda_I^2 - \frac{1}{2}g^2) v^2 c_{2\beta} \\ -\sqrt{\rho} \Delta_I & \frac{1}{2}\sqrt{\rho} (\lambda_I^2 - \frac{1}{2}g^2) v^2 c_{2\beta} & \rho \tilde{m}_I^2 \end{pmatrix}, \quad (2.81)$$

where

$$\begin{aligned} \tilde{M}_{H^\pm}^2 &= M_A^2 + m_W^2 + \frac{1}{2}(\lambda_I^2 - \lambda_Y^2)v^2 - 4\frac{v_I^2}{v^2}\tilde{m}_I^2 + 4\lambda_I^2 v_I^2 - 4\sqrt{2}\mu_n \lambda_I v_I, \\ \Delta_\pm &= (g^2/2 - \lambda_I^2) v_I v s_{2\beta} - (M_I - A_I) \lambda_I v/\sqrt{2}, \end{aligned} \quad (2.82)$$

and Δ_I is introduced in Eq. (2.73). We note in passing that in the $N = \text{SUSY}$ scenario with $\lambda_I = g/\sqrt{2}$ the charged states $s_{1,2}^\pm$ do not mix.

Assuming that $\tilde{m}_I^2 > \tilde{m}_I'^2 > \tilde{M}_{H^\pm}^2$ and $M_I, A_I \sim M_A$, and observing that, again, the charged Higgs/scalar states are weakly coupled at the order of v/\tilde{m}_I or v/\tilde{m}_I' , the block-diagonalization procedure provides approximate solutions as given in Appendix C.

The extension of the Higgs sector by the novel $\text{SU}(2)_I \times \text{U}(1)_Y$ adjoint sigma fields has two important consequences:

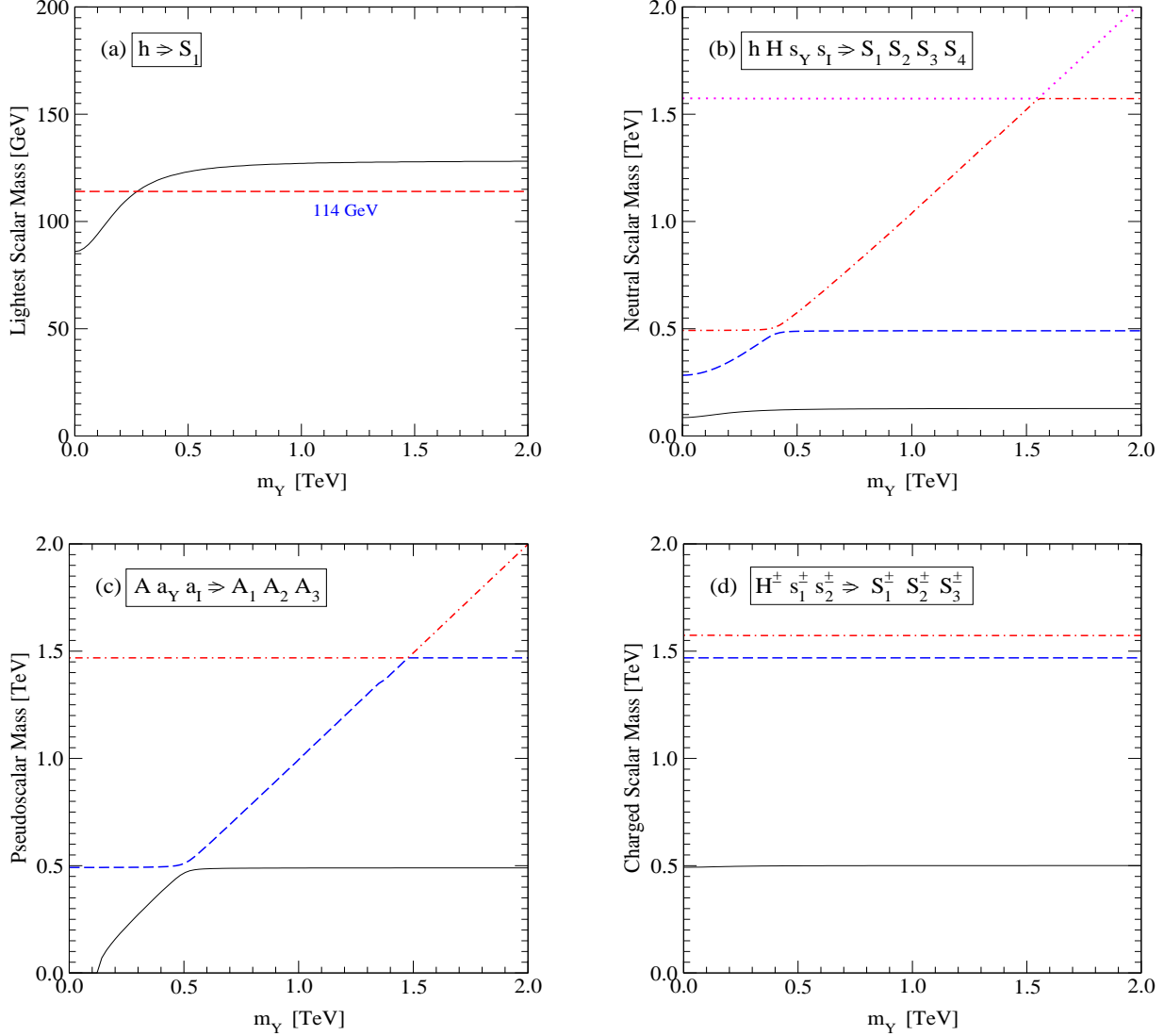


Figure 3: (a) The lightest neutral scalar boson including one-loop top/stop radiative corrections. The red dashed line indicates the present experimental lower bound on the mass $M_{S_1} \gtrsim 114$ GeV; (b) the neutral scalar masses; (c) the neutral pseudoscalar masses; (d) the charged scalar masses, as a function of the hypercharge soft scalar mass m_Y ; the isospin soft scalar mass is set to $m_I = 6v$ to accommodate the small ρ -parameter and the $N=2$ values for the couplings $\lambda_{Y,I}$ in Eq. (2.10) are adopted. The other parameters are fixed to $\tan \beta = 5$, $m_{\tilde{t}_1} = m_{\tilde{t}_2} = 1$ TeV, $M_A = 2v$, $m'_Y = M_Y^D = v/2$, $m'_I = M_I^D = \mu = v$, $A_Y = A_I = 2v$ and $M_Y = M_I = 0$ for Dirac gauginos.

- Each of the neutral pseudoscalar/scalar and charged sectors are extended by two new states with masses of the order of the characteristic scalar parameters m_Y and m_I . As a result, one of the new pseudoscalar/scalar states may acquire mass between a few hundred GeV up to several TeV, while the other will be heavy, *i.e.*, $\mathcal{O}(\text{TeV})$; both the new charged states will be heavy likewise.
- The mass matrix of the Higgs system is modified compared to the MSSM. As pointed out before, the tree-level Higgs masses are independent of the mixing parameter $\tan \beta$. In addition, the lower bound on the [lightest] charged Higgs mass is not guaranteed to exceed the W mass any more [experimentally of course, any charged Higgs boson with mass below ~ 100 GeV is excluded by direct searches [22].]

The tableau in Fig.3 illustrates the evolution of the three neutral pseudoscalar, four neutral scalar, and three

charged masses with the hyper-singlet mass parameter m_Y introduced in the soft SUSY breaking Lagrangian while all other parameters are kept fixed. These parameters have been chosen as indicated in the figure caption.

3. CHARACTERISTIC PHYSICAL PROCESSES

New colored particles like gluinos and squarks are expected to be generated, and detected, at the LHC for masses up to 2–3 TeV, and the strikingly different phenomenology of novel Dirac gluinos and colored adjoint scalars have been discussed in Refs. [7, 8]. In contrast, the mass window for generating non-colored states like charginos/neutralinos directly in quark-antiquark collisions is much smaller as a result of the small electroweak production cross sections. Cascade decays of colored states, however, provide a copious source of non-colored particles with large masses *i.e.* through the decay $\tilde{q} \rightarrow q + \tilde{\chi}$. Pair production of non-colored states at TeV e^+e^- and e^-e^- lepton colliders ILC/CLIC, on the other hand, gives access to the non-colored sector up to masses close to half the c.m. energy, *i.e.* about 0.5 TeV and 1.5 TeV at the ILC and CLIC, respectively, while non-colored adjoint scalars can be produced with high masses in $\gamma\gamma$ collisions. Without specifying the relative size of the masses of the new particles, a myriad of possible cascade decays would be predicted, which can, nevertheless, be analyzed phenomenologically by applying quite similar techniques. To present a transparent overview we, therefore, focus on representative chains in which sigma masses generally exceed the chargino/neutralino masses, as motivated already earlier.

3.1. Charginos and Neutralinos

Below, explicit formulae will be given for the $N=1$ MSSM and the $N=2$ Dirac limit, while scenarios interpolating between the MSSM and the Dirac limit could be obtained by summing up the two individual chargino/Majorana neutralino contributions after the proper diagonalization of the hyper-system.

In the hybrid theory, only the original $N=1$ chargino and neutralino fields couple to the matter fields. The analysis is simplified considerably by restricting ourselves to interactions with first and second generation (s)fermions. In this sector, which is most relevant experimentally, only the gauge components of charginos and neutralinos couple to the matter fields.

In the limit of large supersymmetry scales (in relation to the electroweak scale), the Dirac chargino fields and their charge conjugates are given by

$$\tilde{\chi}_{D1}^- = \tilde{W}'_{L-} + \tilde{W}'_{R-}, \quad \tilde{\chi}_{D1}^+ = -\tilde{W}'_{L+} - \tilde{W}'_{R+}, \quad (3.1)$$

$$\tilde{\chi}_{D2}^- = \tilde{W}'_{L-} + \tilde{W}'_{R-}, \quad \tilde{\chi}_{D2}^+ = -\tilde{W}'_{L+} - \tilde{W}'_{R+}, \quad (3.2)$$

$$\tilde{\chi}_{D3}^- = \tilde{H}'_{dL-} + \tilde{H}'_{uR-}, \quad \tilde{\chi}_{D3}^+ = \tilde{H}'_{uL+} + \tilde{H}'_{dR+}, \quad (3.3)$$

whereas the Dirac neutralino fields and their charge conjugates are

$$\tilde{\chi}_{D1}^0 = \tilde{B}'_L + \tilde{B}'_R, \quad \tilde{\chi}_{D1}^{0c} = -\tilde{B}'_L - \tilde{B}'_R, \quad (3.4)$$

$$\tilde{\chi}_{D2}^0 = \tilde{W}'_{L0} + \tilde{W}'_{R0}, \quad \tilde{\chi}_{D2}^{0c} = -\tilde{W}'_{L0} - \tilde{W}'_{R0}, \quad (3.5)$$

$$\tilde{\chi}_{D3}^0 = i(\tilde{H}'_{dL0} - \tilde{H}'_{uR0}), \quad \tilde{\chi}_{D3}^{0c} = i(\tilde{H}'_{uL0} - \tilde{H}'_{dR0}), \quad (3.6)$$

up to terms of order v/M_{SUSY} . Expressed in terms of these fields, the Lagrangians for matter-chargino/neutralino interactions in the MSSM Majorana limit and in the Dirac theory can be written as

$$\mathcal{L}_{\text{Majo}}^{\text{C}} = g \overline{u_L} \tilde{\chi}_1^+ \tilde{d}_L + g \overline{\tilde{\chi}_1^+} u_L \tilde{d}_L^* - g \overline{d_L} \tilde{\chi}_1^- \tilde{u}_L - g \overline{\tilde{\chi}_1^-} d_L \tilde{u}_L^*, \quad (3.7)$$

$$\mathcal{L}_{\text{Dirac}}^{\text{C}} = g \overline{u_L} \tilde{\chi}_{D2}^+ \tilde{d}_L + g \overline{\tilde{\chi}_{D2}^+} u_L \tilde{d}_L^* - g \overline{d_L} \tilde{\chi}_{D1}^- \tilde{u}_L - g \overline{\tilde{\chi}_{D1}^-} d_L \tilde{u}_L^*, \quad (3.8)$$

and

$$\mathcal{L}_{\text{Majo}}^{\text{N}} = -g_{Li} \overline{f_L} \tilde{\chi}_i^0 \tilde{f}_L - g_{Li}^* \overline{\tilde{\chi}_i^0} f_L \tilde{f}_L^* + g_{Ri} \overline{f_R} \tilde{\chi}_i^0 \tilde{f}_R + g_{Ri}^* \overline{\tilde{\chi}_i^0} f_R \tilde{f}_R^*, \quad (3.9)$$

$$\mathcal{L}_{\text{Dirac}}^{\text{N}} = -g_{Li} \overline{f_L} \tilde{\chi}_{D_i}^0 \tilde{f}_L - g_{Li}^* \overline{\tilde{\chi}_{D_i}^0} f_L \tilde{f}_L^* + g_{Ri} \overline{f_R} \tilde{\chi}_{D_i}^{0c} \tilde{f}_R + g_{Ri}^* \overline{\tilde{\chi}_{D_i}^{0c}} f_R \tilde{f}_R^*, \quad (3.10)$$

where

$$g_{Li} = \sqrt{2} [g' Y_{f_L} \delta_{i1} + g I_f^3 \delta_{i2}] \quad \text{and} \quad g_{Ri} = \sqrt{2} g' Y_{f_R} \delta_{i1}. \quad (3.11)$$

Here u/\tilde{u} correspond to up-type (s)quarks or (s)neutrinos, whereas d/\tilde{d} denote down-type (s)quarks or charged (s)leptons. As mentioned above, mixings from electroweak symmetry breaking as well as from the CKM matrix have been neglected.

In the approximation described by the Dirac Lagrangians a Dirac charge D [7] can be defined which is conserved in all processes:

$$D[\tilde{q}_L^{1,2}] = D[\tilde{\ell}_L^{1,2}] = D[\tilde{\nu}^{1,2}] = D[\tilde{\chi}_D^{0c}] = D[\tilde{\chi}_{D1}^+] = D[\tilde{\chi}_{D2}^-] = -1, \quad (3.12)$$

$$D[\tilde{q}_R^{1,2}] = D[\tilde{\ell}_R^{1,2}] = D[\tilde{\chi}_D^0] = D[\tilde{\chi}_{D1}^-] = D[\tilde{\chi}_{D2}^+] = +1. \quad (3.13)$$

Antiparticles carry the corresponding opposite Dirac charges $-D$. The Dirac charges of all SM particles vanish. The squarks $\tilde{q}^{1,2}$, sleptons $\tilde{\ell}^{1,2}$, and sneutrinos $\tilde{\nu}^{1,2}$ belong to the first and second generation. L, R mixing and large couplings to higgsinos preclude the extension of this approximate scheme to the third generation. Nevertheless, the scheme proves useful for a quick overview of allowed and forbidden processes in the first two generations. For example, in the Dirac limit, the production processes $e_L^- e_L^- \rightarrow \tilde{e}_L^- \tilde{e}_L^-$ and $e_R^- e_R^- \rightarrow \tilde{e}_R^- \tilde{e}_R^-$ with equal helicities are forbidden while the opposite-helicity process $e_L^- e_R^- \rightarrow \tilde{e}_L^- \tilde{e}_R^-$ is allowed.

1. Squark Cascade Decays at LHC

Cascade decays, see *e.g.* Ref. [25], are crucial for the analysis of the non-colored supersymmetry sector at LHC. Following the rules discussed earlier, we will study invariant masses of quark-jets with charged leptons in squark cascade decays:

$$\begin{array}{ll} \underline{\text{Charginos:}} & \text{MSSM:} \quad \tilde{u}_L \rightarrow d \tilde{\chi}_1^+ \rightarrow d \nu_l \tilde{l}_L^+, \quad dl^+ \tilde{\nu}_l \rightarrow dl^+ \nu_l \tilde{\chi}_1^0, \\ & \tilde{d}_L \rightarrow u \tilde{\chi}_1^- \rightarrow u \bar{\nu}_l \tilde{l}_L^-, \quad ul^- \tilde{\nu}_l^* \rightarrow ul^- \bar{\nu}_l \tilde{\chi}_1^0, \end{array} \quad (3.14)$$

$$\begin{array}{ll} \text{Dirac:} & \tilde{u}_L \rightarrow d \tilde{\chi}_{D1}^+ \rightarrow dl^+ \tilde{\nu}_l \rightarrow dl^+ \nu_l \tilde{\chi}_{D1}^{0c}, \\ & \tilde{d}_L \rightarrow u \tilde{\chi}_{D2}^- \rightarrow u \bar{\nu}_l \tilde{l}_L^- \rightarrow ul^- \bar{\nu}_l \tilde{\chi}_{D1}^{0c}, \end{array} \quad (3.15)$$

$$\underline{\text{Neutralinos:}} \quad \text{MSSM:} \quad \tilde{q}_L \rightarrow q \tilde{\chi}_2^0 \rightarrow ql^\pm \tilde{l}_L^\mp \rightarrow ql^\pm l^\mp \tilde{\chi}_1^0, \quad (3.16)$$

$$\text{Dirac:} \quad \tilde{q}_L \rightarrow q \tilde{\chi}_{D2}^0 \rightarrow ql^+ \tilde{l}_L^- \rightarrow ql^+ l^- \tilde{\chi}_1^0. \quad (3.17)$$

Due to CP invariance, the charge conjugated versions of these processes are obtained simply by flipping the gauge/Dirac charges and chiralities at each step.

As evident from the list above, the decay chains differ in their chirality structure between the MSSM and the Dirac theory, which will leave a characteristic imprint on the angular distributions of visible decay jets and leptons. For the squark-chargino cascades this is illustrated by the quark-lepton invariant mass distributions shown in Fig. 4.

Also shown in the figure is an example of the general 2-Majorana hyper-system away from the Dirac limit. In this case one obtains two wino-like charginos $\chi_{1,2}^\pm$ with distinct masses. The dotted lines in the plots corresponds to a

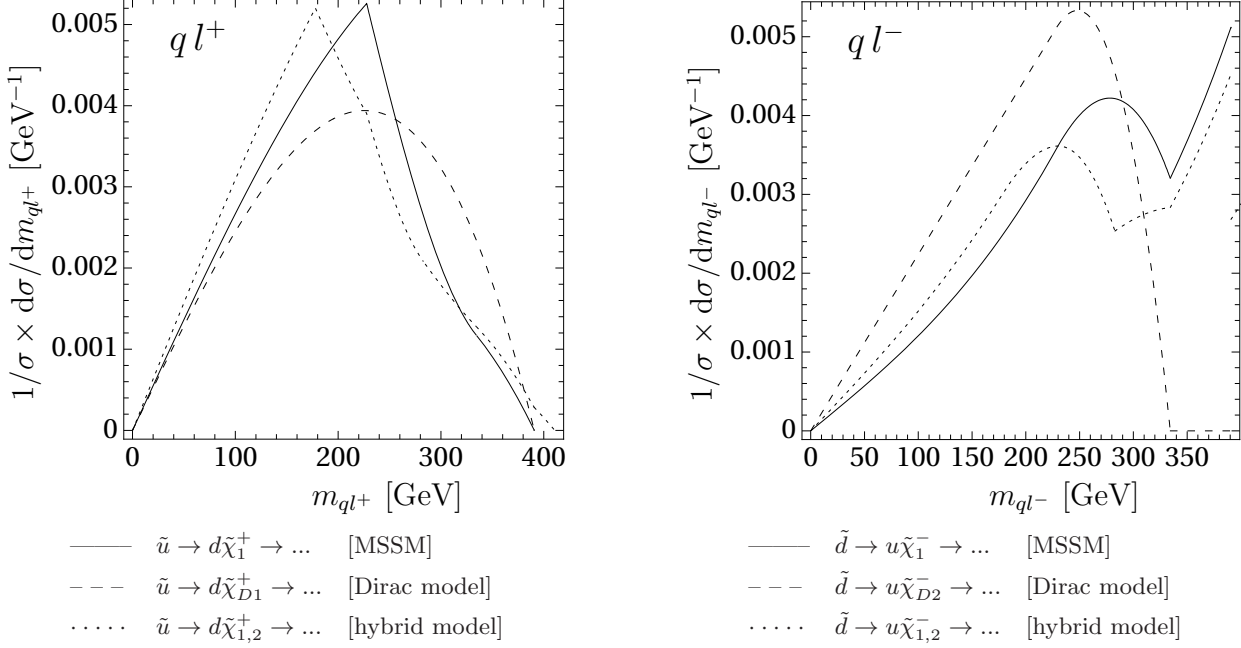


Figure 4: Quark-lepton invariant mass distributions for squark decay chains with intermediate charginos, comparing the $N=1$ MSSM (solid lines) with the $N=2$ Dirac gaugino theory (dashed lines) and the intermediate hybrid theory (dotted lines). Numerical inputs for the plots are $m_{\tilde{q}} = 565$ GeV, $m_{\tilde{\chi}_1^\pm} = m_{\tilde{\chi}_{D1}^\pm} = m_{\tilde{\chi}_{D2}^\pm} = 184$ GeV, $m_{\tilde{t}} = m_{\tilde{b}} = 125.3$ GeV, and $m_{\tilde{\chi}_1^0} = m_{\tilde{\chi}_{D1}^0} = 97.7$ GeV. For the case of the hybrid model, the second chargino mass is $m_{\tilde{\chi}_2^\pm} = 199$ GeV, corresponding to a mixing angle $\cos\theta_2 = 0.6$. Electroweak symmetry breaking effects on the chargino and neutralino mixing matrices have been neglected.

scenario with relatively small departure from the Dirac limit, so that the two chargino masses are of the same order and the \tilde{W}/\tilde{W}' mixing angle is close to maximal mixing.

Nevertheless, the distributions of the 2-Majorana hyper-system are closer to the MSSM in the plots, while the Dirac limit leads to drastically different distributions. This can be understood from the fact that the two independent charginos $\tilde{\chi}_1^\pm$ and $\tilde{\chi}_2^\pm$ in the hybrid model become degenerate in the exact Dirac limit. Interference effects lead to large mixing between the two states in this limit. However, a slight deviation from the Dirac limit is already sufficient to effectively turn off these interference contributions, since the width of both charginos is relatively small.

The squark-neutralino cascades have been worked out in Ref. [7], and are reproduced in Fig. 5. Again, the plots show distinct differences between the MSSM and Dirac limits, which can be exploited to experimentally distinguish the two cases at the LHC.

2. Selectron Pair-Production in e^-e^- and e^+e^- Collisions

Conservation of the Dirac charge D in the first generation forbids the production of selectrons in equal-helicity e^-e^- collisions but allows the production in opposite-helicity collisions in the Dirac theory, while all three helicity combinations are non-trivially realized in Majorana theories:

$$e_L^- e_L^- \rightarrow \tilde{e}_L^- \tilde{e}_L^-, \quad e_R^- e_R^- \rightarrow \tilde{e}_R^- \tilde{e}_R^-, \quad (3.18)$$

$$e_L^- e_R^- \rightarrow \tilde{e}_L^- \tilde{e}_R^-. \quad (3.19)$$

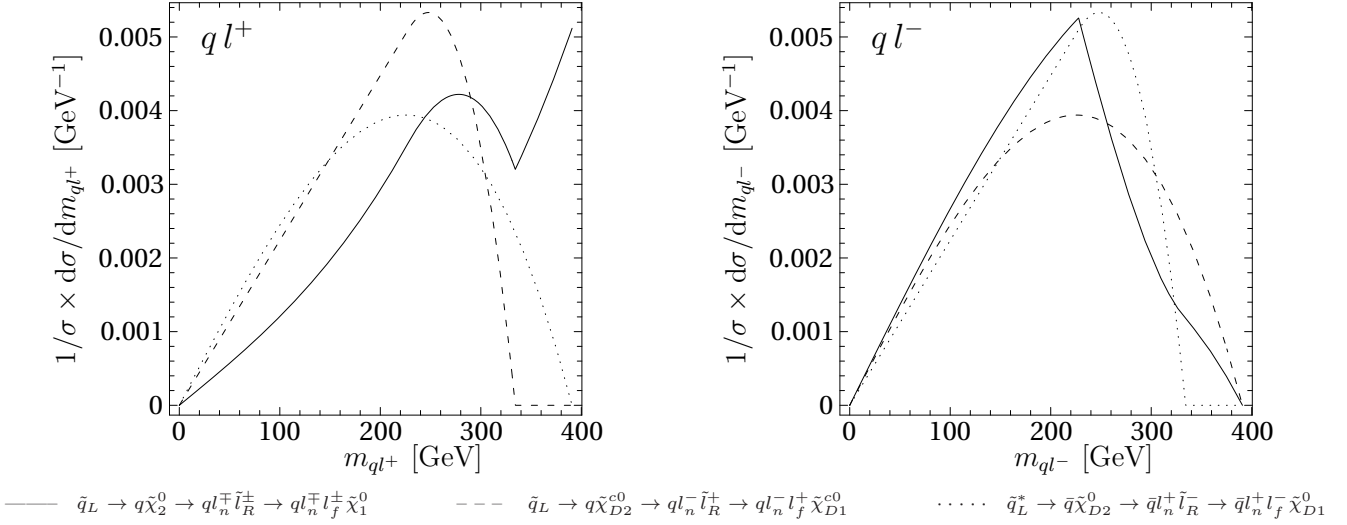


Figure 5: ql invariant mass distributions for squark decay chains involving Majorana or Dirac neutralinos. In the $N=1$ MSSM (solid lines) the squark and anti-squark decay chains lead to identical distributions, in contrast to the $N=2$ Dirac gaugino theory (dashed and dotted lines). Numerical inputs for the plots are $m_{\tilde{q}} = 565$ GeV, $m_{\tilde{\chi}_2^0} = m_{\tilde{\chi}_{D2}^0} = 184$ GeV, $m_{\tilde{l}} = 125.3$ GeV, and $m_{\tilde{\chi}_1^0} = m_{\tilde{\chi}_{D1}^0} = 97.7$ GeV. Electroweak symmetry breaking effects on the chargino and neutralino mixing matrices have been neglected.

Three other independent processes are possible in e^-e^+ collisions:

$$e_L^- e_L^+ \rightarrow \tilde{e}_L^- \tilde{e}_R^+, \quad (3.20)$$

$$e_L^- e_R^+ \rightarrow \tilde{e}_L^- \tilde{e}_L^+, e_R^- e_L^+ \rightarrow \tilde{e}_R^- \tilde{e}_R^+. \quad (3.21)$$

Noting that $(\psi_{L/R})^c = (\psi^c)_{R/L}$, the additional process $e_R^- e_R^+ \rightarrow \tilde{e}_R^- \tilde{e}_L^+$ in the second group is the CP-conjugate of the first process and needs not be analyzed separately. Since non-zero s -channel γ, Z exchange requires opposite lepton helicities, the first electron/positron process is driven only by neutralino exchanges while the other two processes are mediated by both t -channel neutralino and s -channel vector-boson exchanges. Moreover, the first process violates conservation of the D charge and thus is forbidden in the Dirac theory. Simulations of some processes have been presented in Refs. [26, 27].

(i) e^-e^- collisions :

Recalling the definitions introduced in Ref. [7], the e^-e^- scattering amplitudes for selectron pair production in the general hybrid hyper-system on which we have based the detailed analyses, can be written as

$$\mathcal{A}[e_L^- e_L^- \rightarrow \tilde{e}_L^- \tilde{e}_L^-] = -2e^2 [\mathcal{M}_{LL}(s, t) + \mathcal{M}_{LL}(s, u)], \quad (3.22)$$

$$\mathcal{A}[e_R^- e_R^- \rightarrow \tilde{e}_R^- \tilde{e}_R^-] = 2e^2 [\mathcal{M}_{RR}^*(s, t) + \mathcal{M}_{RR}^*(s, u)], \quad (3.23)$$

for same helicity-pairs and

$$\mathcal{A}[e_L^- e_R^- \rightarrow \tilde{e}_L^- \tilde{e}_R^-] = e^2 \lambda_{LR}^{1/2} \sin \theta \mathcal{D}_{LR}(s, t), \quad (3.24)$$

$$\mathcal{A}[e_R^- e_L^- \rightarrow \tilde{e}_L^- \tilde{e}_R^-] = -e^2 \lambda_{LR}^{1/2} \sin \theta \mathcal{D}_{RL}(s, u), \quad (3.25)$$

for opposite helicity-pairs, with the two-body final state kinematic factor $\lambda_{ab} = \lambda(1, m_{\tilde{e}_a}^2/s, m_{\tilde{e}_b}^2/s)$ [$a, b = L, R$] and

$$\lambda(1, x, y) = 1 + x^2 + y^2 - 2(x + y + xy). \quad (3.26)$$

Here θ is the scattering angle, and the dimensionless neutralino functions \mathcal{M}_{ab} and \mathcal{D}_{ab} ($a, b = L, R$) [28] are defined

by

$$\mathcal{M}_{ab}(s, t/u) = \sum_{k=1}^6 \frac{m_{\tilde{\chi}_k^0}}{\sqrt{s}} \mathcal{V}_{ak} \mathcal{V}_{bk} D_{kt/u}, \quad (3.27)$$

$$\mathcal{D}_{ab}(s, t/u) = \sum_{k=1}^6 \mathcal{V}_{ak} \mathcal{V}_{bk}^* D_{kt/u}, \quad (3.28)$$

They are determined by the normalized neutralino propagators $D_{kt} = s/(t - m_{\tilde{\chi}_k^0}^2)$, and similarly for D_{ku} , and the effective mixing coefficients

$$\mathcal{V}_{Lk} = U_{N2k}/(2c_W) + U_{N4k}/(2s_W), \quad \mathcal{V}_{Rk} = U_{N2k}/c_W. \quad (3.29)$$

The neutralino mixing matrix elements $U_{N\alpha k}$, introduced in (2.45), have a very simple structure if effects from electroweak symmetry breaking are neglected, see Eq. (2.49).

After calculating the polarization averaged squared matrix elements and including the phase space factor the differential cross sections are

$$\frac{d\sigma_{LL}}{d\cos\theta} = \frac{\pi\alpha^2}{4s} \lambda_{LL}^{1/2} |\mathcal{M}_{LL}(s, t) + \mathcal{M}_{LL}(s, u)|^2, \quad (3.30)$$

$$\frac{d\sigma_{RR}}{d\cos\theta} = \frac{\pi\alpha^2}{4s} \lambda_{RR}^{1/2} |\mathcal{M}_{RR}(s, t) + \mathcal{M}_{RR}(s, u)|^2, \quad (3.31)$$

$$\frac{d\sigma_{LR}}{d\cos\theta} = \frac{\pi\alpha^2}{4s} \lambda_{LR}^{3/2} \sin^2\theta [|\mathcal{D}_{LR}(s, t)|^2 + |\mathcal{D}_{RL}(s, u)|^2]. \quad (3.32)$$

Finally, the unpolarized total cross sections can be obtained by performing the remaining integration over the scattering angle θ . Note that σ_{LR} and σ_{RL} are not physically distinguishable in the e^-e^- case, unlike for e^+e^- annihilation. The cross sections reduce, on the one side, to the familiar MSSM form, see Ref. [26], while in the Dirac theory, on the other side, they simplify considerably to

$$\sigma[e^-e^- \rightarrow \tilde{e}_L^- \tilde{e}_L^-] = \sigma[e^-e^- \rightarrow \tilde{e}_R^- \tilde{e}_R^-] = 0, \quad (3.33)$$

$$\sigma[e^-e^- \rightarrow \tilde{e}_L^- \tilde{e}_R^-] = \frac{\pi\alpha^2}{2c_W^4 s} \left[(1 + 2m_{\tilde{\chi}_{D1}^0}/s - m_{\tilde{e}_L}^2/s - m_{\tilde{e}_R}^2/s) L'_{D1} - 2\beta' \right], \quad (3.34)$$

with $\beta' = \lambda_{LR}^{1/2}$ and the logarithmic function defined by

$$L'_i = \log \frac{1 + \beta' + (2m_{\tilde{\chi}_i^0}^2 - m_{\tilde{e}_L}^2 - m_{\tilde{e}_R}^2)/s}{1 - \beta' + (2m_{\tilde{\chi}_i^0}^2 - m_{\tilde{e}_L}^2 - m_{\tilde{e}_R}^2)/s}. \quad (3.35)$$

The vanishing of the LL and RR cross sections is obvious from D -charge conservation. In the absence of higgsino exchanges only the bino-exchange can drive the LR process.

The evolution of the total cross section from the MSSM to the Dirac limit is illustrated for the two characteristic processes $e^-e^- \rightarrow \tilde{e}_L^- \tilde{e}_L^-$ and $e^-e^- \rightarrow \tilde{e}_L^- \tilde{e}_R^-$ in the left panel of Fig.6, which demonstrates how the first process is switched off when the Dirac limit is approached.

(ii) e^+e^- collisions :

The analysis of the e^-e^+ processes follows the same path. By introducing a normalized s -channel Z boson propagator $D_Z = s/(s - m_Z^2 + im_Z\Gamma_Z)$ and four bi-linear charges

$$Z_{LL}^+ = 1 + \frac{s_W^2 - 1/2}{c_W^2} D_Z, \quad Z_{LL}^- = 1 + \frac{(s_W^2 - 1/2)^2}{c_W^2 s_W^2} D_Z, \quad (3.36)$$

$$Z_{RR}^+ = 1 + \frac{s_W^2}{c_W^2} D_Z, \quad Z_{RR}^- = 1 + \frac{s_W^2 - 1/2}{c_W^2} D_Z, \quad (3.37)$$

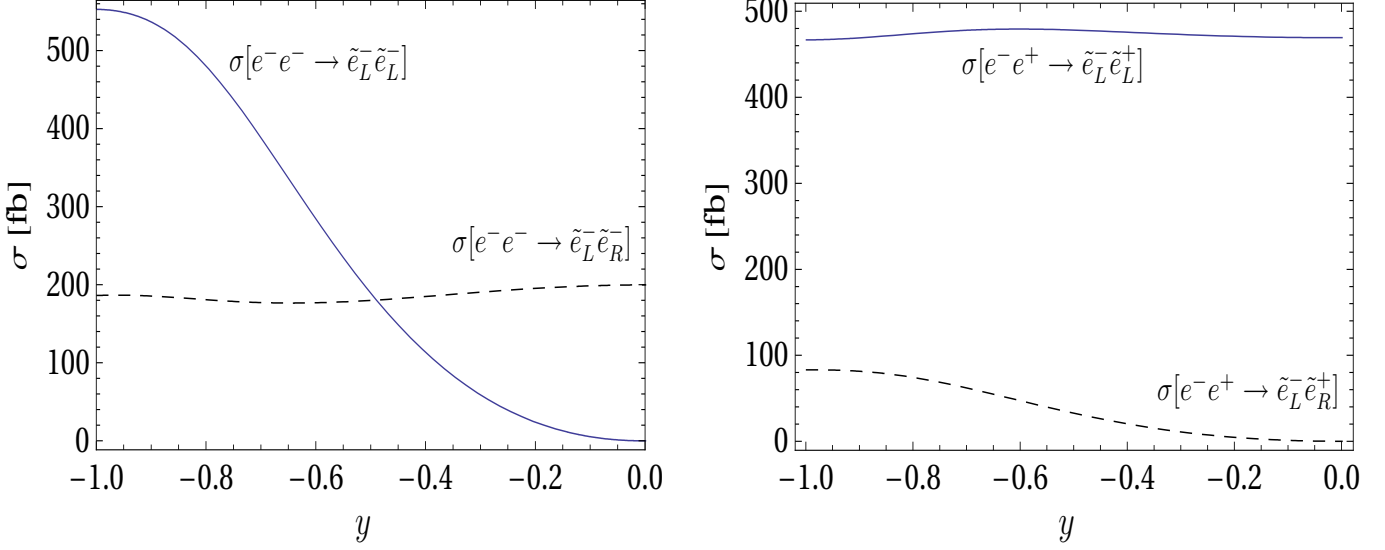


Figure 6: Dependence of the cross sections for same-sign (left) and opposite-sign (right) selectron production on the Dirac/Majorana control parameter y , for $\sqrt{s} = 500$ GeV and SPS1a' parameters [29]. Not shown are the cross sections for $e^-e^\pm \rightarrow \tilde{e}_R^\pm \tilde{e}_R^\pm$, which, apart from the different normalization, shows a similar behavior as the cross section for $e^-e^- \rightarrow \tilde{e}_L^- \tilde{e}_L^\pm$.

we obtain six non-vanishing helicity amplitudes

$$\mathcal{A}[e_L^- e_R^+ \rightarrow \tilde{e}_L^- \tilde{e}_L^+] = -e^2 \lambda_{LL}^{1/2} \sin \theta [\mathcal{D}_{LL}(s, t) + Z_{LL}^-], \quad (3.38)$$

$$\mathcal{A}[e_R^- e_L^+ \rightarrow \tilde{e}_L^- \tilde{e}_L^+] = -e^2 \lambda_{LL}^{1/2} \sin \theta Z_{LL}^+, \quad (3.39)$$

$$\mathcal{A}[e_L^- e_R^+ \rightarrow \tilde{e}_R^- \tilde{e}_R^+] = -e^2 \lambda_{RR}^{1/2} \sin \theta Z_{RR}^-, \quad (3.40)$$

$$\mathcal{A}[e_R^- e_L^+ \rightarrow \tilde{e}_R^- \tilde{e}_R^+] = -e^2 \lambda_{RR}^{1/2} \sin \theta [\mathcal{D}_{RR}(s, t) + Z_{RR}^+], \quad (3.41)$$

$$\mathcal{A}[e_L^- e_L^+ \rightarrow \tilde{e}_L^- \tilde{e}_R^+] = 2e^2 \mathcal{M}_{LR}(s, t), \quad (3.42)$$

$$\mathcal{A}[e_R^- e_R^+ \rightarrow \tilde{e}_R^- \tilde{e}_L^+] = -2e^2 \mathcal{M}_{RL}^*(s, t). \quad (3.43)$$

By squaring the helicity amplitudes, the differential cross sections can easily be derived. The squares are summed incoherently if the initial lepton helicities are not specified experimentally.

As before, the cross sections reduce to the familiar MSSM limit on one side, while in the Dirac limit, on the other side, the processes with LR/RL initial state helicities remain allowed, but the LL and RR processes are excluded by D -charge conservation. The D -charge of the pair $\tilde{e}_L^- \tilde{e}_R^-$ vanishes, thus allowing production in e^-e^- collisions, but the pair $\tilde{e}_L^- \tilde{e}_R^+$ carries the charge $D = 2$ so that production of this pair in e^-e^+ collisions is forbidden.

The continuous transition from the MSSM to the Dirac limit is illustrated in the right panel of Fig. 6, for the two representative total cross sections of $e^-e^+ \rightarrow \tilde{e}_L^- \tilde{e}_R^+$ and $e^-e^+ \rightarrow \tilde{e}_L^- \tilde{e}_L^+$.

3. Chargino and Neutralino Production in e^+e^- Collisions

Direct production of chargino and neutralino pairs in e^+e^- annihilation are ideal laboratories to study the properties of these particles, see *e.g.* Ref. [30]. As will be shown here, the characteristic differences between the Dirac theory and the MSSM also become evident in these processes.

The chargino reactions proceed in general through s -channel γ, Z and t -channel $\tilde{\nu}_e$ exchanges. Focusing on the gaugino sector, doubled in the general hybrid theory compared to the MSSM, the production cross sections for diagonal and non-diagonal charged gaugino pairs are given by

$$\begin{aligned} \frac{d\sigma}{d\cos\theta}[e^+e^- \rightarrow \tilde{\chi}_1^+ \tilde{\chi}_1^-] &= \frac{\pi\alpha^2\lambda_{11}^{1/2}}{16s_W^4 s} \left[\frac{[s^2 - 4s_W^2 m_Z^2 s + 8s_W^4 m_Z^4][2 - \lambda_{11} \sin^2 \theta]}{(s - m_Z^2)^2} \right. \\ &\quad \left. + 2s_2^2 \frac{[s - 2s_W^2 m_Z^2][1 - \lambda_{11} + (1 - \lambda_{11}^{1/2} \cos \theta)^2]}{(s - m_Z^2)(\eta_{11} - \lambda_{11}^{1/2} \cos \theta)} + 2s_2^4 \frac{(1 - \lambda_{11}^{1/2} \cos \theta)^2}{(\eta_{11} - \lambda_{11}^{1/2} \cos \theta)^2} \right], \end{aligned} \quad (3.44)$$

$$\begin{aligned} \frac{d\sigma}{d\cos\theta}[e^+e^- \rightarrow \tilde{\chi}_2^+ \tilde{\chi}_2^-] &= \frac{\pi\alpha^2\lambda_{22}^{1/2}}{16s_W^4 s} \left[\frac{[s^2 - 4s_W^2 m_Z^2 s + 8s_W^4 m_Z^4][2 - \lambda_{22} \sin^2 \theta]}{(s - m_Z^2)^2} \right. \\ &\quad \left. + 2c_2^2 \frac{[s - 2s_W^2 m_Z^2][1 - \lambda_{22} + (1 - \lambda_{22}^{1/2} \cos \theta)^2]}{(s - m_Z^2)(\eta_{22} - \lambda_{22}^{1/2} \cos \theta)} + 2c_2^4 \frac{(1 - \lambda_{22}^{1/2} \cos \theta)^2}{(\eta_{22} - \lambda_{22}^{1/2} \cos \theta)^2} \right], \end{aligned} \quad (3.45)$$

$$\frac{d\sigma}{d\cos\theta}[e^+e^- \rightarrow \tilde{\chi}_1^\pm \tilde{\chi}_2^\mp] = \frac{\pi\alpha^2\lambda_{12}^{1/2}}{4s_W^4 s} c_2^2 s_2^2 \frac{(1 - \lambda_{12} \cos \theta)^2 - (m_{\tilde{\chi}_1^\pm}^2 - m_{\tilde{\chi}_2^\mp}^2)^2/s^2}{(\eta_{12} - \lambda_{12}^{1/2} \cos \theta)^2}, \quad (3.46)$$

and the production cross section of a charged higgsino pair by

$$\frac{d\sigma}{d\cos\theta}[e^+e^- \rightarrow \tilde{\chi}_3^+ \tilde{\chi}_3^-] = \frac{\pi\alpha^2\lambda_{33}^{1/2}}{16s} \frac{(8s_W^4 - 4s_W^2 + 1)(s_W^2 - 1/2)^2}{c_W^4 s_W^4} \frac{s^2(2 - \lambda_{33} \sin^2 \theta)}{(s - m_Z^2)^2}, \quad (3.47)$$

with $\eta_{ij} = 1 + (2m_{\tilde{\nu}}^2 - m_{\tilde{\chi}_i^\pm}^2 - m_{\tilde{\chi}_j^\pm}^2)/s$, where we ignore the Z boson width and introduce the usual Källén functions $\lambda_{ij} = \lambda^{1/2}(1, m_{\tilde{\chi}_i^\pm}^2/s, m_{\tilde{\chi}_j^\pm}^2/s)$. As before electroweak symmetry breaking effects in the chargino mixing matrix have been neglected. The mixing angles c_2 and s_2 , derived from Eq. (2.40) by neglecting v_I and explicitly given by

$$c_2/s_2 = \sqrt{[1 \pm (M_2' - M_2)/\delta_2]/2} \quad \text{with} \quad \delta_2 = \sqrt{(M_2' - M_2)^2 + 4(M_2^D)^2}, \quad (3.48)$$

under the assumption $M_2' + M_2 \leq 0$ and $M_2^{(D)} \geq 0$, only modify the t -channel sneutrino amplitude, so that they can be determined from the angular distribution of $\tilde{\chi}_1^+ \tilde{\chi}_1^-$ production in a straightforward manner. The MSSM limit corresponds to (3.44) with $c_2 = 0$ and $s_2 = 1$. In the Dirac limit, using the basis (3.1),(3.2) for the two degenerate gauginos, one finds

$$\begin{aligned} \frac{d\sigma}{d\cos\theta}[e^+e^- \rightarrow \tilde{\chi}_{D1}^+ \tilde{\chi}_{D1}^-] &= \frac{\pi\alpha^2\lambda_{11}^{1/2}}{16s_W^4 s} \left[\frac{[s^2 - 4s_W^2 m_Z^2 s + 8s_W^4 m_Z^4][2 - \lambda_{11} \sin^2 \theta]}{(s - m_Z^2)^2} \right. \\ &\quad \left. + 2 \frac{[s - 2s_W^2 m_Z^2][2 - 2\lambda_{11}^{1/2} \cos \theta - \lambda_{11} \sin^2 \theta]}{(s - m_Z^2)(\eta_{11} - \lambda_{11}^{1/2} \cos \theta)} + 2 \frac{(1 - \lambda_{11}^{1/2} \cos \theta)^2}{(\eta_{11} - \lambda_{11}^{1/2} \cos \theta)^2} \right], \end{aligned} \quad (3.49)$$

$$\frac{d\sigma}{d\cos\theta}[e^+e^- \rightarrow \tilde{\chi}_{D2}^+ \tilde{\chi}_{D2}^-] = \frac{\pi\alpha^2\lambda_{22}^{1/2}}{16s_W^4 s} \frac{[s^2 - 4s_W^2 m_Z^2 s + 8s_W^4 m_Z^4][2 - \lambda_{22} \sin^2 \theta]}{(s - m_Z^2)^2}, \quad (3.50)$$

$$\frac{d\sigma}{d\cos\theta}[e^+e^- \rightarrow \tilde{\chi}_{D1}^\pm \tilde{\chi}_{D2}^\mp] = 0, \quad (3.51)$$

while the higgsino production is identical to the MSSM case. It is noteworthy that unlike the MSSM, three distinct pairs of charginos can be produced in the Dirac limit, but the cross sections for $\tilde{\chi}_1^+ \tilde{\chi}_1^-$ ($\tilde{\chi}_3^+ \tilde{\chi}_3^-$) production, in the MSSM limit, are identical to those for $\tilde{\chi}_{D1}^+ \tilde{\chi}_{D1}^-$ ($\tilde{\chi}_{D3}^+ \tilde{\chi}_{D3}^-$) production in the Dirac limit. The latter characteristic is in obvious contrast to neutralino and gluino production, which are Majorana particles in one limit and Dirac particles in the other.

As a characteristic example in the neutralino sector we will focus on the production of wino pairs, $e^+e^- \rightarrow \tilde{\chi}_2 \tilde{\chi}_2^{(c)}$ in the MSSM and Dirac limits for the comparison of Majorana and Dirac theories. Neglecting neutralino mixing from

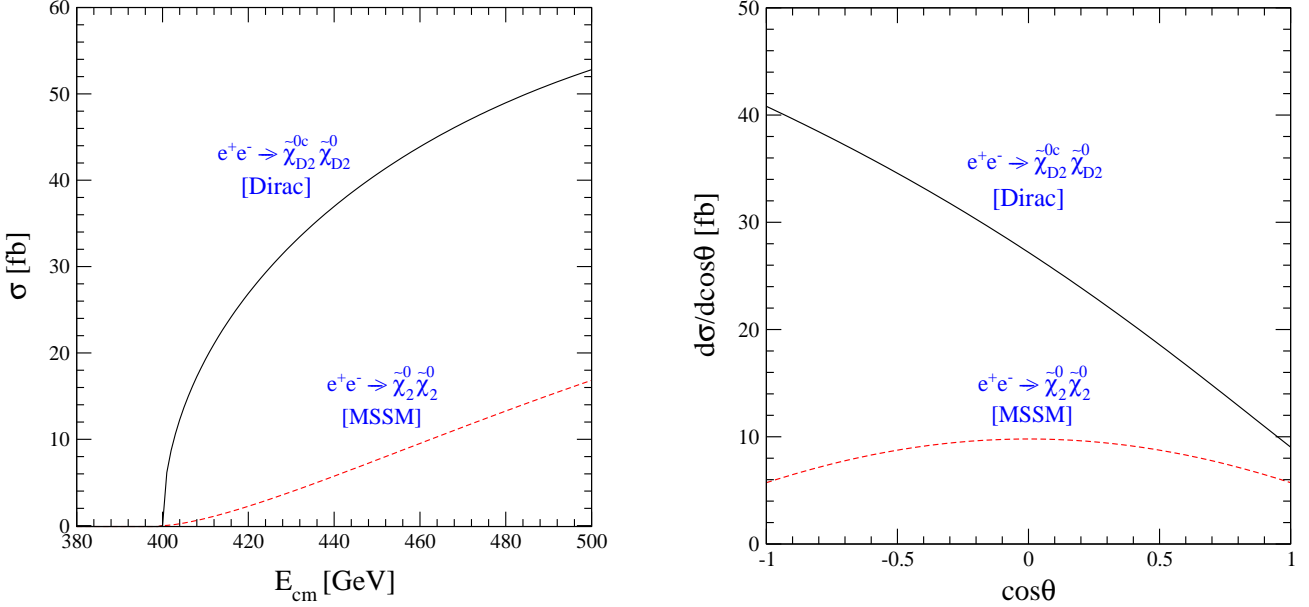


Figure 7: Left: the total cross sections for pair production of wino-like neutralinos near threshold in the MSSM and the Dirac theory. Right: dependence of the cross sections on the production angle θ for $\sqrt{s} = E_{\text{cm}} = 500$ GeV. The sparticle masses in both plots are $m_{\tilde{\chi}_2^0} = m_{\tilde{\chi}_{D2}^0} = 200$ GeV and $m_{\tilde{e}_L} = 400$ GeV.

electroweak symmetry breaking, the production mechanisms proceed via exchange of selectrons in the t -channel for Dirac neutralinos, and both the t, u -channels for Majorana neutralinos. The differential cross sections as a function of the production angle θ read

$$\text{MSSM:} \quad \frac{d\sigma}{d\cos\theta}[e^+e^- \rightarrow \tilde{\chi}_2^0\tilde{\chi}_2^0] = \frac{\pi\alpha^2}{32s_W^4s} \lambda_{22}^{3/2} \frac{\eta_{2L}^2 + (\eta_{2L}^2 - 4\eta_{2L} + 2 - \lambda_{22})\cos^2\theta + \lambda_{22}\cos^4\theta}{(\eta_{2L}^2 - \lambda_{22}\cos^2\theta)^2}, \quad (3.52)$$

$$\text{Dirac:} \quad \frac{d\sigma}{d\cos\theta}[e^+e^- \rightarrow \tilde{\chi}_{D2}^{0c}\tilde{\chi}_{D2}^0] = \frac{\pi\alpha^2}{32s_W^4s} \lambda_{22}^{1/2} \frac{(1 - \lambda_{22}^{1/2}\cos\theta)^2}{(\eta_{2L} - \lambda_{22}^{1/2}\cos\theta)^2}. \quad (3.53)$$

As before, λ_{22} denotes the usual 2-body phase space function and $\eta_{2L} = 1 + 2(m_{\tilde{e}_L}^2 - m_{\tilde{\chi}_2^0}^2)/s$.

Two characteristics distinguish the Dirac from the Majorana cross section, see Fig. 7. Dirac particles are generated in S -waves near threshold, identical Majorana particles in P -waves, giving rise to threshold onsets proportional to the $\tilde{\chi}$ velocity and its third power, respectively. In contrast to identical Majorana particle production, Dirac particle production is not forward-backward symmetric in the production angle θ . The integrated asymmetry is substantial, for example $\mathcal{A}_{\text{FB}} \approx -0.30$ for $m_{\tilde{\chi}_{D2}^0} = 200$ GeV, $m_{\tilde{e}_L} = 400$ GeV and $\sqrt{s} = 500$ GeV. In practice, the measurable asymmetry is somewhat reduced by experimental acceptances and cuts, and the fact that the neutralino cannot be reconstructed fully from its decay products, but it is nevertheless an important tool to discriminate the Dirac theory from the MSSM. It should be noted finally that the cross section for Dirac pair production is equal to the sum of the cross sections for the corresponding $\{kl\}$ diagonal and off-diagonal Majorana pairs as shown explicitly by meticulous accounting of interference effects for gluino production in Ref. [7].

3.2. Scalar Particles

At the Born level the iso-triplet and hyper-singlet sigma fields, σ_I^i and σ_Y^0 , couple to sfermions, charginos/neutralinos and Higgs bosons. The relevant couplings can be derived from the Lagrangian terms and the scalar potential listed in subsection 2.1. The set of new Born and effective loop couplings relevant for the phenomenological analyses of the dominant σ production and decays is displayed in Fig. 8. Only the generic form of the couplings are noted explicitly at the vertices.

1. Sigma Decays

Expressed by the effective couplings, g_B and g_F , in the Lagrangians $\mathcal{L} = g_B s B^* B$ and $\mathcal{L} = g_F \phi \bar{F} [i\gamma_5] F$, $\phi = s, a$, the partial decay widths can be derived generically for bosons B and fermions F as

$$\Gamma[s \rightarrow B\bar{B}] = \frac{g_B^2}{16\pi m_s} \beta, \quad (3.54)$$

$$\Gamma[s \rightarrow F\bar{F}] = \frac{g_F^2 m_s}{8\pi} \beta^3, \quad (3.55)$$

$$\Gamma[a \rightarrow F\bar{F}] = \frac{g_F^2 m_a}{8\pi} \beta, \quad (3.56)$$

with β denoting the velocity of the final state particles. The two standard coefficients β and β^3 correspond to S - and P -wave decays.

In the following analyses we will focus on the gross features of production channels and decay modes of the novel scalar states so that small block mixing can be neglected. The mass eigenstates are therefore approximately identified with the unmixed states $s_{Y,I}$, $a_{Y,I}$ and $s_{1,2}^\pm$, and the MSSM states h, H, A, H^\pm correspondingly.

For unspecified masses and couplings the following decays are the leading modes of the particles s_Y and a_Y :

$$s_Y \rightarrow hh, hH, HH, AA, H^+H^-; \tilde{f}\tilde{f}^*; \tilde{\chi}^+\tilde{\chi}^-, \tilde{\chi}^0\tilde{\chi}^{0(c)}, \quad (3.57)$$

$$a_Y \rightarrow \tilde{\chi}^+\tilde{\chi}^-, \tilde{\chi}^0\tilde{\chi}^{0(c)}. \quad (3.58)$$

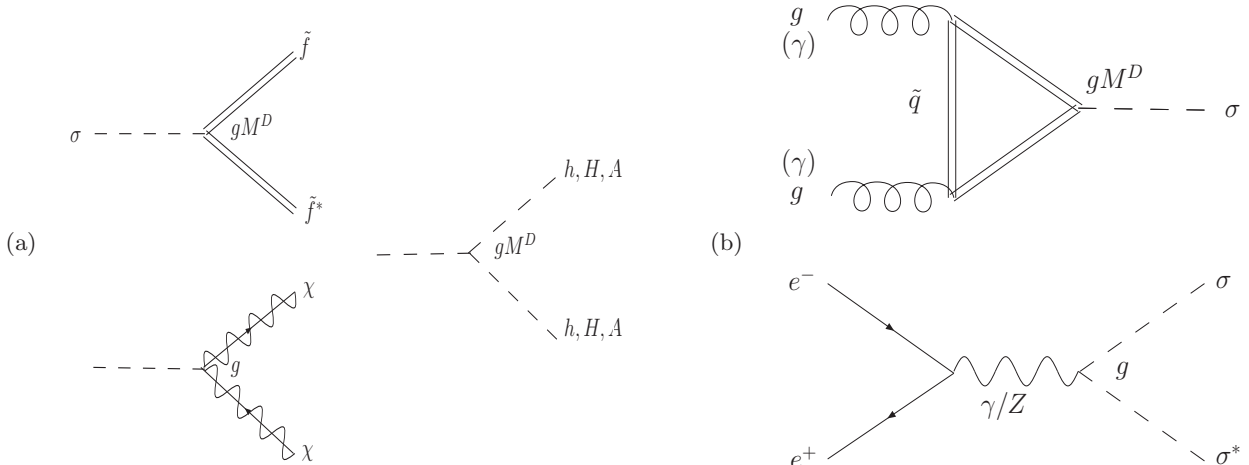


Figure 8: Diagrams relevant for (a) electroweak σ decays and (b) electroweak σ production. The $\gamma\gamma$ couplings to σ include also loops of charginos, W and charged Higgs bosons. [Values of the couplings denoted at the vertices, are generic.]

The pseudoscalar particle a_Y decays only to (higgsino-type) neutralino or chargino pairs, with equal probability sufficiently above the threshold region. If 2-body decays are kinematically forbidden, 3-body decays to a (higgsino-type) neutralino, (bino-type) neutralino and Higgs boson, as well as loop-decays to $t\bar{t}$ pairs and photons are predicted. It should also be noted that the mass eigenstate proper, A_2 , may decay through channels opened by the mixing with the pseudoscalar A Higgs boson. As the couplings are of size $\mathcal{O}(g'M_Y^D)$ and/or $\mathcal{O}(\lambda_Y\mu, \lambda_Y M_Y, \lambda_Y A_Y)$, the ensuing partial widths are typically of electroweak size above the 2-body threshold regions.

A detailed set of leading decay branching ratios is shown for the hyper-singlet scalar particle s_Y in Fig. 9. The relevant couplings g_B and g_F for the scalar s_Y to Higgs bosons are:

$$\begin{aligned}
g_B[s_Y hh] &= -\sqrt{2}\lambda_Y\mu_n + g'M_Y^D c_{2\beta} + (M_Y + A_Y)\lambda_Y s_{2\beta}/\sqrt{2}, \\
g_B[s_Y hH] &= -g'M_Y^D s_{2\beta} + (M_Y + A_Y)\lambda_Y c_{2\beta}/\sqrt{2}, \\
g_B[s_Y HH] &= g_B[s_Y AA] = -\sqrt{2}\lambda_Y\mu_n - g'M_Y^D c_{2\beta} - (M_Y + A_Y)\lambda_Y s_{2\beta}/\sqrt{2}, \\
g_B[s_Y H^+ H^-] &= -\sqrt{2}\lambda_Y\mu_c + g'M_Y^D c_{2\beta} - (M_Y + A_Y)\lambda_Y s_{2\beta}/\sqrt{2},
\end{aligned} \tag{3.59}$$

those to supersymmetric particles are:

$$\begin{aligned}
g_B[s_Y \tilde{f}_L \tilde{f}_L^*] &= -2g'M_Y^D Y_{f_L}, \\
g_B[s_Y \tilde{f}_R \tilde{f}_R^*] &= 2g'M_Y^D Y_{f_R}, \\
g_F[s_Y \tilde{H}_u^+ \tilde{H}_d^-] &= g_F[s_Y \tilde{\chi}_{D3}^+ \tilde{\chi}_{D3}^-] = -\lambda_Y/\sqrt{2}, \\
g_F[s_Y \tilde{H}_u^0 \tilde{H}_d^0] &= -g_F[s_Y \tilde{\chi}_{D3}^0 \tilde{\chi}_{D3}^{0c}] = \lambda_Y/\sqrt{2},
\end{aligned} \tag{3.60}$$

and the relevant couplings for the pseudoscalar a_Y are:

$$\begin{aligned}
g_F[a_Y \tilde{H}_u^+ \tilde{H}_d^-] &= g_F[a_Y \tilde{\chi}_{D3}^+ \tilde{\chi}_{D3}^-] = \lambda_Y/\sqrt{2}, \\
g_F[a_Y \tilde{H}_u^0 \tilde{H}_d^0] &= -g_F[a_Y \tilde{\chi}_{D3}^0 \tilde{\chi}_{D3}^{0c}] = -\lambda_Y/\sqrt{2}.
\end{aligned} \tag{3.61}$$

The Dirac chargino and neutralino, $\tilde{\chi}_{D3}^\pm$ and $\tilde{\chi}_{D3}^0$, are defined in terms of higgsinos in Eqs. (3.3) and (3.6), respectively. For the specific set of parameters the hyper-singlet scalar s_Y decays dominantly to Higgs bosons and sleptons. The decays to gaugino-like neutralinos are forbidden due to gauge symmetry and the decays to higgsino-like neutralinos and charginos are kinematically allowed only when the particle is very heavy.

The iso-triplet scalar states, s_I, a_I and $s_{1,2}^\pm$, have been assumed very heavy. Several features of the iso-triplet scalar interactions determine their potential decay modes. In parallel to the hypercharge states, they do not couple to quarks and leptons, but they couple to gauginos, higgsinos and scalar pairs, sfermions, as well as Higgs bosons and/or gauge bosons. Thus, if kinematically allowed, the gauge/Higgs bosons, sfermions, charginos and neutralinos constitute the dominant decay channels for the s_I, a_I and $s_{1,2}^\pm$ states:

$$s_I \rightarrow hh, hH, HH, AA, H^+ H^-; \tilde{f}\tilde{f}^*; \tilde{\chi}^+ \tilde{\chi}^-, \tilde{\chi}^0 \tilde{\chi}^{0(c)}, \tag{3.62}$$

$$a_I \rightarrow \tilde{\chi}^+ \tilde{\chi}^-, \tilde{\chi}^0 \tilde{\chi}^{0(c)}, \tag{3.63}$$

$$s_{1,2}^\pm \rightarrow H^\pm h, H^\pm H, H^\pm A; \tilde{f}\tilde{f}^*; \tilde{\chi}^+ \tilde{\chi}^0 / \tilde{\chi}^- \tilde{\chi}^{0c}, \tag{3.64}$$

with partial widths of the electroweak scale. In addition, the small couplings to electroweak gauge bosons, developed by the small iso-triplet vev v_I , lead to the two-boson decay $s_I \rightarrow W^+ W^-$, albeit at reduced rate. Furthermore, the iso-triplet scalar states may decay to gluons, photons, electroweak bosons, quarks and leptons through sfermion and chargino/neutralino loops.

2. Stop and Stau Decays to Sigma Particles

Sigma fields carry positive R -parity, but they couple preferentially to gaugino and squark/slepton pairs. Assuming, as before, that they are heavier than charginos and neutralinos, this leaves us with heavy sfermion decays as a possible

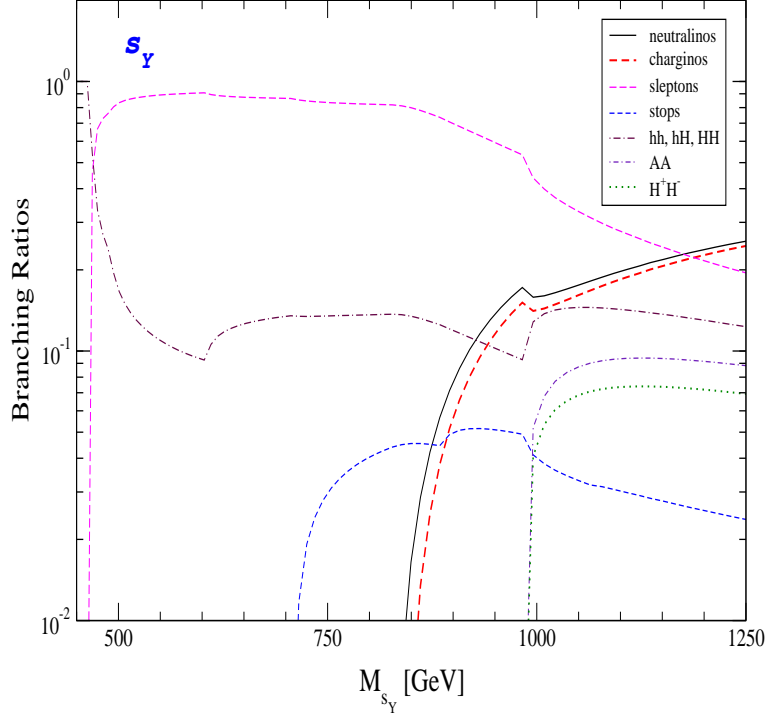


Figure 9: Dependence of the branching ratios for s_Y decays on the mass M_{s_Y} . The values of the relevant SUSY parameters are taken to be $\tan\beta=5$, $\mu = 400$ GeV, $m'_Y = M_Y^D = v/2$, $m'_I = M_I^D = v$, $A_Y = A_I = 2v$, together with $m_{\tilde{t}_L} = v$, $m_{\tilde{e}_R} = 0.95m_{\tilde{t}_L}$, $m_{\tilde{q}_L} = 2v$, $m_{\tilde{q}_R} = 0.95m_{\tilde{q}_L}$, $m_{\tilde{t}_R} = 0.8m_{\tilde{q}_L}$, $m_{\tilde{t}_L} = X_t = 0.9m_{\tilde{q}_L}$, $m_H = m_A = m_{H^\pm} = 2v$, $m_h = 114$ GeV. For the charginos and neutralinos the Dirac limit with $M_{1,2}^{(0)} = 0$ is assumed. Only the leading 2-body decays are shown.

source for neutral sigma particles:

$$\tilde{f}_2 \rightarrow \tilde{f}_1 + s_Y. \quad (3.65)$$

While the s_I channel is likely too heavy to be open, the pseudoscalars $a_{Y,I}$ do not couple.

Since the mass splitting between the two stops is typically large, let us examine the process $\tilde{t}_2 \rightarrow \tilde{t}_1 + s_Y$ first. The partial width for this decay mode is given by

$$\Gamma_{\tilde{t}_2} = \frac{g_{\tilde{t}}^2}{16\pi m_{\tilde{t}_2}} \lambda^{1/2}(1, m_{\tilde{t}_1}^2/m_{\tilde{t}_2}^2, M_{s_Y}^2/m_{\tilde{t}_2}^2), \quad (3.66)$$

with λ denoting the usual phase space function defined in (3.26) and the coupling

$$g_{\tilde{t}} = \frac{5}{6\sqrt{2}} g' M_Y^D \sin 2\theta_{\tilde{t}}. \quad (3.67)$$

Even for large values of the stop mixing angle $\theta_{\tilde{t}}$, $\Gamma_{\tilde{t}}$ is typically less than 1 GeV for sparticle masses of a few 100 GeV, compared to a typical \tilde{t}_2 total width of a few tens of GeV. Thus the branching ratio for $\tilde{t}_2 \rightarrow \tilde{t}_1 + s_Y$ can amount to a few per-cent at most, so that experimental discovery of this decay channel will be very challenging.

In the stau system, the decay mode $\tilde{\tau}_2 \rightarrow \tilde{\tau}_1 + s_Y$ only becomes viable for large values of the mass splitting $m_{\tilde{\tau}_2} - m_{\tilde{\tau}_1}$ and of $\tan\beta$. In such a scenario, however, one typically obtains sizable branching ratios of order 10%. This can be explained by the larger hypercharges of the staus compared to the stops, leading to a similar expression for the partial width as above but with $g_{\tilde{t}}$ replaced by

$$g_{\tilde{\tau}} = \frac{3}{2\sqrt{2}} g' M_Y^D \sin 2\theta_{\tilde{\tau}}. \quad (3.68)$$

While heavy staus will be swamped by background at hadron colliders, the process $\tilde{\tau}_2 \rightarrow \tilde{\tau}_1 + s_Y$ could be a possible discovery mode for the s_Y scalar at high-energy lepton colliders.

3. Production of Sigma Particles at LHC

The neutral hyper-singlet and iso-triplet scalar particles s_Y and s_I can, in principle, be generated singly in gluon fusion processes at the LHC, analogous to Higgs bosons:

$$pp \rightarrow gg \rightarrow s_{Y,I}. \quad (3.69)$$

Since the pseudoscalar states $a_{Y,I}$ do not couple to gluons through squark loops, their single formation channel is shut. The adjoint $s_{Y,I}$ scalar coupling to the gluons are mediated by squark triangles, the D -terms providing the interactions of the squarks with the sigma fields.

The partonic fusion cross section for s_Y production, with the Breit-Wigner function in units of $1/M_{s_Y}^2$ factored off,

$$\hat{\sigma}[gg \rightarrow s_Y] = \frac{\pi^2}{8M_{s_Y}} \Gamma(s_Y \rightarrow gg), \quad (3.70)$$

can be expressed in terms of the partial width for $s_Y \rightarrow gg$,

$$\Gamma[s_Y \rightarrow gg] = \frac{\alpha_Y \alpha_s^2}{8\pi^2} \frac{(M_a^D)^2}{M_{s_Y}} \left| \sum [Y_L \tau_L f(\tau_L) - Y_R \tau_R f(\tau_R)] \right|^2. \quad (3.71)$$

with $\alpha_Y = g'^2/4\pi$. The standard triangular function $f(\tau)$ is defined by

$$f(\tau) = [\sin^{-1}(1/\sqrt{\tau})]^2 \quad \text{if } \tau \geq 1, \quad \text{and} \quad -\frac{1}{4} \left[\ln \left(\frac{1 + \sqrt{1-\tau}}{1 - \sqrt{1-\tau}} \right) - i\pi \right]^2 \quad \text{if } 0 \leq \tau < 1, \quad (3.72)$$

with $\tau_{L,R} = 4M_{\tilde{q}_{L,R}}^2/M_{s_Y}^2$ and $Y_{L,R}$ being the hypercharges of the L and R -squarks. It should be noted that the hypercharges add up to zero for complete generations, but not individually for up- and down-type states for which the L/R hypercharge difference amounts to ∓ 1 . While for mass-degenerate complete generations the sum of the form factors in the partial width vanishes, the cancellation is lifted for stop states, in particular, with the non-zero difference enhanced by the different L/R hypercharges.

The pp cross section is finally found by convoluting the parton cross section with the gg luminosity [31],

$$\sigma[pp \rightarrow s_Y] = \frac{\pi^2}{8s} \frac{\Gamma(s_Y \rightarrow gg)}{M_{s_Y}} \int_{M_{s_Y}^2/s}^1 \frac{dx}{x} g(x; M_{s_Y}^2) g(\tau/x; M_{s_Y}^2), \quad (3.73)$$

in the usual notation. The cross section for s_Y production is shown in Fig. 10 as a function of the s_Y mass.

An analogous expression holds for s_I production in pp collisions. However, since the mass of s_I needs to be very large due to the ρ -parameter constraint, the actual size of the fusion cross section will be significantly below 1 fb.

Other production channels are offered by Higgs-strahlung and electroweak boson fusion. Pairs of electroweak gauge bosons couple to the lightest Higgs boson h and the iso-vector s_I . All these couplings involve either the electroweak vev v or the iso-scalar vev v_I . Rotating the mass eigenstates s_i to the current eigenstates h etc, the cross sections for Higgs-strahlung and vector-boson fusion can easily be expressed by the corresponding cross section for the production of the SM Higgs boson with equivalent mass:

$$\sigma[pp \rightarrow W \rightarrow W s_i] = \left(\mathcal{O}_{S1i} + 4 \frac{v_I}{v} \mathcal{O}_{S4i} \right)^2 \sigma[pp \rightarrow W \rightarrow W H_{SM}], \quad (3.74)$$

$$\sigma[pp \rightarrow Z \rightarrow Z s_i] = (\mathcal{O}_{S1i})^2 \sigma[pp \rightarrow Z \rightarrow Z H_{SM}], \quad (3.75)$$

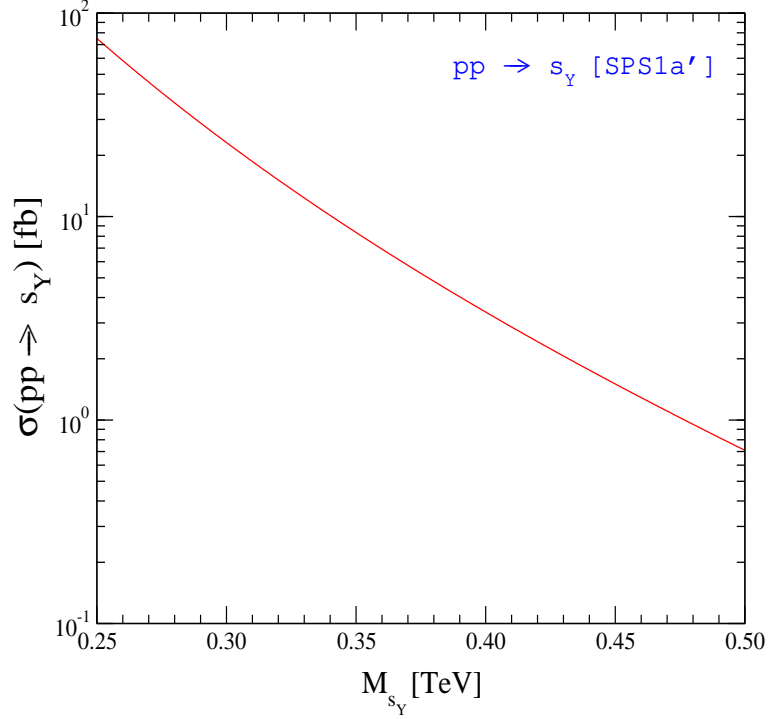


Figure 10: Cross sections for single s_Y production through gg fusion in pp collisions at LHC ($\sqrt{s} = 14$ TeV). The MSSM benchmark point SPS1a', Ref. [29], is adopted for the numerical analysis.

with \mathcal{O}_S denoting the 4×4 rotation matrix diagonalizing the scalar mass matrix squared \mathcal{M}_S^2 in Eq. (2.70) as $\mathcal{O}_S^T \mathcal{M}_S^2 \mathcal{O}_S = \text{diag}(M_{S_1}^2, \dots, M_{S_4}^2)$. Cross sections for vector boson fusion are related in the same way.

Numerical analyses taking into account the experimental constraint on the ρ parameter and the mass bound on the lightest neutral scalar lead to mixing coefficients of 10^{-2} and less so that these channels are presumably of little value in practice.

4. Charged Adjoint Scalar Pair-Production in e^+e^- and $\gamma\gamma$ Collisions

(i) e^+e^- collisions :

Resonance production of sigma particles in e^+e^- collisions is strongly suppressed as the production amplitude scales with the electron mass. Since the quantum numbers Q, I_3, Y of the neutral sigma states $\sigma_{I,Y}^0$ all vanish, these particles cannot be pair-produced in e^+e^- collisions. However, production channels open up for diagonal charged scalar pairs $s_{1,2}^\pm$ defined in Eq. (2.80),

$$e^+e^- \rightarrow s_n^+ s_n^- \quad [n = 1, 2], \quad (3.76)$$

through s -channel γ, Z exchanges. With effective charges

$$\begin{aligned} g_{L*}[s_n^\pm] &= 1 - \frac{s_W^2 - 1/2}{s_W^2} \frac{s}{s - m_Z^2} \approx 2, & g_{R*}[s_n^\pm] &= 1 - \frac{s}{s - m_Z^2} \approx 0, \\ g_{L*}[H^\pm] &= 1 + \frac{(s_W^2 - 1/2)^2}{c_W^2 s_W^2} \frac{s}{s - m_Z^2} \approx \frac{4}{3}, & g_{R*}[H^\pm] &= 1 + \frac{s_W^2 - 1/2}{c_W^2} \frac{s}{s - m_Z^2} \approx \frac{2}{3}, \end{aligned} \quad (3.77)$$

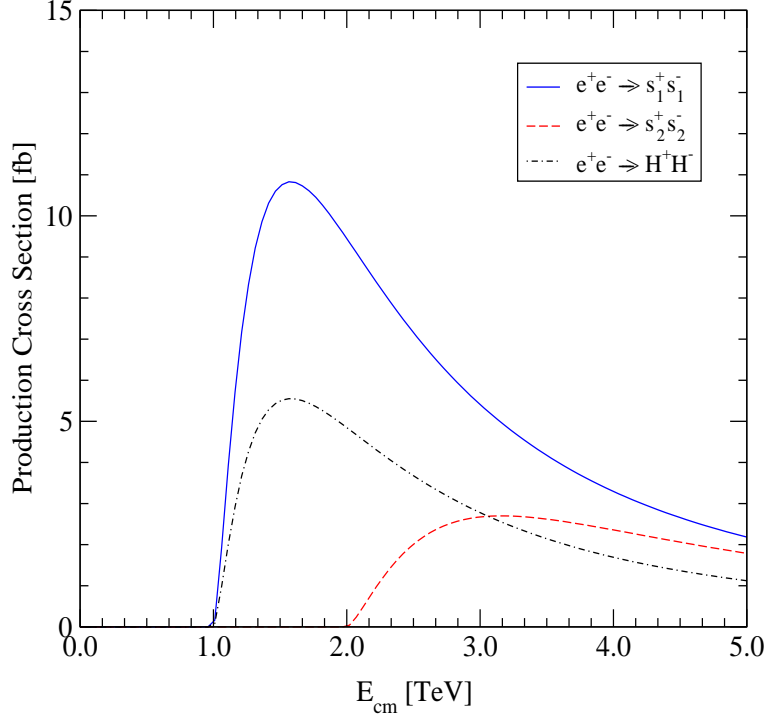


Figure 11: The cross sections for charged $s_{1,2}^{\pm}$ pair production in e^+e^- collisions at TeV energies. The charged scalar masses are assumed to be $M_{s_1^{\pm}} = 0.5$ TeV and $M_{s_2^{\pm}} = 1.0$ TeV. For comparison, the cross section for charged Higgs pair production is shown with its mass $M_{H^{\pm}} = 0.5$ TeV.

with $n=1, 2$ for L and R -chiral electron pairs coupled to the $s_{1,2}^{\pm}$ pairs and equivalently to the H^{\pm} pair, the cross section reads:

$$\sigma = \frac{\pi\alpha^2}{3s} \frac{g_{L*}^2 + g_{R*}^2}{2} \beta^3, \quad (3.78)$$

where s is the total c.m. energy squared and β the velocity of the particles $s_{1,2}^{\pm}$ and H^{\pm} ; $s_W^2 = \sin^2 \theta_W$ denotes the electroweak mixing parameter. The size of the three production cross sections, identical in form, is illustrated in Fig. 11 for two different mass values $M_{s_1^{\pm}, H^{\pm}} = 0.5$ TeV and $M_{s_2^{\pm}} = 1.0$ TeV.

(ii) $\gamma\gamma$ collisions :

Excellent instruments for searching for heavy scalar/pseudoscalar particles and studying their properties are $\gamma\gamma$ colliders, see Ref. [32]. About 80% of the incoming electron energy can be converted to a high-energy photon by Compton back-scattering of laser light, with the spectrum peaking at the maximal energy by choosing proper helicities.

Depending on the nature of the neutral scalars/pseudoscalars, their couplings to the two photons is mediated by charged W -bosons, charginos, and charged scalars and Higgs bosons. As before, the formation cross sections for the states $\phi = s_Y, s_I$ and a_Y, a_I can be expressed by the $\gamma\gamma$ widths of the particles and the $\gamma\gamma$ luminosity:

$$\begin{aligned} \langle \sigma(\gamma\gamma \rightarrow \phi) \rangle &= 8\pi^2 \frac{\Gamma(\phi \rightarrow \gamma\gamma)}{M_\phi^3} \tau_\phi \frac{d\mathcal{L}_{\gamma\gamma}}{\tau_\phi} \\ &= \sigma_0(\gamma\gamma \rightarrow \phi) \tau_\phi \frac{d\mathcal{L}_{\gamma\gamma}}{\tau_\phi}, \end{aligned} \quad (3.79)$$

with $\tau_\phi = M_\phi^2/s$. For qualitative estimates the luminosity function $\tau_\phi d\mathcal{L}_{\gamma\gamma}/d\tau_\phi$ can be approximated by unity after splitting off the overall e^+e^- luminosity [33].

The partial $\gamma\gamma$ widths are parameterized by couplings and loop functions,

$$\Gamma(s/a \rightarrow \gamma\gamma) = \frac{\alpha^2}{64\pi^3} M_{s/a} \left| \sum_i N_{c_i} e_i^2 g_i^{s/a} A_i^{s/a} \right|^2. \quad (3.80)$$

The factor N_{c_i} denotes the color factor of the loop line, while the couplings $g_i^{s/a}$ are expressed by

$$g_{\tilde{H}_D^\pm}^{s_Y} = \lambda_Y/\sqrt{2}, \quad g_{f_{L,R}}^{s_Y} = \pm Y_{f_{L,R}} M_Y^D/M_{s_Y},$$

$$g_{\tilde{H}^\pm}^{s_Y} = \left(\sqrt{2}\lambda_Y\mu_c - g' M_Y^D c_{2\beta} + \lambda_Y(M_Y + A_Y) s_{2\beta}/\sqrt{2} \right) / M_{s_Y}, \quad (3.81)$$

$$g_{W^\pm}^{s_I} = 2g^2 v_I/M_{s_I}, \quad g_{\tilde{H}_D^\pm}^{s_I} = \lambda_I/\sqrt{2}, \quad g_{\tilde{W}_{1,2}^\pm}^{s_I} = \mp g, \quad g_{f_{L,R}}^{s_I} = \pm g I_3^f M_I^D/M_{s_I},$$

$$g_{\tilde{H}^\pm}^{s_I} = - \left(\sqrt{2}\lambda_I\mu_c - g M_I^D c_{2\beta} + \lambda_I(M_I - A_I) s_{2\beta}/\sqrt{2} \right) / M_{s_I}, \quad (3.82)$$

for the hyper-singlet scalar s_Y and the iso-triplet scalar s_I , and

$$g_{\tilde{H}_D^\pm}^{a_Y} = -\lambda_Y/\sqrt{2},$$

$$g_{\tilde{H}_D^\pm}^{a_I} = \lambda_I/\sqrt{2}, \quad g_{\tilde{W}_{1,2}^\pm}^{a_I} = \pm g, \quad (3.83)$$

for the hyper-singlet pseudoscalar a_Y . The loop functions $A_i^{s/a}$, identical in form for the particles of a given spin, include the standard triangular function $f(\tau)$ in Eq. (3.72) as

$$A_0^s = 1 - \tau f(\tau), \quad A_{1/2}^s = -2\sqrt{\tau} [1 + (1 - \tau)f(\tau)], \quad A_1^s = 2/\tau + 3 + 3(2 - \tau)f(\tau), \quad (3.84)$$

for the scalar s , and

$$A_{1/2}^a = -2\sqrt{\tau} f(\tau), \quad (3.85)$$

for the pseudoscalar a , where the subscripts 0, 1/2 and 1 stand for spin-0, spin-1/2 and spin-1 intermediate particles.

Adopting the SPS1a' parameters in the SUSY sector [29], the reduced $\gamma\gamma$ cross section $\sigma_0(\gamma\gamma \rightarrow \phi)$ for $\phi = s_{Y,I}$ and $a_{Y,I}$, defined in Eq. (3.79), amounts to order 1 fb as shown in Fig. 12 so that for an overall luminosity of several hundred fb^{-1} a sizable sample of neutral scalars $s_{Y,I}$ and pseudoscalars $a_{Y,I}$ can be generated in $\gamma\gamma$ collisions.

4. SUMMARY

In minimal supersymmetric extensions of the Standard Model the fermionic partners of color and electroweak gauge bosons are self-conjugate Majorana fields. Their properties are characteristically distinct from Dirac fields. To investigate this point quantitatively, we have adopted an $N=1/N=2$ hybrid supersymmetry model in which the gauge and Higgs sectors are extended to $N=2$ while the matter sector remains restricted to $N=1$. This extension is wide enough to allow the joining of Majorana to Dirac fields while keeping the matter sector chiral. By properly varying gaugino mass matrices, the original MSSM Majorana theory can be transformed smoothly to the Dirac theory.

The transition from $N=1$ to $N=2$ expands the gauge sector by a matter supermultiplet composed of a new gaugino and adjoint scalar multiplet.

- (i) The doubling of the gauginos in $N=2$ gives rise to new particles along the path from the MSSM to the Dirac theory:

$$- 8 \text{ Majorana gluinos} \rightarrow 16 \text{ Majorana gluinos} \rightarrow 8 \text{ Dirac gluinos}$$

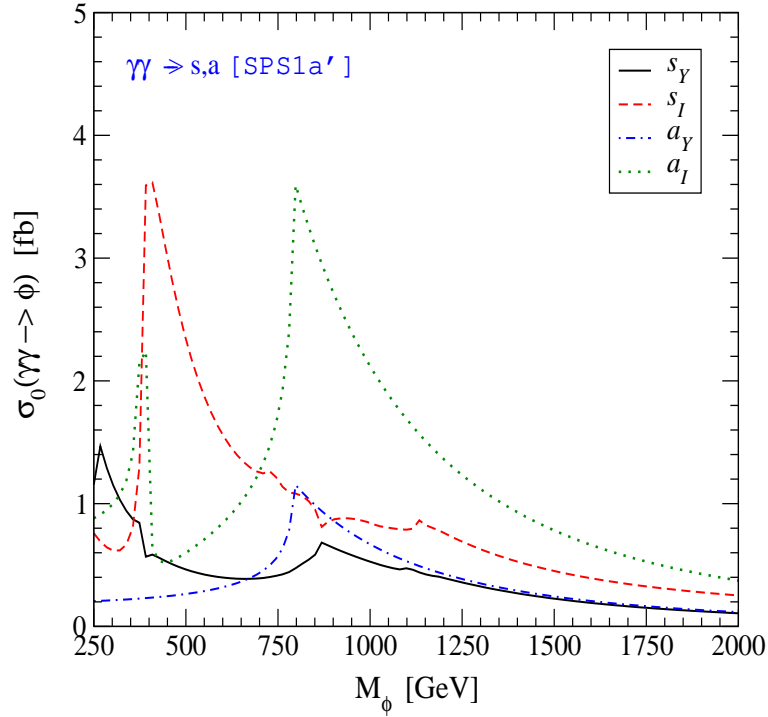


Figure 12: The reduced production cross sections $\sigma_0(\gamma\gamma \rightarrow \phi)$ for $\phi = s_{Y,I}$ and $a_{Y,I}$. The SPS1a' parameter set [29] for the (s)particle masses, couplings and mixing parameters are adopted for the numerical analysis.

- 2 charginos \rightarrow 3 charginos
- 4 Majorana neutralinos \rightarrow 6 Majorana neutralinos \rightarrow 3 Dirac neutralinos

(ii) The adjoint scalars expand also the number of states originally present in the MSSM scalar sector; the new $SU(2)_I \times U(1)_Y$ scalars mix with the Higgs fields in the electroweak sector:

- 8 octet complex scalar gluons, generally termed sgluons
- 1 pseudoscalar state \rightarrow 3 pseudoscalar states
- 2 scalar states \rightarrow 4 scalar states
- 1 charged scalar $[\pm]$ pair \rightarrow 3 charged scalar $[\pm]$ pairs

The scale of the new degrees of freedom is strongly restricted by the experimentally allowed deviation of the ρ parameter from unity. Since the new electroweak $SU(2)_I$ and $U(1)_Y$ scalars acquire vacuum expectation values, the $SU(2)_I$ iso-triplet vev must be small, and the iso-triplet scalar mass parameter is driven into the TeV region. The $U(1)_Y$ hyper-singlet vev , on the other hand, is not restricted by the ρ parameter and the hyper-singlet scalar mass may still be characterized by a fraction of TeV.

The new degrees of freedom are coupled to the original MSSM fields rather weakly at the order gv/\tilde{M} . This allows us to solve the complicated chargino, neutralino and scalar systems analytically in a systematic expansion, *i.e.* mass eigenvalues and mixings. This leads in a straightforward way to the prediction of production channels and decay modes.

The Majorana or Dirac character of gluinos and neutralinos can nicely be discriminated in sfermion-sfermion production. While allowed by Majorana exchanges, equal L - or R -sfermion pair production is forbidden in Dirac theories, *i.e.* $\tilde{q}_L \tilde{q}_L$ and $\tilde{e}_L \tilde{e}_L$ production in pp and e^-e^- collisions. In addition, cascade decays involving Majorana

neutralinos give rise to charge-symmetric lepton final states, while Dirac neutralinos predict charge sequences as governed by the conservation of Dirac charges. Total cross sections and angular distributions in pair production of charginos and neutralinos in e^+e^- collisions depend on the Majorana or Dirac nature of the underlying gaugino theory.

A variety of production channels are predicted for the scalar states, depending on the nature of the particles:

- Scalar and pseudoscalar sgluons can be produced in pairs in pp collisions, and scalars singly via gluon-gluon fusion.
- The $U(1)_Y$ scalar state can be generated in pp collisions via gluon fusion or in stop or stau decays, but not the corresponding pseudoscalar partner.
- $\gamma\gamma$ collisions offer production channels for all neutral scalar and pseudoscalar, iso-scalar and iso-vector states.
- The charged iso-vector states can be generated pairwise in e^+e^- collisions.

Thus in contrast to the color sector it is quite difficult to cover experimentally the electroweak hyper-singlet and iso-triplet states, the main reason being the expected heavy masses of the new scalar and pseudoscalar particles. Nevertheless, given the joint potential of hadron and lepton colliders, all the new scalar and pseudoscalar particles introduced by the $N=1/N=2$ supersymmetric hybrid theory can in principle be accessed. Only the basics of the processes have been investigated in this report, while detailed analyses of final states under realistic detector conditions are far beyond the scope of this study.

On the other hand, the suppression of reaction channels and cascade decays in gaugino Dirac theories as opposed to Majorana theories for color and electroweak gauginos should provide unique signatures for the Majorana or Dirac nature of gluinos and electroweak gauginos.

Acknowledgments

The work was partially supported by the Korea Research Foundation Grant funded by the Korean Government (MOERHRD, Basic Research Promotion Fund) (KRF-2008-521-C00069), by Bundesministerium für Bildung und Forschung under contract no. 05HT6PDA, by the Marie Curie Training Research Networks “UniverseNet” under contract no. MRTN-CT-2006-035863, “ForcesUniverse” under contract no. MRTN-CT-2004-005104, “Tools and Precision Calculations for Physics Discoveries at Collider” under contract no. MRTN-CT-2006-035505, “The Quest for Unification” under contract no. MRTN-CT-2004-503369, “Particle Physics and Cosmology: the Interface” under contract no. MTKD-CT-2005-029466, by the Polish Ministry of Science and Higher Education Grant no N N202 230337, the Department of Science and Technology, India, under project number SR/S2/RFHEP-05/2006, as well as by the National Science Foundation under grant no. PHY-0854782. PMZ thanks the Institut für Theoretische Teilchenphysik und Kosmologie for the warm hospitality extended to him at RWTH Aachen University. JMK thanks for the hospitality of Korea Institute for Advanced Study where this work was partially done. DC is thankful to the Institute of Theoretical Physics for warm hospitality extended to him during his visit at University of Warsaw.

Appendix A: Analytic analysis of the singular value decomposition of a 2×2 matrix

For any $n \times n$ complex matrix, there exist two unitary matrices U_L and U_R such that

$$U_L^T \mathcal{M} U_R = \mathcal{M}_D = \text{diag}(m_1, m_2, \dots, m_n), \quad (\text{A.1})$$

where the diagonal elements m_k are real and non-negative. This procedure is the singular value decomposition (SVD) of the matrix \mathcal{M} . If the matrix \mathcal{M} is symmetric, there exists a single unitary matrix U such that $U^T \mathcal{M} U = \mathcal{M}_D$ with $U_L = U_R = U$, called the Takagi diagonalization of the symmetric matrix \mathcal{M} .

The singular value decomposition of a 2×2 real matrix can be performed analytically. The result is more involved than the standard diagonalization of a 2×2 symmetric matrix by a single orthogonal matrix. The 2×2 matrix is defined as:

$$\mathcal{M} = \begin{pmatrix} a & c \\ \tilde{c} & b \end{pmatrix}, \quad (\text{A.2})$$

where at least c or \tilde{c} be non-zero. Generally we can parameterize two 2×2 unitary matrices U_L and U_R in Eq. (A.1) by

$$U_L = O_L P = \begin{pmatrix} \cos \theta_L & \epsilon_L \sin \theta_L \\ -\epsilon_L \sin \theta_L & \cos \theta_L \end{pmatrix} \begin{pmatrix} \alpha & 0 \\ 0 & \beta \end{pmatrix}, \quad (\text{A.3})$$

$$U_R = O_R P = \begin{pmatrix} \cos \theta_R & \epsilon_R \sin \theta_R \\ -\epsilon_R \sin \theta_R & \cos \theta_R \end{pmatrix} \begin{pmatrix} \alpha & 0 \\ 0 & \beta \end{pmatrix}, \quad (\text{A.4})$$

where $0 \leq \theta_{L,R} \leq \pi/2$, $\epsilon_{L,R} = \pm 1$ and $\alpha, \beta = 1, i$. The two phase matrices, which map the singular values onto non-negative values, can be identified without loss of generality, as only their product is fixed.

If two singular values $m_{1,2}$ of the matrix \mathcal{M} are non-degenerate, they can be determined by taking the positive square root of the non-negative eigenvalues $m_{1,2}^2$ of the orthogonal matrix $\mathcal{M}^T \mathcal{M}$:

$$m_{1,2} = \frac{1}{2} |\sigma_+ \mp \sigma_-| \quad \text{with} \quad \sigma_{\pm} = \sqrt{(a \pm b)^2 + (c \mp \tilde{c})^2}. \quad (\text{A.5})$$

Two eigenvalues become identical only if $a = \pm b$ and $c = \mp \tilde{c}$. The smaller eigenvalue, m_1 , vanishes if the invariant determinant vanishes, $\det \mathcal{M} = ab - c\tilde{c} = 0$.

Explicitly performing the diagonalization of $\mathcal{M}^T \mathcal{M}$ by U_R and $\mathcal{M} \mathcal{M}^T$ by U_L , the rotation angles and signs can be computed:

$$\cos \theta_{L,R} = \sqrt{\frac{\sigma_+ \sigma_- + b^2 - a^2 \pm \tilde{c}^2 \mp c^2}{2 \sigma_+ \sigma_-}}, \quad \sin \theta_{L,R} = \sqrt{\frac{\sigma_+ \sigma_- - b^2 + a^2 \mp \tilde{c}^2 \pm c^2}{2 \sigma_+ \sigma_-}}, \quad (\text{A.6})$$

$$\epsilon_L = \text{sign}(a\tilde{c} + bc), \quad \epsilon_R = \text{sign}(ac + b\tilde{c}). \quad (\text{A.7})$$

In the final step of the computation the phase parameters α and β can be determined by inserting Eqs. (A.6) and (A.7) into Eq. (A.1):

$$\alpha = \sqrt{\text{sign}[a(\sigma_+ \sigma_- + b^2 - a^2) - a(c^2 + \tilde{c}^2) - 2bc\tilde{c}]}, \quad (\text{A.8})$$

$$\beta = \sqrt{\text{sign}[b(\sigma_+ \sigma_- + b^2 - a^2) + b(c^2 + \tilde{c}^2) + 2ac\tilde{c}]}, \quad (\text{A.9})$$

up to an arbitrary overall sign of both parameters. If the smaller singular value m_1 vanishes for $\det(\mathcal{M}) = 0$, the parameter α is undefined while all the other angles are uniquely determined.

In the case $a = b = 0$ and $\tilde{c} = c$, two singular values are degenerate with $m_{1,2} = |c|$, and the unitary matrices U_L and U_R reduce to a single unitary matrix U :

$$U = \begin{pmatrix} 1/\sqrt{2} & -1/\sqrt{2} \\ 1/\sqrt{2} & 1/\sqrt{2} \end{pmatrix} \cdot \begin{pmatrix} 1 & 0 \\ 0 & i \end{pmatrix} = \begin{pmatrix} 1/\sqrt{2} & -i/\sqrt{2} \\ 1/\sqrt{2} & i/\sqrt{2} \end{pmatrix}, \quad (\text{A.10})$$

corresponding to a $\pi/4$ rotation matrix and a phase matrix, which turns the second eigenvalue positive.

Appendix B: The small-mixing approximation in the singular value decomposition

In this second appendix, we provide details of the singular value decomposition of the mass matrix⁴ in the small mixing approximation, in which the coupling by two off-diagonal matrix blocks is weak and can be treated perturbatively. For mathematical clarity, we present the solution for a general $(N + M) \times (N + M)$ matrix in which the $N \times N$ and $M \times M$ submatrices are coupled weakly so that their mixing is small:

$$\mathcal{M}_{N+M} = \begin{pmatrix} \mathcal{M}_N & X_{NM} \\ \tilde{X}_{NM}^T & \mathcal{M}_M \end{pmatrix}. \quad (\text{B.1})$$

To obtain the corresponding physical masses, we must perform a singular value decomposition of \mathcal{M}_{N+M} :⁵

$$L_{N+M}^T \mathcal{M}_{N+M} R_{N+M} = \text{diag}(m_{1'}, m_{2'}, \dots, m_{N'+M'}), \quad m_{k'} \geq 0, \quad (\text{B.2})$$

where L_{N+M} and R_{N+M} are unitary.⁶ The non-negative diagonal elements $m_{k'}$ are called the singular values of \mathcal{M}_{N+M} , which are defined as the non-negative square roots of the eigenvalues of $\mathcal{M}_{N+M}^\dagger \mathcal{M}_{N+M}$ or, equivalently, $\mathcal{M}_{N+M} \mathcal{M}_{N+M}^\dagger$.

In Eq. (B.1), \mathcal{M}_N and \mathcal{M}_M are $N \times N$ and $M \times M$ symmetric submatrices with singular values assumed to be generally larger than the matrix elements of the $N \times M$ rectangular matrices, X_{NM} and \tilde{X}_{NM} . In this case, one can treat the off-diagonal parts X_{NM} and \tilde{X}_{NM} as a perturbation as long as there are no accidental near-degeneracies between the singular values of \mathcal{M}_N and \mathcal{M}_M , respectively.

(1) In the first step, we separately perform a singular value decomposition of \mathcal{M}_N and \mathcal{M}_M :

$$\overline{\mathcal{M}}_N^D = L_N^T \mathcal{M}_N R_N = \text{diag}(\overline{m}_{1'}, \dots, \overline{m}_{N'}), \quad (\text{B.3})$$

$$\overline{\mathcal{M}}_M^D = L_M^T \mathcal{M}_M R_M = \text{diag}(\overline{m}_{N'+1'}, \dots, \overline{m}_{N'+M'}), \quad (\text{B.4})$$

where the diagonal elements $\overline{m}_{k'}$ are real and non-negative. The ordering of the diagonal elements may conveniently be chosen according to footnote 5.

Step (1) results in a partial singular value decomposition of \mathcal{M}_{N+M} :

$$\overline{\mathcal{M}}_{N+M} \equiv \begin{pmatrix} L_N^T & \mathbb{O} \\ \mathbb{O}^T & L_M^T \end{pmatrix} \begin{pmatrix} \mathcal{M}_N & X_{NM} \\ \tilde{X}_{NM}^T & \mathcal{M}_M \end{pmatrix} \begin{pmatrix} R_N & \mathbb{O} \\ \mathbb{O}^T & R_M \end{pmatrix} = \begin{pmatrix} \overline{\mathcal{M}}_N^D & L_N^T X_{NM} R_M \\ L_M^T \tilde{X}_{NM}^T R_N & \overline{\mathcal{M}}_M^D \end{pmatrix} \equiv \begin{pmatrix} \overline{\mathcal{M}}_N^D & Y_{NM} \\ \tilde{Y}_{NM}^T & \overline{\mathcal{M}}_M^D \end{pmatrix}, \quad (\text{B.5})$$

where \mathbb{O} is an $N \times M$ matrix of zeros. The upper left and lower right blocks of $\overline{\mathcal{M}}_{N+M}$ are diagonal with real non-negative entries, but the upper right and lower left off-diagonal blocks are non-zero.

(2) The ensuing $(N + M) \times (N + M)$ matrix, $\overline{\mathcal{M}}_{N+M}$, can be subsequently block-diagonalized by performing an $(N + M) \times (N + M)$ singular value decomposition of $\overline{\mathcal{M}}_{N+M}$ in an approximate expansion. Since the elements of the off-diagonal blocks in $\overline{\mathcal{M}}_{N+M}$ are small compared to the diagonal elements $\overline{m}_{k'}$, we may treat Y_{NM} and \tilde{Y}_{NM} as a perturbation. More precisely, Y_{NM} and \tilde{Y}_{NM} can be treated as a perturbation if

$$\left| \frac{(Y_{NM})_{i'j'}}{\overline{m}_{i'} - \overline{m}_{j'}} \right| \ll 1 \quad \text{and} \quad \left| \frac{(\tilde{Y}_{NM})_{i'j'}}{\overline{m}_{i'} - \overline{m}_{j'}} \right| \ll 1, \quad (\text{B.6})$$

⁴ The formalism applies also to general complex matrices [34].

⁵ In Eq. (B.2), we use primed subscripts to indicate that the corresponding states are continuously connected to the states of the unperturbed block matrix, $\text{diag}(\overline{\mathcal{M}}_N^D, \overline{\mathcal{M}}_M^D)$, where the diagonal matrices $\overline{\mathcal{M}}_N^D$ and $\overline{\mathcal{M}}_M^D$ are defined in Eqs. (B.3) and (B.4).

⁶ When N and M are used in subscripts of matrices, they refer to the dimension of the corresponding square matrices. For rectangular matrices, two subscripts will be used.

for all choices of $i' = 1', \dots, N'$ and $j' = N' + 1' \dots, N' + M'$. These conditions, as can generally be anticipated, will naturally emerge from the formalism below.

The perturbative block-diagonalization is accomplished by introducing two $(N + M) \times (N + M)$ unitary matrices:

$$\mathcal{L}_{N+M} \simeq \begin{pmatrix} \mathbb{1}_{N \times N} - \frac{1}{2} \Omega_L \Omega_L^\dagger & \Omega_L \\ -\Omega_L^\dagger & \mathbb{1}_{M \times M} - \frac{1}{2} \Omega_L^\dagger \Omega_L \end{pmatrix}, \quad (\text{B.7})$$

$$\mathcal{R}_{N+M} \simeq \begin{pmatrix} \mathbb{1}_{N \times N} - \frac{1}{2} \Omega_R \Omega_R^\dagger & \Omega_R \\ -\Omega_R^\dagger & \mathbb{1}_{M \times M} - \frac{1}{2} \Omega_R^\dagger \Omega_R \end{pmatrix}, \quad (\text{B.8})$$

where Ω_L and Ω_R are $N \times M$ complex matrices that vanish when X_{NM} and \tilde{X}_{NM} vanish and hence, like X_{NM} and \tilde{X}_{NM} , are perturbatively small. Straightforward matrix multiplication then yields:

$$\mathcal{L}_{N+M}^T \begin{pmatrix} \overline{\mathcal{M}}_N^D & Y_{NM} \\ \tilde{Y}_{NM}^T & \overline{\mathcal{M}}_M^D \end{pmatrix} \mathcal{R}_{N+M} \approx \begin{pmatrix} \mathcal{M}'_N{}^D & Y_{NM} - \Omega_L^* \overline{\mathcal{M}}_M^D + \overline{\mathcal{M}}_N^D \Omega_R \\ \tilde{Y}_{NM}^T - \overline{\mathcal{M}}_M^D \Omega_R^\dagger + \Omega_L^T \overline{\mathcal{M}}_N^D & \mathcal{M}'_M{}^D \end{pmatrix}, \quad (\text{B.9})$$

where

$$\mathcal{M}'_N{}^D \equiv \overline{\mathcal{M}}_N^D + \Omega_L^* \overline{\mathcal{M}}_M^D \Omega_R^\dagger - \Omega_L^* \tilde{Y}_{NM}^T - Y_{NM} \Omega_R^\dagger - \frac{1}{2} \Omega_L^* \Omega_L^T \overline{\mathcal{M}}_N^D - \frac{1}{2} \overline{\mathcal{M}}_N^D \Omega_R \Omega_R^\dagger, \quad (\text{B.10})$$

$$\mathcal{M}'_M{}^D \equiv \overline{\mathcal{M}}_M^D + \Omega_L^T \overline{\mathcal{M}}_N^D \Omega_R + \Omega_L^T Y_{NM} + \tilde{Y}_{NM}^T \Omega_R - \frac{1}{2} \Omega_L^T \Omega_L^* \overline{\mathcal{M}}_M^D - \frac{1}{2} \overline{\mathcal{M}}_M^D \Omega_R^\dagger \Omega_R, \quad (\text{B.11})$$

The block-diagonalization is achieved by demanding that

$$Y_{NM} = \Omega_L^* \overline{\mathcal{M}}_M^D - \overline{\mathcal{M}}_N^D \Omega_R, \quad (\text{B.12})$$

$$\tilde{Y}_{NM} = \Omega_R^* \overline{\mathcal{M}}_M^D - \overline{\mathcal{M}}_N^D \Omega_L. \quad (\text{B.13})$$

Inserting these relations in Eqs. (B.10) and (B.11) and eliminating Y_{NM} and \tilde{Y}_{NM} , we obtain:

$$\mathcal{M}'_N{}^D = \overline{\mathcal{M}}_N^D + \frac{1}{2} \overline{\mathcal{M}}_N^D \Omega_R \Omega_R^\dagger + \frac{1}{2} \Omega_L^* \Omega_L^T \overline{\mathcal{M}}_N^D - \Omega_L^* \overline{\mathcal{M}}_M^D \Omega_R^\dagger, \quad (\text{B.14})$$

$$\mathcal{M}'_M{}^D = \overline{\mathcal{M}}_M^D + \frac{1}{2} \overline{\mathcal{M}}_M^D \Omega_R^\dagger \Omega_R + \frac{1}{2} \Omega_L^T \Omega_L^* \overline{\mathcal{M}}_M^D - \Omega_L^T \overline{\mathcal{M}}_N^D \Omega_R. \quad (\text{B.15})$$

The results above simplify somewhat when we recall that $\overline{\mathcal{M}}_N^D$ and $\overline{\mathcal{M}}_M^D$ are diagonal matrices [see Eq. (B.3) and (B.4)]. Combining the matrix elements of Eqs. (B.12) and (B.13) yields two equations for the elements of Ω_L and Ω_R :

$$\Omega_{L i' j'} \equiv \frac{1}{\overline{m}_{j'}^2 - \overline{m}_{i'}^2} \left[\overline{m}_{i'} \tilde{Y}_{NM i' j'} + Y_{NM i' j'}^* \overline{m}_{j'} \right], \quad (\text{B.16})$$

$$\Omega_{R i' j'} \equiv \frac{1}{\overline{m}_{j'}^2 - \overline{m}_{i'}^2} \left[\overline{m}_{i'} Y_{NM i' j'} + \tilde{Y}_{NM i' j'}^* \overline{m}_{j'} \right], \quad (\text{B.17})$$

with $i' = 1', \dots, N'$ and $j' = N' + 1' \dots, N' + M'$. Since the elements $\Omega_{L i' j'}$ and $\Omega_{R i' j'}$ are the small parameters of the perturbation expansion, the perturbativity conditions previously given in Eq. (B.6) arise naturally.

At this stage, the result of the perturbative block diagonalization is:

$$\mathcal{L}_{N+M}^T \begin{pmatrix} \overline{\mathcal{M}}_N^D & Y_{NM} \\ \tilde{Y}_{NM}^T & \overline{\mathcal{M}}_M^D \end{pmatrix} \mathcal{R}_{N+M} = \begin{pmatrix} \mathcal{M}'_N{}^D & \mathbb{O} \\ \mathbb{O} & \mathcal{M}'_M{}^D \end{pmatrix}, \quad (\text{B.18})$$

up to third order in Ω in the off-diagonal blocks. The $\mathcal{O}(\Omega^3)$ terms can be neglected consistently. Also the re-diagonalization of the two diagonal blocks can be omitted. Though the off-diagonal elements of $\mathcal{M}'_N{}^D$ and $\mathcal{M}'_M{}^D$ are of $\mathcal{O}(\Omega^2)$, they only effect, in the singular value decomposition, the corresponding diagonal elements at $\mathcal{O}(\Omega^4)$, which

we neglect in this analysis. However, the diagonal elements of $\mathcal{M}'_N{}^D$ and $\mathcal{M}'_M{}^D$ also contain terms of $\mathcal{O}(\Omega^2)$, which generate second-order shifts of the diagonal elements relative to the $\bar{m}_{k'}$ obtained at step (1). These corrections are easily obtained from the diagonal matrix elements of Eqs. (B.14) and (B.15) after making use of Eq. (B.16):

$$m_{i'} \simeq \bar{m}_{i'} + \frac{1}{2} \sum_{j'=N'+1'}^{N'+M'} \left\{ \frac{\bar{m}_{i'} (|Y_{NMi'j'}|^2 + |\tilde{Y}_{NMi'j'}|^2)}{\bar{m}_{i'}^2 - \bar{m}_{j'}^2} + 2 \frac{\bar{m}_{j'} Y_{NMi'j'} \tilde{Y}_{NMi'j'}}{\bar{m}_{i'}^2 - \bar{m}_{j'}^2} \right\}, \quad (\text{B.19})$$

$$m_{j'} \simeq \bar{m}_{j'} - \frac{1}{2} \sum_{i'=1'}^{N'} \left\{ \frac{\bar{m}_{j'} (|Y_{NMi'j'}|^2 + |\tilde{Y}_{NMi'j'}|^2)}{\bar{m}_{i'}^2 - \bar{m}_{j'}^2} + 2 \frac{\bar{m}_{i'} Y_{NMi'j'} \tilde{Y}_{NMi'j'}}{\bar{m}_{i'}^2 - \bar{m}_{j'}^2} \right\}, \quad (\text{B.20})$$

with $i' = 1', \dots, N'$ and $j' = N' + 1', \dots, N' + M'$. The shifted mass parameters correspond to the physical mass values if the original mass matrix is real.

(3) However, for complex mass matrices the shifted mass parameters would in general be complex. These phases can be removed by substituting $\mathcal{L} \rightarrow \mathcal{L}\mathcal{P}$ and $\mathcal{R} \rightarrow \mathcal{R}\mathcal{P}$ with properly chosen phases

$$\mathcal{P} = \text{diag}(e^{-i\alpha_{1'}}, \dots, e^{-i\alpha_{N'+M'}}). \quad (\text{B.21})$$

Starting from Eqs. (B.19) and (B.20), one can evaluate \mathcal{P} to second order in the perturbation $\Omega_{L,R}$. In particular, for $\epsilon_{1,2} \ll a$, we have $a + \epsilon_1 + i\epsilon_2 \simeq (a + \epsilon_1)e^{i\epsilon_2/a}$. From this result, we easily derive the second-order expressions for the physical masses by just substituting

$$Y\tilde{Y} \rightarrow \Re(Y\tilde{Y}), \quad (\text{B.22})$$

while the phases are given by the imaginary part of $Y\tilde{Y}$,

$$\alpha_{i'} \simeq \frac{1}{2} \sum_{j'=N'+1'}^{N'+M'} \frac{\bar{m}_{j'}}{\bar{m}_{i'}(\bar{m}_{i'}^2 - \bar{m}_{j'}^2)} \Im \left(Y_{NMi'j'} \tilde{Y}_{NMi'j'} \right), \quad (\text{B.23})$$

$$\alpha_{j'} \simeq -\frac{1}{2} \sum_{i'=1'}^{N'} \frac{\bar{m}_{i'}}{\bar{m}_{j'}(\bar{m}_{i'}^2 - \bar{m}_{j'}^2)} \Im \left(Y_{NMi'j'} \tilde{Y}_{NMi'j'} \right), \quad (\text{B.24})$$

with $i' = 1', \dots, N'$ and $j' = N' + 1', \dots, N' + M'$.

This completes the perturbative singular value decomposition of the mass matrix for N -dimensional and M -dimensional subsystems of fermions weakly coupled by an off-diagonal perturbation. Thus the physical masses and the elements of the mixing matrices can be derived from the parameters of the $N \times N$ and $M \times M$ subsystems and the weak couplings X_{NM}, \tilde{X}_{NM} of the subsystems [rotated to Y_{NM}, \tilde{Y}_{NM} finally].

As noted in Eq. (B.6), the perturbation theory breaks down if any mass $\bar{m}_{i'}$ from the N -dimensional subsystem is nearly degenerate with a corresponding mass $\bar{m}_{j'}$ from the M -dimensional subsystem (if the corresponding residues do not vanish). In this case the formalism developed in Ref. [23] can be adopted to calculate the physical masses also in the cross-over zones analytically.

Appendix C: Chargino, neutralino and scalar masses and mixing elements by block-diagonalization

When the weak couplings among the gaugino and higgsino sectors are switched on the mass eigenvalues and mixing parameters are calculated using the block-diagonalization method adopting the formulae in the preceding appendices.

Charginos

Using the short-hand notation $m_{\tilde{\chi}_i^\pm} = m_i^\pm$, the chargino mass eigenvalues are given approximately by

$$m_1^\pm = \bar{m}_1^\pm + \frac{v^2}{2((\bar{m}_1^\pm)^2 - \mu_c^2)} \left\{ \bar{m}_1^\pm \left[(\lambda_I v_u c_+ + g v_d \epsilon_+ s_+ / \sqrt{2})^2 + (\lambda_I v_d c_- - g v_u \epsilon_- s_- / \sqrt{2})^2 \right] - 2\mu_c \alpha_c^2 (\lambda_I v_u c_+ + g v_d \epsilon_+ s_+ / \sqrt{2})(\lambda_I v_d c_- - g v_u \epsilon_- s_- / \sqrt{2}) \right\}, \quad (\text{C.1})$$

$$m_2^\pm = \bar{m}_2^\pm + \frac{v^2}{2((\bar{m}_2^\pm)^2 - \mu_c^2)} \left\{ \bar{m}_2^\pm \left[(\lambda_I v_u \epsilon_+ s_+ - g v_d c_+ / \sqrt{2})^2 + (\lambda_I v_d \epsilon_- s_- + g v_u c_- / \sqrt{2})^2 \right] - 2\mu_c \beta_c^2 (\lambda_I v_u \epsilon_+ s_+ - g v_d c_+ / \sqrt{2})(\lambda_I v_d \epsilon_- s_- + g v_u c_- / \sqrt{2}) \right\}, \quad (\text{C.2})$$

$$m_3^\pm = \mu_c - \frac{v^2}{2((\bar{m}_1^\pm)^2 - \mu_c^2)} \left\{ \mu_c \left[(\lambda_I v_u c_+ + g v_d \epsilon_+ s_+ / \sqrt{2})^2 + (\lambda_I v_d c_- - g v_u \epsilon_- s_- / \sqrt{2})^2 \right] - 2\bar{m}_1^\pm \alpha_c^2 (\lambda_I v_u c_+ + g v_d \epsilon_+ s_+ / \sqrt{2})(\lambda_I v_d c_- - g v_u \epsilon_- s_- / \sqrt{2}) \right\} - \frac{v^2}{2((\bar{m}_2^\pm)^2 - \mu_c^2)} \left\{ \mu_c \left[(\lambda_I v_u \epsilon_+ s_+ - g v_d c_+ / \sqrt{2})^2 + (\lambda_I v_d \epsilon_- s_- + g v_u c_- / \sqrt{2})^2 \right] - 2\bar{m}_2^\pm \beta_c^2 (\lambda_I v_u \epsilon_+ s_+ - g v_d c_+ / \sqrt{2})(\lambda_I v_d \epsilon_- s_- + g v_u c_- / \sqrt{2}) \right\}, \quad (\text{C.3})$$

where the signs ϵ_\pm and the phases α_\pm and β_\pm are defined by

$$\epsilon_\pm = \text{sign}[(M'_2 + M_2)M_2^D \pm g(M'_2 - M_2)v_I], \quad (\text{C.4})$$

$$\alpha_c = \sqrt{\text{sign}[M'_2(\sigma_+ \sigma_- - M_2'^2 + M_2^2) - 2(M'_2 + M_2)(M_2^D)^2 - 2g^2(M'_2 - M_2)v_I]}, \quad (\text{C.5})$$

$$\beta_c = \sqrt{\text{sign}[M_2(\sigma_+ \sigma_- - M_2'^2 + M_2^2) + 2(M'_2 + M_2)(M_2^D)^2 - 2g^2(M'_2 - M_2)v_I]}, \quad (\text{C.6})$$

and the abbreviations $c_\pm = \cos \theta_\pm$ and $s_\pm = \sin \theta_\pm$, and $c_{2\beta} = \cos 2\beta$, $s_{2\beta} = \sin 2\beta$ have been adopted.

The gaugino/higgsino mixing elements read in this approximation

$$\begin{aligned} U_{\pm 11} &= \alpha_c c_\pm, & U_{\pm 12} &= \beta_c \epsilon_\pm s_\pm, & U_{\pm 13} &= \alpha_c c_\pm \Omega_{\pm 13} + \beta_c \epsilon_\pm s_\pm \Omega_{\pm 23}, \\ U_{\pm 21} &= -\alpha_c \epsilon_\pm s_\pm, & U_{\pm 22} &= \beta_c c_\pm, & U_{\pm 23} &= -\alpha_c \epsilon_\pm s_\pm \Omega_{\pm 13} + \beta_c c_\pm \Omega_{\pm 23}, \\ U_{\pm 31} &= -\Omega_{\pm 13}^*, & U_{\pm 32} &= -\Omega_{\pm 23}^*, & U_{\pm 33} &= 1, \end{aligned} \quad (\text{C.7})$$

The matrix elements of the rectangular Ω_\pm matrices, which block-diagonalize the mass matrix are as follows

$$\begin{aligned} \Omega_{+13} &= \left[\bar{m}_1^\pm \alpha_c (\lambda_I v_d c_- - g v_u \epsilon_- s_- / \sqrt{2}) - \mu_c \alpha_c^* (\lambda_I v_u c_+ + g v_d \epsilon_+ s_+ / \sqrt{2}) \right] / (\mu_c^2 - (\bar{m}_1^\pm)^2), \\ \Omega_{+23} &= \left[\bar{m}_2^\pm \beta_c (\lambda_I v_d \epsilon_- s_- + g v_u c_- / \sqrt{2}) - \mu_c \beta_c^* (\lambda_I v_u \epsilon_+ s_+ - g v_d c_+ / \sqrt{2}) \right] / (\mu_c^2 - (\bar{m}_2^\pm)^2), \end{aligned} \quad (\text{C.8})$$

and

$$\begin{aligned} \Omega_{-13} &= - \left[\bar{m}_1^\pm \alpha_c (\lambda_I v_u c_+ + g v_d \epsilon_+ s_+ / \sqrt{2}) - \mu_c \alpha_c^* (\lambda_I v_d c_- - g v_u \epsilon_- s_- / \sqrt{2}) \right] / (\mu_c^2 - (\bar{m}_1^\pm)^2), \\ \Omega_{-23} &= - \left[\bar{m}_2^\pm \beta_c (\lambda_I v_u \epsilon_+ s_+ - g v_d c_+ / \sqrt{2}) - \mu_c \beta_c^* (\lambda_I v_d \epsilon_- s_- + g v_u c_- / \sqrt{2}) \right] / (\mu_c^2 - (\bar{m}_2^\pm)^2), \end{aligned} \quad (\text{C.9})$$

where the signs ϵ_\pm and the phase factors α_c and β_c are defined in Eqs. (C.4) to (C.6).

As a numerical check for the analytic expansion we show in Fig. 13 the evolution of the approximate versus exact chargino masses as a function of the control parameter y from the MSSM doublet ($y = -1$) to the Dirac ($y = 0$)

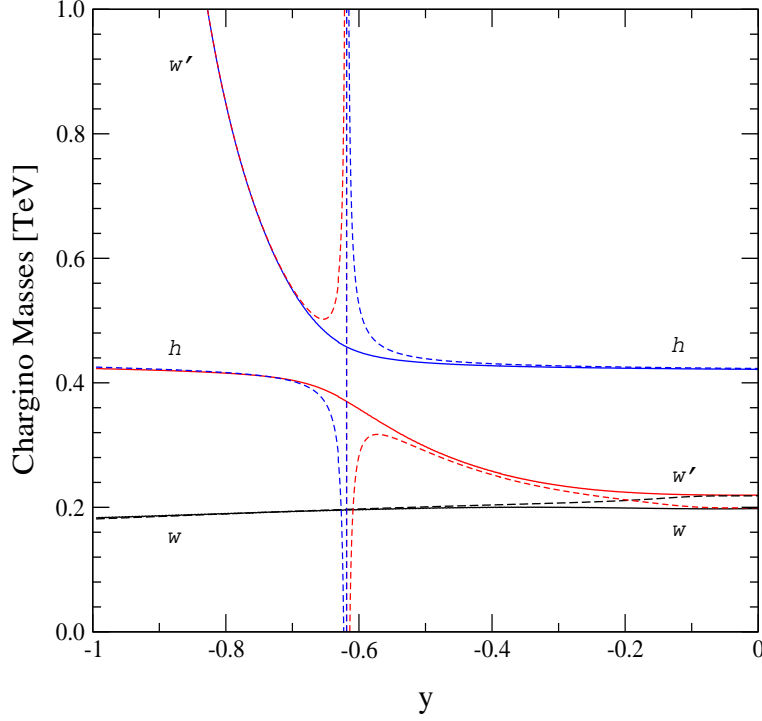


Figure 13: Evolution of the approximate versus exact chargino masses as a function of the control parameter y from the MSSM doublet ($y = -1$) to the Dirac ($y = 0$) triplet along the path \mathcal{P}_C in Eq. (2.42) for $m = 200$ GeV and $\tan \beta = 5$. The singularity in the cross-over zone can be removed by using the specific formalism for degenerate states as developed in Ref. [23].

triplet along the path \mathcal{P}_C in Eq. (2.42) for the same parameter set used in Fig. 1. The descending order of the physical masses in the figure reflects, in obvious notation, the pattern $w' \gg h > w$ in the MSSM limit. When the states w' and h become degenerate near $y = -0.6$, the standard analytical expansion cannot be applied any more. In this situation the mass spectrum must either be obtained numerically or analytical expansions tailored specifically for cross-over phenomena, see Ref. [23]. On the other hand, the ordering $h > w' > w$ is kept until the Dirac limit is reached. The level-crossing phenomenon near $y = -0.2$ is due to the mixing between the gaugino and higgsino sectors but not due to the $w'-w$ cross-over, as $\overline{m}_2^\pm > \overline{m}_1^\pm$ along the entire path.

Neutralinos

With $m_{\tilde{\chi}_i^0} = m_i^0$ the neutralino mass eigenvalues are given by

bino sector :

$$m_1^0 = \overline{m}_1^0 - \frac{1}{4(\overline{m}_1^0 + \mu)} \left[g'v_{-s_1}/\sqrt{2} - \lambda_Y v_{+c_1} \right]^2 - \frac{1}{4(\overline{m}_1^0 - \mu)} \left[g'v_{+s_1}/\sqrt{2} + \lambda_Y v_{-c_1} \right]^2, \quad (\text{C.10})$$

$$m_2^0 = \overline{m}_2^0 - \frac{1}{4(\overline{m}_2^0 - \mu)} \left[g'v_{-c_1}/\sqrt{2} + \lambda_Y v_{+s_1} \right]^2 - \frac{1}{4(\overline{m}_2^0 + \mu)} \left[g'v_{+c_1}/\sqrt{2} - \lambda_Y v_{-s_1} \right]^2, \quad (\text{C.11})$$

wino sector :

$$m_3^0 = \bar{m}_3^0 - \frac{1}{4(\bar{m}_3^0 + \mu)} \left[g v_{-s_2}/\sqrt{2} + \lambda_I v_{+c_2} \right]^2 - \frac{1}{4(\bar{m}_3^0 - \mu)} \left[g v_{+s_2}/\sqrt{2} - \lambda_I v_{-c_2} \right]^2, \quad (\text{C.12})$$

$$m_4^0 = \bar{m}_4^0 - \frac{1}{4(\bar{m}_4^0 - \mu)} \left[g v_{+c_2}/\sqrt{2} - \lambda_I v_{+s_2} \right]^2 - \frac{1}{4(\bar{m}_4^0 + \mu)} \left[g v_{+c_2}/\sqrt{2} + \lambda_I v_{-s_2} \right]^2, \quad (\text{C.13})$$

higgsino sector :

$$m_5^0 = \mu_n + \frac{1}{4(\bar{m}_1^0 + \mu)} \left[g' v_{-s_1}/\sqrt{2} - \lambda_Y v_{+c_1} \right]^2 - \frac{1}{4(\bar{m}_2^0 - \mu)} \left[g' v_{-c_1}/\sqrt{2} + \lambda_Y v_{+s_1} \right]^2 \\ + \frac{1}{4(\bar{m}_3^0 + \mu)} \left[g v_{+s_2}/\sqrt{2} + \lambda_I v_{+c_2} \right]^2 - \frac{1}{4(\bar{m}_4^0 - \mu)} \left[g v_{-c_2}/\sqrt{2} - \lambda_I v_{+s_2} \right]^2, \quad (\text{C.14})$$

$$m_6^0 = \mu_n - \frac{1}{4(\bar{m}_1^0 - \mu)} \left[g' v_{+s_1}/\sqrt{2} + \lambda_Y v_{-c_1} \right]^2 + \frac{1}{4(\bar{m}_2^0 + \mu)} \left[g' v_{+c_1}/\sqrt{2} - \lambda_Y v_{-s_1} \right]^2 \\ - \frac{1}{4(\bar{m}_3^0 - \mu)} \left[g v_{ud}^+ s_2/\sqrt{2} - \lambda_I v_{ud}^- c_2 \right]^2 + \frac{1}{4(\bar{m}_4^0 + \mu)} \left[g v_{+c_2}/\sqrt{2} + \lambda_I v_{-s_2} \right]^2, \quad (\text{C.15})$$

where $v_{\pm} = v_u \pm v_d$.

The final 6×6 diagonalization matrix reads approximately:

$$U_N = \bar{U}_N \begin{pmatrix} \mathbf{1}_{4 \times 4} & \Omega_{4 \times 2} \\ -\Omega_{4 \times 2}^\dagger & \mathbf{1}_{2 \times 2} \end{pmatrix}, \quad (\text{C.16})$$

where the elements of the rectangular matrix $\Omega_{4 \times 2}$ are as follows:

$$\text{bino sector} : \Omega_{15} = \frac{-i}{2(\bar{m}_1^0 + \mu)} \left[g' v_{-s_1}/\sqrt{2} - \lambda_Y v_{+c_1} \right], \quad \Omega_{16} = \frac{1}{2(\bar{m}_1^0 - \mu)} \left[g' v_{+s_1}/\sqrt{2} + \lambda_Y v_{-c_1} \right], \\ \Omega_{25} = \frac{1}{2(\bar{m}_2^0 - \mu)} \left[g' v_{-c_1}/\sqrt{2} - \lambda_Y v_{-s_1} \right], \quad \Omega_{26} = \frac{i}{2(\bar{m}_2^0 + \mu)} \left[g' v_{+c_1}/\sqrt{2} - \lambda_Y v_{-s_1} \right], \quad (\text{C.17})$$

and

$$\text{wino sector} : \Omega_{35} = \frac{i}{2(\bar{m}_3^0 + \mu)} \left[g v_{-s_2}/\sqrt{2} + \lambda_I v_{+c_2} \right], \quad \Omega_{36} = \frac{1}{2(\bar{m}_3^0 - \mu)} \left[g v_{+s_2}/\sqrt{2} - \lambda_I v_{-c_2} \right], \\ \Omega_{45} = \frac{-1}{2(\bar{m}_4^0 - \mu)} \left[g v_{-c_2}/\sqrt{2} - \lambda_I v_{+s_2} \right], \quad \Omega_{46} = \frac{i}{2(\bar{m}_4^0 + \mu)} \left[g v_{+c_2}/\sqrt{2} + \lambda_I v_{-s_2} \right], \quad (\text{C.18})$$

with abbreviations as before.

Scalar/Higgs Particles

The block-diagonalization of the Higgs/scalar mass matrix when the weak coupling between the Higgs and the sigma fields is included gives the following results.

(i) neutral pseudoscalars:

The physical pseudoscalar masses are given approximately by

$$M_{A_1}^2 = M_A^2 - \frac{(M_Y - A_Y)^2}{2(\tilde{m}_Y'^2 - M_A^2)} \lambda_Y^2 v^2 - \frac{(M_I - A_I)^2}{2(\tilde{m}_I'^2 - M_A^2)} \lambda_I^2 v^2, \quad (\text{C.19})$$

$$M_{A_2}^2 = \tilde{m}_Y'^2 + \frac{(M_Y - A_Y)^2}{2(\tilde{m}_Y'^2 - M_A^2)} \lambda_Y^2 v^2, \quad (\text{C.20})$$

$$M_{A_3}^2 = \tilde{m}_I'^2 + \frac{(M_I - A_I)^2}{2(\tilde{m}_I'^2 - M_A^2)} \lambda_I^2 v^2, \quad (\text{C.21})$$

up to the order of $v^2/m_{I,Y}^2$, while the physical pseudoscalar states are mixed according to the relation $O_P^T \mathcal{M}_P^2 O_P = \text{diag}(M_{A_1}^2, M_{A_2}^2, M_{A_3}^2)$ with the mixing elements given approximately by

$$\begin{aligned} O_{P11} = O_{P22} = O_{P33} &= 1, & O_{P12} = -O_{P21} &= -\frac{(M_Y - A_Y)\lambda_Y v}{\sqrt{2}(\tilde{m}_Y'^2 - M_A^2)}, \\ O_{P13} = -O_{P31} &= -\frac{(M_I - A_I)\lambda_I v}{\sqrt{2}(\tilde{m}_I'^2 - M_A^2)}, & O_{P23} = -O_{P32} &= \frac{\lambda_Y \lambda_I v^2}{2(\tilde{m}_I'^2 - \tilde{m}_Y'^2)}, \end{aligned} \quad (\text{C.22})$$

up to the order of $v/m_{I,Y}$.

(ii) neutral scalars:

The block diagonalization is described by the 2×2 matrix Ω_S with its elements

$$\begin{aligned} \Omega_{S13} &= -\frac{(2\tilde{m}_Y^2 - \lambda_Y^2 v^2)v_Y}{(\tilde{m}_Y^2 - m_Z^2)v}, & \Omega_{S23} &= \frac{\Delta_Y}{\tilde{m}_Y^2 - M_A^2}, \\ \Omega_{S14} &= -\frac{(2\tilde{m}_I^2 - \lambda_I^2 v^2)v_I}{(\tilde{m}_I^2 - m_Z^2)v}, & \Omega_{S24} &= \frac{\Delta_I}{\tilde{m}_I^2 - M_A^2}, \end{aligned} \quad (\text{C.23})$$

up to the order of $v/M_A, v/m_{Y,I}$. Performing these subsequent transformations gives rise to the four physical masses

$$M_{S_1}^2 = m_Z^2 + \delta_H s_{2\beta} + \epsilon_H - \frac{(\delta_H c_{2\beta} + \epsilon_H/t_\beta)^2}{M_A^2 - m_Z^2} - \frac{(2\tilde{m}_Y^2 - \lambda_Y^2 v^2)^2 v_Y^2}{(\tilde{m}_Y^2 - m_Z^2)v^2} - \frac{(2\tilde{m}_I^2 - \lambda_I^2 v^2)^2 v_I^2}{(\tilde{m}_I^2 - m_Z^2)v^2}, \quad (\text{C.24})$$

$$M_{S_2}^2 = M_A^2 - \delta_H s_{2\beta} + \epsilon_H/t_\beta^2 + \frac{(\delta_H c_{2\beta} + \epsilon_H/t_\beta)^2}{M_A^2 - m_Z^2} - \frac{\Delta_Y^2}{\tilde{m}_Y^2 - M_A^2} - \frac{\Delta_I^2}{\tilde{m}_I^2 - M_A^2}, \quad (\text{C.25})$$

$$M_{S_3}^2 = \tilde{m}_Y^2 + \frac{(2\tilde{m}_Y^2 - \lambda_Y^2 v^2)^2 v_Y^2}{(\tilde{m}_Y^2 - m_Z^2)v^2} + \frac{\Delta_Y^2}{\tilde{m}_Y^2 - M_A^2}, \quad (\text{C.26})$$

$$M_{S_4}^2 = \tilde{m}_I^2 + \frac{(2\tilde{m}_I^2 - \lambda_I^2 v^2)^2 v_I^2}{(\tilde{m}_I^2 - m_Z^2)v^2} + \frac{\Delta_I^2}{\tilde{m}_I^2 - M_A^2}, \quad (\text{C.27})$$

up to the order of $v^2/M_A^2, v^2/m_{Y,I}^2$, and the 4×4 mixing matrix \mathcal{O}_S , connecting current with mass eigenstates as $\mathcal{O}_S^T \mathcal{M}_S^2 \mathcal{O}_S = \text{diag}(M_{S_1}^2, \dots, M_{S_4}^2)$, with its elements:

$$\begin{aligned} \mathcal{O}_{S11} = \mathcal{O}_{S22} = \mathcal{O}_{S33} = \mathcal{O}_{S44} &= 1, & \mathcal{O}_{S12} = -\mathcal{O}_{S21} &= s_h, & \mathcal{O}_{S34} = -\mathcal{O}_{S43} &= 0, \\ \mathcal{O}_{S13} = -\mathcal{O}_{S31} &= -\frac{(2\tilde{m}_Y^2 - \lambda_Y^2 v^2)v_Y}{(\tilde{m}_Y^2 - m_Z^2)v}, & \mathcal{O}_{S23} = -\mathcal{O}_{32} &= \frac{\Delta_Y}{\tilde{m}_Y^2 - M_A^2}, \\ \mathcal{O}_{S14} = -\mathcal{O}_{S41} &= -\frac{(2\tilde{m}_I^2 - \lambda_I^2 v^2)v_I}{(\tilde{m}_I^2 - m_Z^2)v}, & \mathcal{O}_{S24} = -\mathcal{O}_{42} &= \frac{\Delta_I}{\tilde{m}_I^2 - M_A^2}, \end{aligned} \quad (\text{C.28})$$

up to the order of $v/M_A, v/m_{Y,I}$ with the abbreviation $s_h = \sin \theta_h$.

(iii) charged scalars:

In the weak coupling limit the charged H^\pm and $s_{1,2}^\pm$ states are mixed by the 3×3 matrix \mathcal{O}_S^\pm with components

$$\begin{aligned} \mathcal{O}_{S11}^\pm = \mathcal{O}_{S22}^\pm = \mathcal{O}_{S33}^\pm &= 1, & \mathcal{O}_{S12}^\pm = -\mathcal{O}_{S21}^\pm &= \Delta_{1\pm}/(\tilde{m}_I'^2 - M_A^2), \\ \mathcal{O}_{S13}^\pm = -\mathcal{O}_{S31}^\pm &= \Delta_{2\pm}/(\tilde{m}_I'^2 - M_A^2), & \mathcal{O}_{S23}^\pm = -\mathcal{O}_{S32}^\pm &= 0, \end{aligned} \quad (\text{C.29})$$

up to the order of $v/M_A, v/m_{Y,I}$ to generate the physical charged scalar masses

$$M_{S_1^\pm}^2 = \tilde{M}_{H^\pm}^2 - \Delta_{1\pm}^2/(\tilde{m}_I'^2 - M_A^2) - \Delta_{2\pm}^2/(\tilde{m}_I'^2 - M_A^2), \quad (\text{C.30})$$

$$M_{S_2^\pm}^2 = \tilde{m}_I'^2 + g^2 v_I^2 c_{2\beta}^2/4(\tilde{m}_I'^2 - \tilde{m}_I'^2) + \Delta_{1\pm}^2/(\tilde{m}_I'^2 - M_A^2), \quad (\text{C.31})$$

$$M_{S_3^\pm}^2 = \rho \tilde{m}_I'^2 c_{2\beta}^2/4(\tilde{m}_I'^2 - \tilde{m}_I'^2) + \Delta_{2\pm}^2/(\tilde{m}_I'^2 - M_A^2), \quad (\text{C.32})$$

up to the order of $v^2/M_A^2, v^2/m_{Y,I}^2$.

-
- [1] Yu. A. Golfand and E. P. Likhtman, JETP Lett. **13** (1971) 3214; J. Wess and B. Zumino, Nucl. Phys. B **70** (1974) 39.
- [2] H. P. Nilles, Phys. Rept. **110** (1984) 1; H. E. Haber and G. L. Kane, Phys. Rept. **117** (1985) 75.
- [3] M. Drees, R. Godbole and P. Roy, “Theory and phenomenology of sparticles: An account of four-dimensional $N=1$ supersymmetry in high energy physics,” *Hackensack, USA: World Scientific (2004) 555 p*; P. Binetruy, “Supersymmetry: Theory, experiment and cosmology,” *Oxford, UK: Oxford Univ. Pr. (2006) 520 p*; J. Wess and J. Bagger, “Supersymmetry and supergravity,” *Princeton, USA: Univ. Pr. (1992) 259 p*.
- [4] P. Fayet, Nucl. Phys. B **113** (1976) 135; P. Fayet, Nucl. Phys. B **246** (1984) 89; F. del Aguila, M. Dugan, B. Grinstein, L. J. Hall, G. G. Ross and P. C. West, Nucl. Phys. B **250** (1985) 225; L. Girardello, M. Porrati and A. Zaffaroni, Nucl. Phys. B **505** (1997) 272 [arXiv:hep-th/9704163].
- [5] L. Álvarez-Gaumé and S. F. Hassan, Fortsch. Phys. **45** (1997) 159 [arXiv:hep-th/9701069].
- [6] M. M. Nojiri and M. Takeuchi, Phys. Rev. D **76** (2007) 015009 [arXiv:hep-ph/0701190];
- [7] S. Y. Choi, M. Drees, A. Freitas and P. M. Zerwas, Phys. Rev. D **78** (2008) 095007 [arXiv:0808.2410 [hep-ph]]; M. Kramer, E. Popeno, M. Spira and P. M. Zerwas, Phys. Rev. D **80** (2009) 055002 [arXiv:0902.3795 [hep-ph]].
- [8] S. Y. Choi, M. Drees, J. Kalinowski, J. M. Kim, E. Popeno and P. M. Zerwas, Phys. Lett. B **672** (2009) 246 [arXiv:0812.3586 [hep-ph]]; Acta Phys. Polon. B **40** (2009) 1947 [arXiv:0902.4706 [hep-ph]].
- [9] T. Plehn and T. M. P. Tait, J. Phys. G **36** (2009) 075001 [arXiv:0810.3919 [hep-ph]].
- [10] K. Benakli and C. Moura, in M. M. Nojiri *et al.*, arXiv:0802.3672 [hep-ph].
- [11] K. Benakli and M. D. Goodsell, arXiv:1003.4957 [Unknown].
- [12] L. J. Hall and L. Randall, Nucl. Phys. B **352** (1991) 289; L. Randall and N. Rius, Phys. Lett. B **286** (1992) 299.
- [13] G. D. Kribs, E. Poppitz and N. Weiner, arXiv:0712.2039 [hep-ph]; A. E. Blechman and S. P. Ng, JHEP **0806** (2008) 043 [arXiv:0803.3811 [hep-ph]]; for [general] flavor aspects of scalar fields, see *e.g.* C. P. Burgess, M. Trott and S. Zuberi, JHEP **0909** (2009) 082 [arXiv:0907.2696 [hep-ph]].
- [14] N. Polonsky and S. Su, Phys. Lett. B **508**, 103 (2001) [arXiv:hep-ph/0010113].
- [15] G. Belanger, K. Benakli, M. Goodsell, C. Moura and A. Pukhov, JCAP **0908** (2009) 027 [arXiv:0905.1043 [hep-ph]].
- [16] An alternative treatment of Dirac gaugino as a leptophilic candidate for dark matter has been discussed in E. J. Chun and J. C. Park, JCAP **0902** (2009) 026 [arXiv:0812.0308 [hep-ph]].
- [17] K. Hsieh, Phys. Rev. D **77** (2008) 015004 [arXiv:0708.3970 [hep-ph]].
- [18] E. J. Chun, J. C. Park and S. Scopel, JCAP **1002** (2010) 015 [arXiv:0911.5273 [hep-ph]].
- [19] P. J. Fox, A. E. Nelson and N. Weiner, JHEP **0208** (2002) 035 [arXiv:hep-ph/0206096].
- [20] I. Antoniadis, K. Benakli, A. Delgado and M. Quiros, Adv. Stud. Theor. Phys. **2** (2008) 645 [arXiv:hep-ph/0610265].
- [21] K. Benakli and M. D. Goodsell, Nucl. Phys. B **830** (2010) 315 [arXiv:0909.0017 [hep-ph]].
- [22] C. Amsler *et al.* [Particle Data Group], Phys. Lett. B **667** (2008) 1.
- [23] S. Y. Choi, H. E. Haber, J. Kalinowski and P. M. Zerwas, Nucl. Phys. B **778** (2007) 85 [arXiv:hep-ph/0612218].
- [24] E. Komatsu *et al.* [WMAP Collaboration], Astrophys. J. Suppl. **180** (2009) 330 [arXiv:0803.0547 [astro-ph]]; J. Dunkley *et al.* [WMAP Collaboration], Astrophys. J. Suppl. **180** (2009) 306 [arXiv:0803.0586 [astro-ph]].
- [25] A. J. Barr and C. G. Lester, arXiv:1004.2732 [hep-ph].
- [26] A. Freitas, A. von Manteuffel and P. M. Zerwas, Eur. Phys. J. C **34** (2004) 487 [arXiv:hep-ph/0310182]; Addendum, Eur. Phys. J. C **40** (2005) 435 [arXiv:hep-ph/0408341].
- [27] J. A. Aguilar-Saavedra and A. M. Teixeira, Nucl. Phys. B **675** (2003) 70 [arXiv:hep-ph/0307001].
- [28] M. E. Peskin, Int. J. Mod. Phys. A **13** (1998) 2299 [arXiv:hep-ph/9803279]; S. Y. Choi, M. Drees and B. Gaissmaier, Phys. Rev. D **70** (2004) 014010 [arXiv:hep-ph/0403054].
- [29] J. A. Aguilar-Saavedra *et al.*, Eur. Phys. J. C **46** (2006) 43 [arXiv:hep-ph/0511344].
- [30] S. Y. Choi, A. Djouadi, M. Guchait, J. Kalinowski, H. S. Song and P. M. Zerwas, Eur. Phys. J. C **14** (2000) 535 [arXiv:hep-ph/0002033]; S. Y. Choi, J. Kalinowski, G. A. Moortgat-Pick and P. M. Zerwas, Eur. Phys. J. C **22** (2001) 563 [Addendum-ibid. C **23** (2002) 769] [arXiv:hep-ph/0108117].
- [31] J. Pumplin, D. R. Stump, J. Huston, H. L. Lai, P. M. Nadolsky and W. K. Tung, JHEP **0207** (2002) 012 [arXiv:hep-ph/0201195].
- [32] M. M. Mühlleitner and P. M. Zerwas, Acta Phys. Polon. B **37** (2006) 1021 [arXiv:hep-ph/0511339].
- [33] D. M. Asner, J. B. Gronberg and J. F. Gunion, Phys. Rev. D **67** (2003) 035009 [arXiv:hep-ph/0110320].
- [34] S. Y. Choi and H. E. Haber, in preparation.